JUSTUS-LIEBIG-UNIVERSITÄT GIESSEN

INSTITUT FÜR ANORGANISCHE UND ANALYTISCHE CHEMIE

Investigation of Chromium Complexes with N-donor Ligands

Inaugural-Dissertation

zur Erlangung des Doktorgrades der Naturwissenschaften im Fachbereich Biologie und Chemie der Justus-Liebig-Universität Gießen

vorgelegt von

Sabrina Schäfer

aus

Haiger

For my family

„Die Neugier steht immer an erster Stelle eines Problems, das gelöst werden will."

Galileo Galilei

Danksagung

Mein herzlicher Dank gilt Prof. Dr. Siegfried Schindler für die interessante Themenstellung, die Unterstützung und die Ermöglichung meiner Promotion in seiner Arbeitsgruppe.

Des Weiteren gilt mein herzlicher Dank PD Dr. Dr. Dirk Walter für die gute Zusammenarbeit und die Einblicke in neue Themengebiete. Danke für die Bemühungen, das Engagement und die „Stärkungen" zwischendurch.

Ein weiterer Dank gilt Dr. Christian Würtele für die Hilfestellung während meiner Arbeit. Außerdem danke ich sehr meinen lieben Kollegen Jenny Blank, Anja Henß, Alexander Beitat, Jörg Müller, Thomas Nebe, Janine Will und Sabrina Turba. Ihr habt die Zeit unvergesslich werden lassen! Außerdem danke ich Melanie Jopp, Lars Valentin, Tobias Hoppe, Sandra Kisslinger, Jonathan Becker, Sabine Löw, Natascha Kempf, Stefan Schaub, Cornelius Brombach, Frank Mehlich, Miriam Wern und Andreas Miska für die gute Zusammenarbeit und das abwechslungsreiche Arbeitsklima.
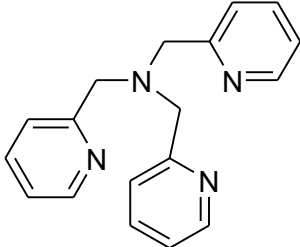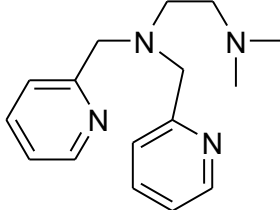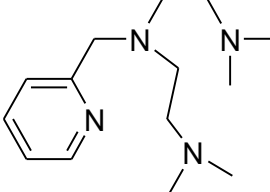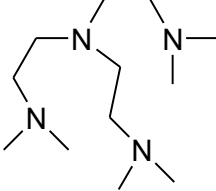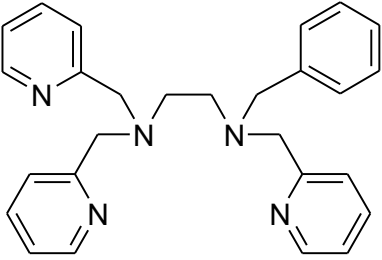
Ein großes Dankeschön geht an Dr. Michael Serafin für die Hilfe bei der „Bombenrohr-Synthese" und für die Beantwortung aller Fragen.

Günter Koch, Christian Kleeberg, Alexander Beitat, Christian Würtele, Jonathan Becker und Sabine Löw danke ich für die Bemühungen bei der Messung und Strukturlösung meiner Kristalle, auch wenn diese noch so klein und hässlich waren.

Ganz besonders danke ich meiner Familie, ohne die diese Arbeit niemals möglich gewesen wäre. Danke für den Rückhalt und die aufmunternden Worte immer dann, wenn sie nötig waren. Dies gilt auch für meine engen Freunde, die immer ein offenes Ohr für mich hatten.

Zuletzt danke ich Jörg für die immer wiederkehrende Erinnerung daran einen Schritt nach dem anderen zu machen. Danke für jede Aufmunterung, wenn sie nötig war, für den Versuch die Arbeit zu lesen und einfach für alles!

Ligands Used

Name	Abbreviation	Structure and Formula	Molar Mass [g·mol⁻¹]
Tris(2-pyridylmethyl)amine	**tmpa**	$C_{18}H_{18}N_4$	290.37
(2-Dimethyl-aminoethyl)bis(2-pyridylmethyl)amine	**Me₂uns-penp**	$C_{16}H_{22}N_4$	270.38
Bis(2-dimethyl-aminoethyl)(2-pyridylmethyl)amine	**Me₄apme**	$C_{14}H_{26}N_4$	250.39
Tris(2-Dimethyl-aminoethyl)amine	**Me₆tren**	$C_{12}H_{30}N_4$	230.40
N-benzyl-N,N',N'-tris(2-methylpyridyl)-ethylenediamine	**bztpen**	$C_{27}H_{29}N_5$	423.55

Abbreviations

approx.	approximately
BPh_4^-	tetraphenylborate
bz	benzyl
ClO_4^-	perchlorate
δ	chemical shift (NMR)
ε	extinction coefficient
e. g.	for example (Latin: *exempli gratia*)
et al.	*et alii*
GC-MS	gas chromatography-mass spectrometry
Hc	hemocyanin
IR	infrared
KBr	Potassium bromide
λ	wavelength
Me	methyl
NMR	nuclear magnetic resonance
OTf$^-$	triflate (trifluoromethanesulfonate)
PF_6^-	hexafluorophosphate
PhIO	iodosobenzene
py	pyridyl
s	singulett (NMR)
THF	tetrahydrofuran
τ	trigonality index parameter $\tau = (\beta-\alpha)/60°$, with α and β being the two largest coordination angles around the metal atom $\tau = 0$ for ideal square pyramidal arrangement and $\tau = 1$ for trigonal bipyramidal arrangement
TMS	tetramethylsilane (NMR)
UV/Vis	ultraviolet-visible
vs.	*versus*

Table of Contents

Table of Figures

1 Introduction

1.1 Motivation

Oxidation reactions play an important role in biochemistry, industrial processes and organic syntheses.[1] Especially interesting are oxidation reactions occurring in nature because here the oxidant is oxygen from air and the reactions take place under ambient conditions in aqueous solutions. Therefore, there is high interest to model such reactions for an industrial use. A number of research groups in the field of bioinorganic chemistry are interested in establishing functional model systems to gain better understanding of these reactions. In general, oxidation reactions of organic substrates with dioxygen are described by a two-step reaction mechanism.[2] In the first step dioxygen is activated at the active site and in the second step oxygen is transferred to a substrate according to the following scheme:

$$\text{Metalloenzyme or Metal Complex} \xrightleftharpoons{O_2} \text{"Oxy-Form"} \xrightarrow{\text{Substrate}} \text{Product}$$
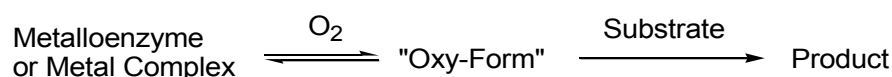
Scheme 1-1: Two-step reaction mechanism of general oxidation reactions of organic substrates using dioxygen as an oxidant.

The activation step, the reversible binding of dioxygen, is analogous to the reaction of oxygen-carrier proteins such as hemoglobin (myoglobin), hemocyanin and hemoerythrin. In contrast to that, metalloenzymes do not only activate dioxygen, but also transfer oxygen on substrates, either one oxygen atom (monooxygenases) or both oxygen atoms from the dioxygen molecule (dioxygenases).

It is well-known that in these naturally occurring oxidation reactions, iron or copper ions are located at the active sites of the metalloenzymes. Therefore, in recent years many iron or copper complexes have been studied as functional model complexes for these enzymes.[2-3] Based on these investigations one can be optimistic that new catalysts for homogeneous catalysis for selective oxidations under ambient conditions will be developed in the near future. Regarding this background it is important to study the activation of dioxygen in great detail.[4-7]

However, in many cases it turned out that the investigation of these complexes is quite challenging due to the difficulty in handling the intermediate, "dioxygen adduct complexes". Usually, these intermediates can only be observed spectroscopically as a transient short-lived (many times only at low temperatures) species. In contrast to that, "dioxygen adduct complexes" of chromium such as peroxido or oxido complexes are well-known and can often

be isolated and fully characterized. Therefore, it seemed reasonable to investigate chromium complexes with analogous ligands of which copper and iron complexes are known. In the following the motivation and background of this work are described in more detail.

1.2 Characterized Copper and Iron "Dioxygen Adduct Complexes"

A full description of all copper and iron "dioxygen adduct complexes" is not possible in this thesis. However, a large number of review articles on this topic were published.[2-6,8-15] In the following some selected examples being important for this thesis are presented.[12] Scheme 1-2 depicts a listing of possible reactive "dioxygen adduct complexes" occurring in oxygenation reactions using metal complexes.
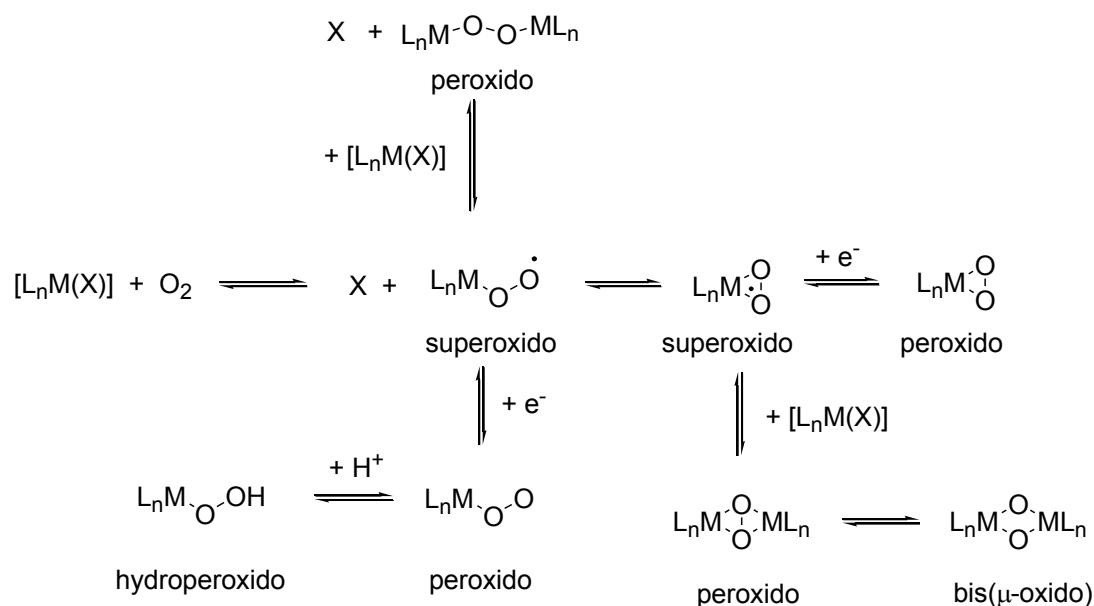
Scheme 1-2: General scheme including possible reactive species. The charges have been omitted for clarity.

In 1989 Kitajima and co-workers characterized the first side-on copper peroxido complex using the ligand hydrotris(3,5-diisopropyl-1-pyrazolyl)borate (HB(3,5-iPr$_2$pz)$_3$). This compound is known as the first model substance for hemocyanin (Hc). Such a peroxido moiety shows many similarities to the oxy-Hc form.[16] The molecular structure of the synthesized complex is shown in Figure 1-1 a).

The first synthetic copper peroxido complex using the tripodal ligand tris(2-pyridylmethyl)amine (tmpa) was structurally characterized by Karlin and co-workers in 1988 (Figure 1-1 b)).[17-18] This compound did not mimic the natural binding of dioxygen, but it showed another possibility of a copper "dioxygen adduct complex" as shown in Scheme 1-2. It is a dinuclear copper peroxido complex with end-on coordination of the peroxido ligand. The molecular structure of the complex is presented in Figure 1-1 b).
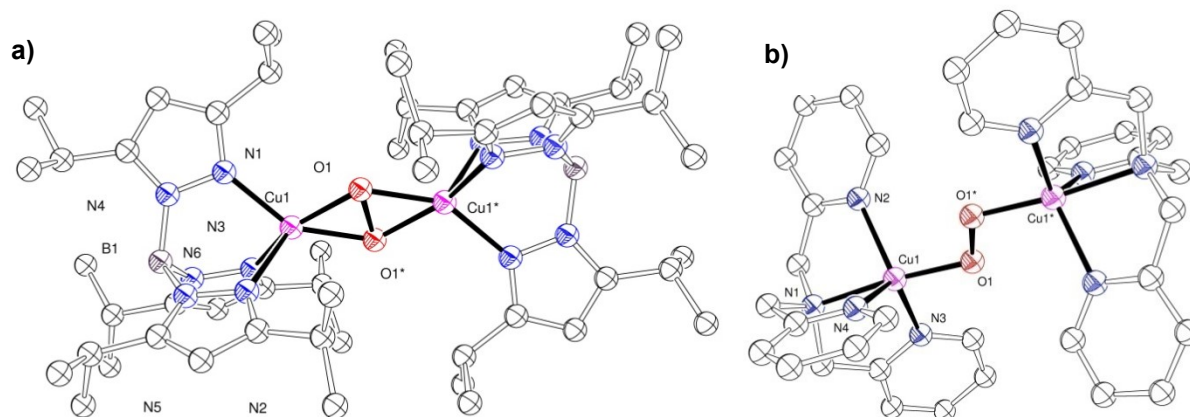
Figure 1-1: a) Molecular structure of the cation of the side-on coordinated copper peroxido complex [Cu$_2$(HB(3,5-iPrpz)$_3$)$_2$(O$_2$)].[16] b) Molecular structure of the cation of the end-on coordinated copper peroxido complex [Cu$_2$(tmpa)$_2$(O$_2$)](PF$_6$)$_2$.[17]

A similar end-on peroxido complex with the tren-based ligand Bz$_3$tren (tris(N-benzyl-N-methylaminoethyl)amine) was structurally characterized by Suzuki and co-workers in 2004.[19] (Figure 1-2)
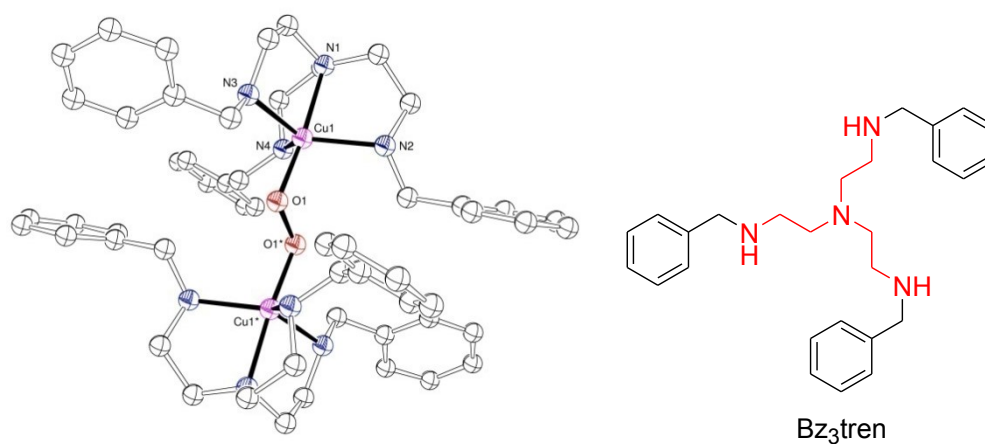
Figure 1-2: Molecular structure of the copper peroxido complex [Cu$_2$(Bz$_3$tren)$_2$(O$_2$)] and the ligand Bz$_3$tren.[19]

Until that time, the structurally characterized copper peroxido complexes were thermally very labile and could only be handled at very low temperatures. With a variation of the anions Würtele *et al.* were able to structurally characterize a copper peroxido complex with the ligand Me$_6$tren (Figure 1-11) that is stable in the solid state at room temperature (and even at higher temperatures).[20] The stability is caused by the shielding of eight tetraphenylborate anions. The molecular structure of the cation of the peroxido complex and also the anion shielding with a space-filling model are shown in Figure 1-3.
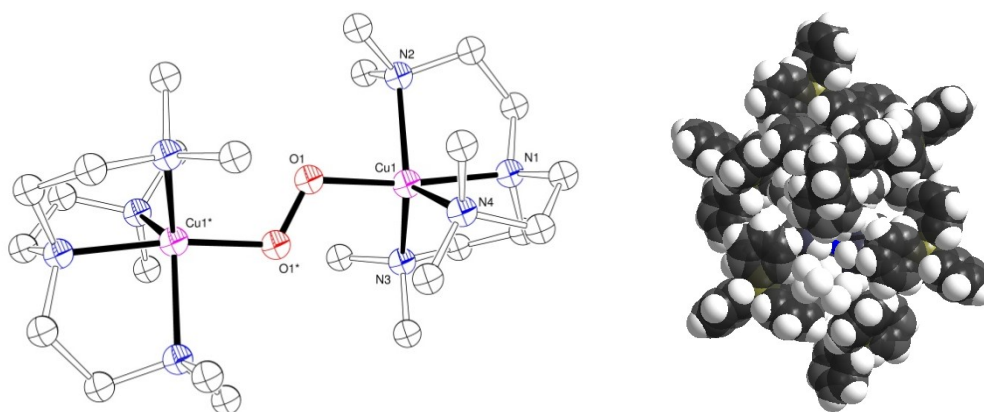
Figure 1-3: Molecular structure of the cation of a stable copper peroxido complex $[Cu_2(Me_6tren)(O_2)](BPh_4)_2$ (left) and the anion shielding shown with a space-filling model (right).[20]

The above mentioned tripodal ligands proved useful to obtain complexes for modeling reactive intermediates of metalloenzymes. Another interesting group of ligands being used to obtain such model compounds are macrocyclic ligands. In 2012, Hoppe *et al.* structurally characterized a first copper peroxido complex with the macrocyclic ligand rac-5,5,7,12,12,14-hexamethyl-1,4,8,11-tetraazacyclotetradecane (tet b). Again, the peroxido ligand has end-on coordination.[21] (Figure 1-4)
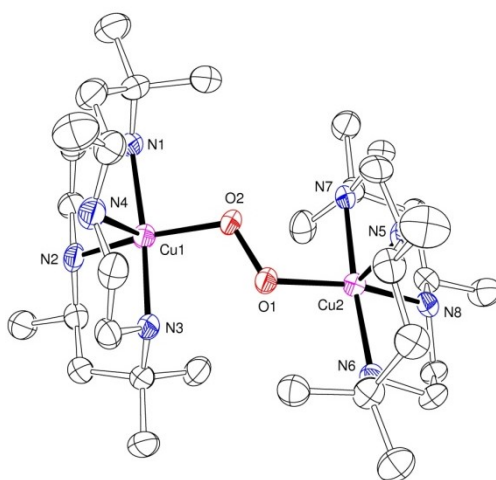
Figure 1-4: Molecular structure of the cation of $[Cu_2(tet\ b)_2(O_2)](OTf)_2$.[21]

In contrast to the studies of copper complexes, which are regularly used to model the active sites of proteins, only a small number of iron "dioxygen adduct complexes" were structurally characterized. One of the more recent complexes in that regard is a mononuclear non-heme side-on iron(III) peroxido complex with the macrocyclic ligand 1,4,8,11-tetramethyl-1,4,8,11-tetraazacyclotetradecane (14-TMC). The N-tetramethylated cyclam (TMC)[22] ligands, such as n-TMC (in this case n=14), are versatile ligands in the field of biomimetic chemistry.[23] The complex $[Fe^{II}14\text{-}TMC(OTf)_2]$ reacted with hydrogen peroxide in the presence of triethylamine to obtain the iron side-on peroxido complex (Figure 1-5). Herein, the iron atom has distorted octahedral coordination.[24]
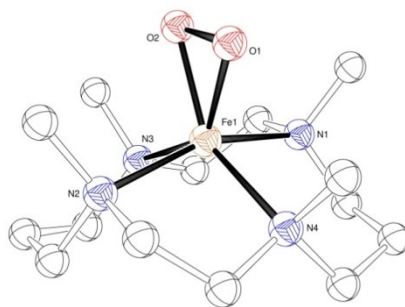
Figure 1-5: Molecular structure of the cation of the side-on iron peroxido complex [Fe(14-TMC)(O$_2$)]OTf.[24]

The same precursor complex [Fe^{II}14-TMC(OTf)$_2$] reacted with iodosobenzene (PhIO) in acetonitrile at –40 °C to a pale green intermediate. Que and co-workers structurally characterized the intermediate as Fe^{IV}=O species.[25] The 14-TMC ligand forms a plane with the iron cation, and the oxido ligand is coordinated in axial position. All four N-methyl groups are *anti*-positioned to the oxido ligand.[25] The molecular structure of the mononuclear non-heme Fe^{IV}=O complex is shown in Figure 1-6.
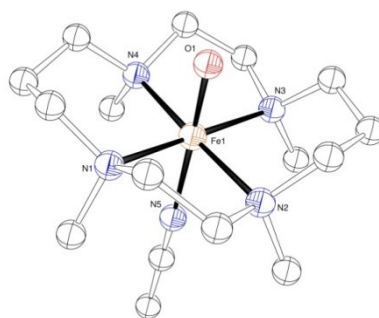
Figure 1-6: Molecular structure of the cation of the iron oxido complex *trans*-[Fe^{IV}(O)(14-TMC)(NCCH$_3$)](OTf)$_2$.[25]

1.3 Chromium "Dioxygen Adduct Complexes"

In organic chemistry, chromium(VI) salts are well-known as oxidants. Particularly chromiumtrioxide (CrO$_3$), chromate (CrO$_4^{2-}$), and dichromate (Cr$_2$O$_7^{2-}$) are often used e. g. for the oxidation of alcohols to aldehydes or ketones.[26] However, a problematic feature of these reactions is that primary alcohols often cannot simply be oxidized to aldehydes. Instead, they react further to form carboxylic acids. To avoid this problem, the anhydrous salt pyridiniumchloridochromate (PCC, C$_5$H$_5$NH[CrO$_3$Cl]) is used for selective oxidations of alcohols to aldehydes.[26] However, the use of chromium(VI) salts in oxidation reactions is furthermore problematic due to their toxicity. In this context, the reaction of dioxygen with low valent chromium compounds is little-known.

There are a number of reports in literature on stable chromium "dioxygen adduct complexes". In 2002 Qin *et al.* structurally characterized a chromium(III) superoxido complex [Tp^{tBu,Me}Cr(pz'H)(O$_2$)]BARF (Tp^{tBu,Me} = hydrotris(3-*tert*-butyl-5-methylpyrazolyl-)borate; pz'H =

3-*tert*-butyl-5-methylpyrazole; BARF = tetrakis(3,5-bis(trifluoridomethyl)phenyl)borate) with a side-on binding of dioxygen.[27] In 2003 Ramsey *et al.* described the side-on chromium(IV) peroxido complex [Cr(dien)(O$_2$)$_2$].[28]
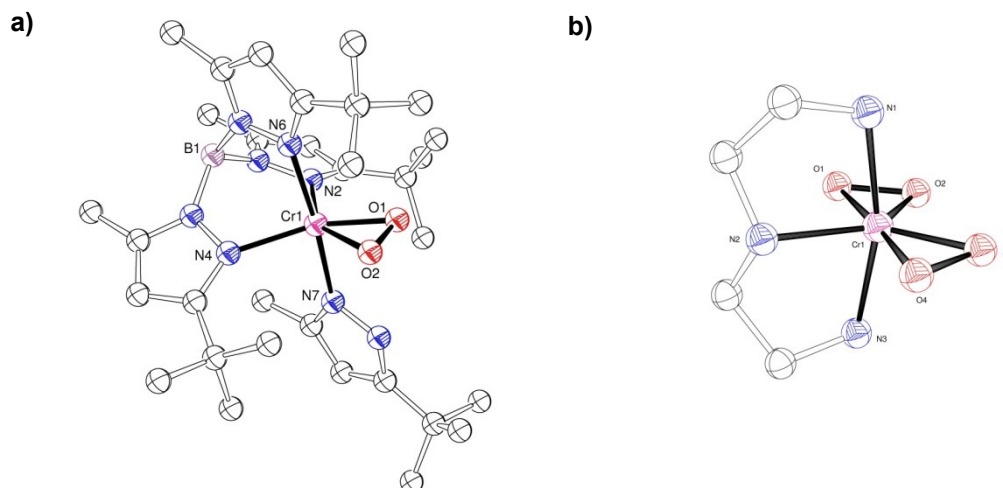
Figure 1-7: a) Molecular structure of the cation of a side-on chromium superoxido complex [Tp^{tBu,Me}Cr(pz'H)(O$_2$)]BARF.[27] b) Molecular structure of a side-on chromium peroxido complex [Cr(dien)(O$_2$)$_2$]·H$_2$O.[28]

Furthermore, Nam and co-workers recently structurally characterized a mononuclear chromium(III) superoxido complex.[29] To synthesize this complex, they used the macrocyclic ligand 14-TMC. They prepared the chromium(II) complex [Cr(14-TMC)Cl]Cl·2CH$_3$CN and by bubbling dioxygen through the according complex solution in acetonitrile at –10 °C, the chromium(III) superoxido complex [Cr(14-TMC)(O$_2$)Cl]·2CH$_3$CN was obtained (Figure 1-8).
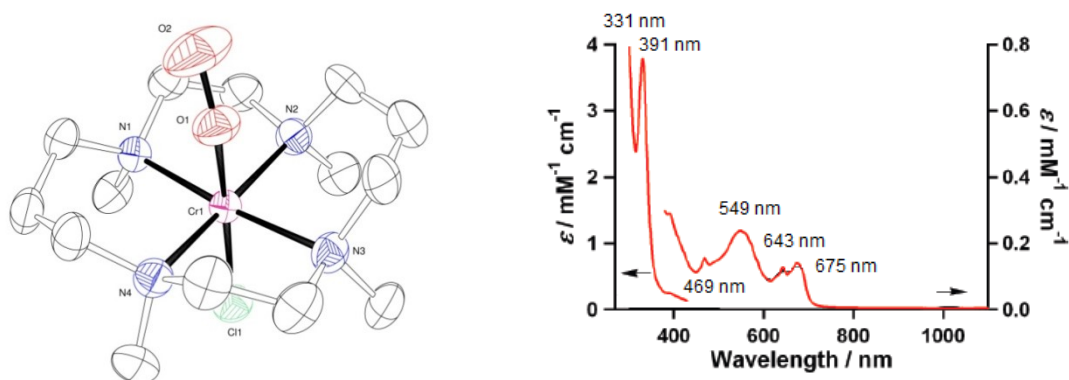
Figure 1-8: Molecular structure of the cation of a chromium(III) end-on superoxido complex [Cr(14-TMC)(O$_2$)Cl]·2CH$_3$CN.[29] UV/Vis spectrum of the chromium(III) superoxido complex in acetonitrile at –10 °C.[29]

By reaction of the chromium(II) complex [Cr(14-TMC)(CH$_3$CN)](ClO$_4$)$_2$ with iodosobenzene (PhIO) at –30 °C, Nam and co-workers synthesized and structurally characterized a chromium(V) oxido complex.[30] The chromium(V) oxido complex showed absorption maxima

at 353 nm and 446 nm and a shoulder at 520 nm (Figure 1-9). The mononuclear complex has distorted octahedral coordination.
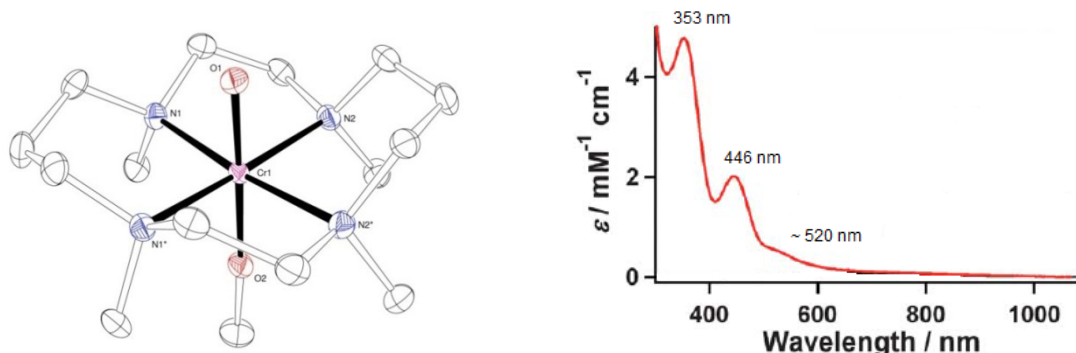
Figure 1-9: Molecular structure of the cation of the chromium(V) oxido complex [Cr(14-TMC)(O)(OCH$_3$)](ClO$_4$)$_2$.[30] UV/Vis spectrum of the chromium(V) oxido complex in acetonitrile at 25 °C.[30]

Furthermore, Nam and co-workers synthesized and structurally characterized a chromium(IV) oxido complex with the same ligand.[31] Using the smaller macrocycle 12-TMC (12-TMC = 1,4,7,10-tetramethyl-1,4,7,10-tetraazacyclododecane) as a ligand, a chromium(IV) side-on peroxido complex could was synthesized and structurally characterized.[32]

1.4 Tripodal Ligands

Tripodal ligands turned out to be useful ligands in bioinorganic chemistry to investigate model substances as described above. These ligands are tetradentate chelate ligands with the general structure of a central donor atom X and three arms each with a donor atom Y (Figure 1-10).[33] A large number of tripodal ligands is based on the parent amine tren (tris(2-aminoethyl)amine). The related tripodal ligand tmpa (tris(2-pyridylmethyl)amine), was first prepared in 1967 and has been extensively used in coordination and bioinorganic chemistry.[34] Figure 1-10 depicts the relationship between the ligands tren und tmpa.

general structure   tren   tmpa
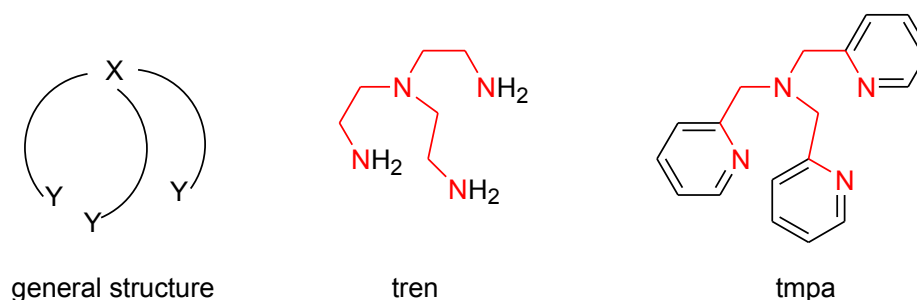
Figure 1-10: General structure of tripodal ligands and the ligands tren and related tmpa.

Systematic modifications of the ligands tmpa and tren were performed to obtain more information about the influence of the ligand on the reactivity of the complexes. As an example the pyridine N-donor atoms in tmpa were systematically substituted with aliphatic amine donor atoms, thus, leading from tmpa to Me$_2$uns-penp ((2-dimethyl-aminoethyl)bis(2-pyridylmethyl)amine) to Me$_4$apme (bis(2-dimethyl-aminoethyl)(2-pyridylmethyl)amine) and finally to Me$_6$tren (tris(2-dimethyl-aminoethyl)amine).[35] The ligand series is shown in Figure 1-11.
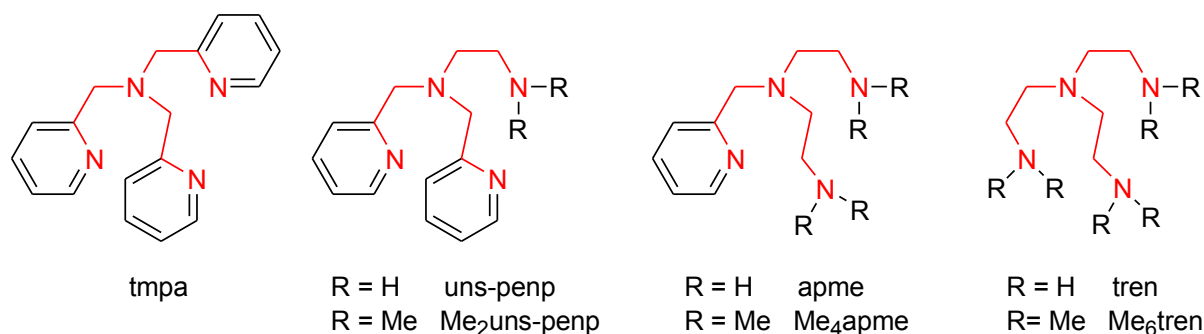
Figure 1-11: Variation of tripodal ligands bases on tren. The tren skeleton emphasized in red.

Chromium(II) complexes with tripodal ligands were previously reported in literature by Robertson *et al.*[36] They described different chromium(II) and chromium(III) complexes with the ligand tmpa, which are depicted in Figure 1-12. They characterized chromium(II) complexes with chloride and tetraphenylborate as anion. The ligand tmpa with CrCl$_2$ formed the monomeric [Cr(tmpa)Cl$_2$] complex. Subsequent substitution of the chloride ion with BPh$_4^-$ as anion yielded the dimeric complex [Cr(tmpa)Cl]$_2$(BPh$_4$)$_2$. This complex reacted with traces of water or air in the according solvent and a chromium "oxygen adduct complex" {[Cr(tmpa)Cl]$_2$(μ-O)}(BPh$_4$)$_2$ could be structurally characterized.[36]

[Cr(tmpa)Cl$_2$]   [Cr(tmpa)Cl]$_2$(BPh$_4$)$_2$ {[Cr(tmpa)Cl]$_2$(μ-O)}(BPh$_4$)$_2$
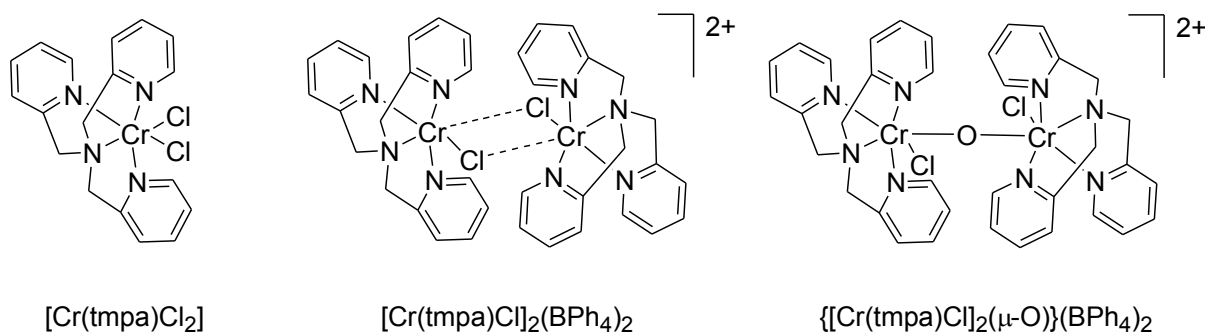
Figure 1-12: Structurally characterized chromium(II) complexes with the ligand tmpa by Robertson *et al.*[36]

Another variation of the tren/tmpa ligand system led to the ligand bztpen, a pentadentate ligand. Firstly, substituting the organic rest (R) of the ligand uns-penp (N,N-bis(2-pyridylmethyl)ethylenediamine) by a pyridyl arm led to the ligand Rtpen (Figure 1-13). The

8

ligand bztpen (R = bz, N-benzyl-N,N',N'-tris(2-methylpyridyl)-ethylenediamine, Figure 1-13) was used in this work.

R = H   uns-penp
R = Me   Me$_2$uns-penp
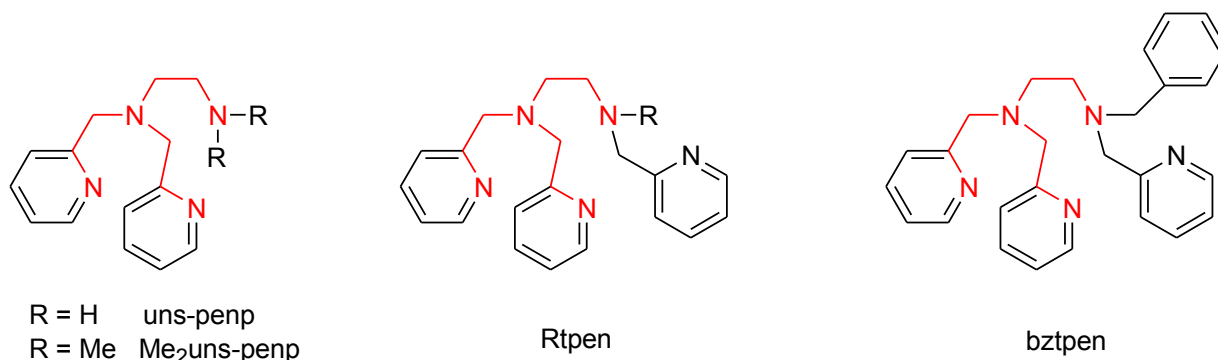
Rtpen

bztpen

Figure 1-13: Variation of the ligand uns-penp leading to the ligands Rtpen and bztpen.

Iron complexes using these types of ligands, especially the ligand bztpen, are described in literature.[13,37-40] The formation of iron bztpen hydroperoxido complexes was investigated in detail. The [Fe(bztpen)OOH]$^{2+}$ complex was obtained by reaction of the iron(II) complex with excess hydrogen peroxide in methanol.[37,40] Furthermore, iron oxido complexes with the ligand bztpen were reported.[38-39] A solution of an iron(II) precursor complex in acetonitrile reacted at room temperature with excess solid iodosobenzene to yield the complex [Fe(bztpen)(O)]$^{2+}$. These complexes could not be crystallographically characterized so far. The proposed reaction scheme is presented in Scheme 1-3.
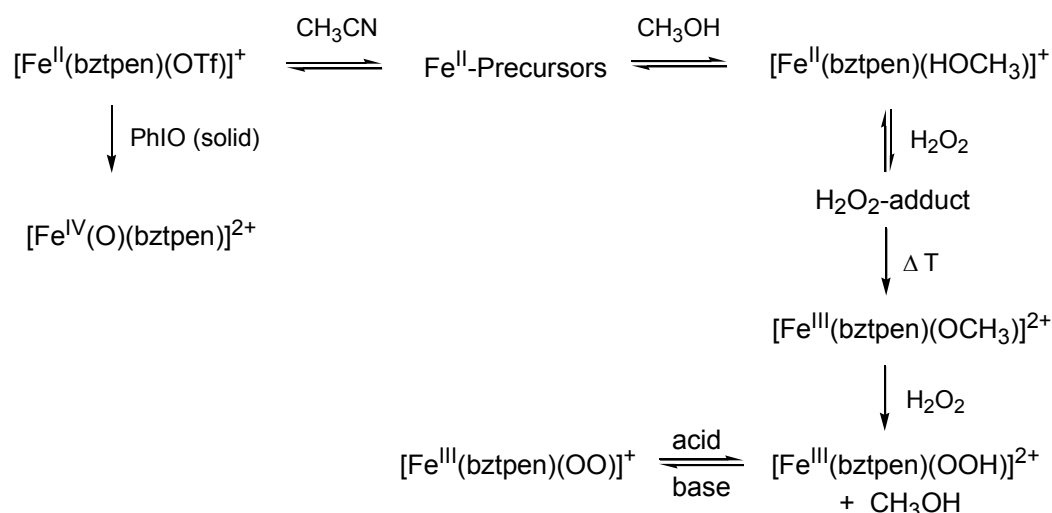
Scheme 1-3: Several "dioxygen adduct complexes" of iron bztpen complexes that could be spectroscopically characterized.[37]

The formation of superoxido complexes is somehow related to the oxidation of complexes by nitric oxide to form nitrosyl complexes. Compared to dioxygen, nitric oxide lacks an electron. Therefore, NO$^-$ and O$_2$ are isoelectronic and a comparison of the coordination of nitric oxide

and the coordination of dioxygen in metal complexes is interesting. Iron(III) nitrosyl complexes using bztpen as a ligand have been investigated previously.[41-42] In 2010, Nebe *et al.* structurally characterized an iron(III) nitrosyl complex with the ligand bztpen.[37] The molecular structure is shown in Figure 1-14.
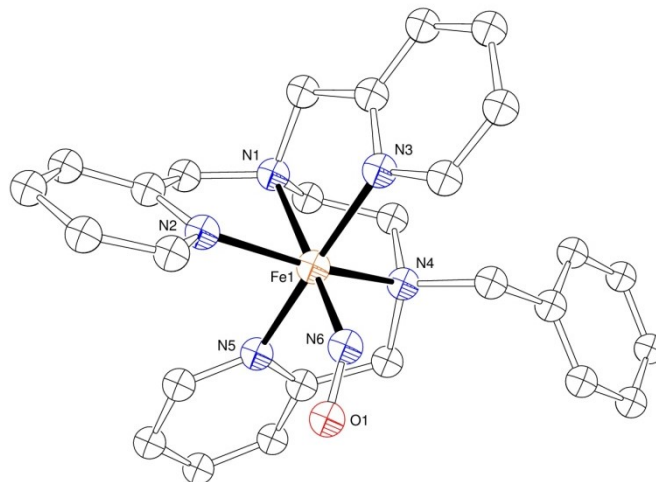
Figure 1-14: Molecular structure of the cation of the iron(III) nitrosyl complex [Fe(bztpen)NO](OTf)$_2$.[37]

1.5 Organometallic Complexes

The organometallic chemistry of chromium is well-known, especially because of the most famous species, the compound bis(benzene)chromium (Cr(η^6-C$_6$H$_6$)$_2$) (Figure 1-16). In the past a number of organochromium species were investigated.[43] This first transition metal sandwich complex with two neutral benzene molecules bound to a neutral, zerovalent metal atom was synthesized by Fischer and Hafner in 1955.[44] Based on the π-interaction between the neutral fragments, a stable metal–ligand bond formed (18-electron rule).[45-46] The molecular structure of the sandwich complex was obtained in 1956 by Weiss and Fischer.[47] These results were refined and confirmed and the symmetry was described by several scientists in the following years.[48-51] During the investigations in this thesis, the structure as well characterized. The obtained molecular structure is shown in Figure 1-15.

Different methods were used to synthesize bis(benzene)chromium and related complexes. It turned out that the method using aluminum chloride and aluminum powder in a Friedel-Crafts reaction with chromium(III) chloride and benzene was quite efficient. It first leads to the bis(benzene)chromium cation, which is reduced with dithionite to yield the final product. This method was further used for the syntheses of di-aromatic-metal complexes with the transition metals V, Mo, W, Re, Fe, Ru, Os, Co, Rh and Ir.[52]
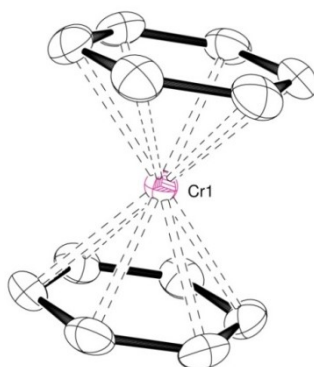
Figure 1-15: Molecular structure of bis(benzene)chromium.

Based on these compounds Elschenbroich *et al*. reported the first η^6-coordination with unsubstituted pyridine.[53] The different complexes are shown in Figure 1-16.
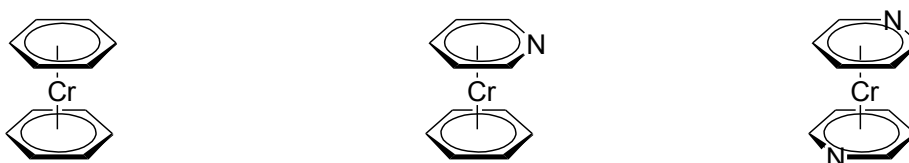
bis(η^6-benzene)chromium   (η^6-benzene)(η^6-pyridine)chromium   bis(η^6-pyridine)chromium

Figure 1-16: Structural formula of a selection of bis(arene)chromium complexes.

As expected, bis(benzene)chromium is quite sensitive towards oxidation and is thus rapidly oxidized by air or dioxygen.[44] Elschenbroich and co-workers observed that the oxidation of bis(benzene)chromium with dioxygen led to a yellow product that could not be characterized so far. They suggested that this complex could be similar to the proposed oxidation product of cobaltocene.[54-55] Unpublished calculations by Holthausen indicated the formation of a chromium peroxido complex.[56]

1.6 Projects

a) As described in the introduction, copper and iron complexes with tripodal ligands based on the ligand system tren have proved to be versatile model compounds for according metalloenzymes. Due to the instability of the intermediate complexes it was however assumed that the kinetically more inert chromium(III) complexes would allow isolation and characterization of analogous chromium "dioxygen adduct complexes". Based on previous work on chromium complexes with tmpa described in literature, chromium(II) and chromium(III) complexes with the tripodal ligands presented in Figure 1-11 should be synthesized and characterized.[36] In the following the oxidation potential of the [Cr(L)Cl]⁺/dioxygen system when oxidizing toluene should be tested (Figure 1-17). This

outcome should then be compared to a previous study that used the according copper complexes.
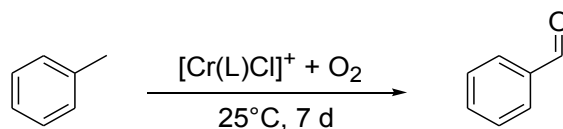
Figure 1-17: Oxidation of the substrate toluene with the synthesized chromium(II) complexes with dioxygen (L = tmpa, Me₂uns-penp, Me₄apme and Me₆tren).

b) In line with the reactivity of the iron complex with the ligand bztpen above described, the according chromium complex should be synthesized and its reactivity should be investigated as for example described in Figure 1-18. Since the spectroscopically detected iron "dioxygen adduct complexes" could not be isolated and fully characterized until now, it was hoped that the analogous, yet inert chromium(III) compounds might enable for isolation and characterization.
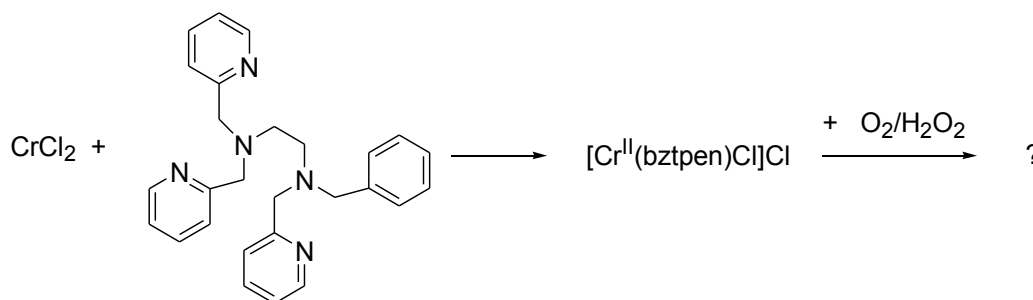
Figure 1-18: Synthesis of the chromium(II) complex with the ligand bztpen (here with chloride as anion) and the planned investigations of its reactivity.

c) As mentioned in Chapter 1, the formation of a chromium peroxido complex was proposed during the reaction of bis(benzene)chromium with dioxygen. However, up to now an experimental verification for this compound has been missing. Therefore, the reaction of bis(benzene)chromium with dioxygen should be studied in detail to gain further information on the formed yellow reaction product (Figure 1-19).
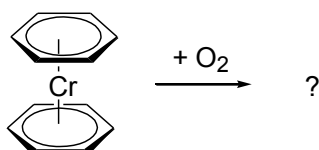
Figure 1-19: Investigation of the reactivity of bis(benzene)chromium with dioxygen under anhydrous conditions.

2 Investigation of Chromium Complexes with a Series of Tripodal Ligands

This work has been published previously in *Zeitschrift für Anorganische und Allgemeine Chemie.*

Sabrina Schäfer, Jonathan Becker, Alexander Beitat and Christian Würtele

2.1 Abstract

A series of chromium(II) complexes containing the tripodal ligands tmpa, Me$_2$uns-penp, Me$_4$apme and Me$_6$tren were prepared and investigated with regard to their reactivity towards dioxygen. It was possible to structurally characterize the complexes [Cr(Me$_2$uns-penp)Cl]$_2$(BPh$_4$)$_2$, [Cr(Me$_6$tren)Cl]Cl, [Cr(Me$_4$apme)Cl]BPh$_4$ and [Cr(Me$_4$apme)Cl$_3$]. The complexes show reactions with dioxygen, but it was not possible to characterize intermediates of these reactions. The oxidation behavior of the complexes towards organic substrates like toluene was investigated and oxidation of toluene to benzaldehyde was observed.

2.2 Introduction

Oxidation reactions play an important role in biochemistry, industrial processes, and organic syntheses.[1] Therefore, there is high interest in the direct oxidation of organic substrates using a metal catalyst and air as the oxidant.

The activation of dioxygen leads to different "dioxygen adduct" transition metal complexes such as, for example, superoxido, peroxido or oxido species. The formation of "dioxygen adduct complexes" can cause the transfer of oxygen to a substrate. In that regard Würtele *et al.* as well as Karlin and co-workers recently demonstrated that a copper peroxido complex could be used to oxidize toluene to benzaldehyde and benzyl alcohol.[20,57] The copper peroxido complexes used in these investigations were based on the tripodal ligands shown in Figure 2-1. However, oxidations in organic syntheses are still often performed using chromium(VI) compounds such as K$_2$Cr$_2$O$_7$. These compounds are problematic with regard to selective oxidation reactions and their toxicity.[58] With this background it seemed interesting to investigate the possibility to perform selective oxidation reactions with low valent chromium complexes and dioxygen using the tripodal ligands shown in Figure 2-1.

Especially tris(2-pyridylmethyl)amine (tmpa, Figure 2-1) has turned out to be a versatile ligand in bioinorganic chemistry to model the reactivity of different metal enzymes based on iron, copper, manganese or zinc in the active centre as well as in other applications.[12,33,59-62] Most importantly, tmpa was used in copper chemistry where Karlin and co-workers succeeded in structurally characterizing a dinuclear copper peroxido complex for the first time. They were able to model the reversible uptake of dioxygen of copper enzymes.[17]
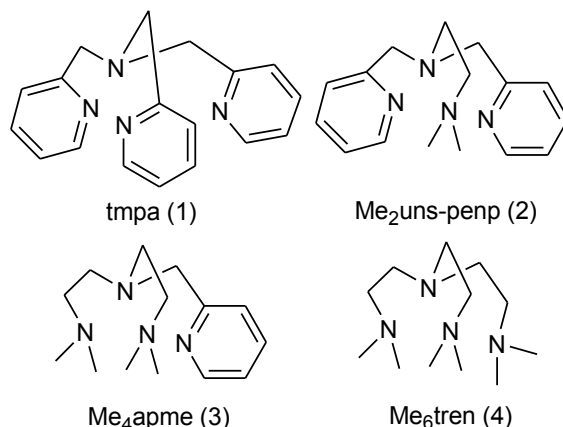
Figure 2-1: Tripodal ligands investigated in this work.

Systematic variation of the ligand tmpa was performed in the past in an effort to gain better understanding of the reactivity of copper(I) complexes towards dioxygen and the potential of the formed intermediates to oxidize organic substrates.[2,63-64] In the ligands in Figure 2-1 the pyridine N-donor atoms of tmpa were systematically substituted with aliphatic amine donor atoms leading from tmpa (**1**) to (2-dimethyl-aminoethyl)bis(2-pyridylmethyl)amine (Me$_2$uns-penp (**2**)), bis(2-dimethyl-aminoethyl)(2-pyridylmethyl)amine (Me$_4$apme (**3**)) and tris(2-dimethylaminoethyl)amine (Me$_6$tren (**4**)). Copper(I) complexes with all of these four ligands react with dioxygen to form a mononuclear end-on superoxido copper complex that further reacts to a dinuclear copper peroxido complex according to the mechanism in Figure 2-2.[65-66]
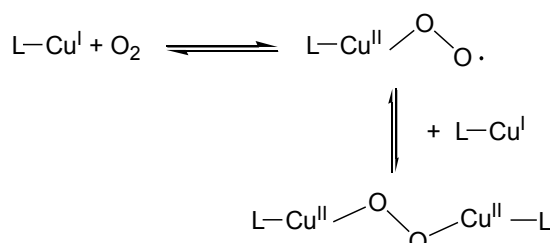
Figure 2-2: Mechanism for the reaction of copper(I) complexes (L = tripodal ligand) with dioxygen (Charges are omitted for clarity).

The peroxido complex $[(Me_6tren)CuO_2(Me_6tren)]^{2+}$ was structurally characterized.[20] As described above it could be demonstrated that these complexes can be used to catalytically oxidize toluene to benzaldehyde.[20] However, one of the problems to investigate these compounds in solution is the necessity to perform all these studies at low temperatures. Therefore, low temperature stopped-flow measurements were performed. Unfortunately, even at –80 °C detection, many times the reaction intermediates could not be spectroscopically identified fast enough.[63,65-66]

Due to the fact that stable chromium peroxido complexes are well-known, e. g. $[Cr(dien)(O_2)_2] \cdot H_2O$ (dien = diethylenetriamine),[28] we assumed that we might overcome some of these problems using chromium complexes with the tripodal ligands shown in Figure 2-1. Further support for this assumption came from Nam and co-workers who recently succeeded to structurally characterize a superoxido chromium(III) complex using TMC (= 1,4,8,11-tetramethyl-1,4,8,11-tetraazacyclotetradecane) as a ligand.[29] Furthermore, they obtained the according chromium(IV) or chromium(V) oxido complexes.[30-31] Using the smaller macrocycle cyclen as a ligand a side-on peroxido chromium(IV) complex was prepared and structurally characterized by the same group.[32] Reactivity studies demonstrated the interesting potential of these complexes.

2.3 Results and Discussion

Chromium(II) complexes with the ligand tmpa were previously reported by Robertson *et al.*[36] They structurally characterized complexes $[Cr(tmpa)Cl_2]$ (**1a**) and $[Cr(tmpa)Cl]_2(BPh_4)_2$ (**1b**). We were able to reproduce their syntheses of both compounds. Furthermore, they described that from the reaction of **1b** in acetonitrile (with traces of water or air in the solvent) the formation of a μ-oxido chromium(III) complex, $\{[Cr(tmpa)Cl]_2(\mu\text{-}O)\}(BPh_4)_2$, was observed as an impurity. This compound was structurally characterized as well, however, no spectroscopic data were reported. We thus reacted **1b** with dioxygen in acetonitrile to enforce this reaction and observed the spectral changes in the UV/Vis spectrum shown in Figure 2-3.

The spectrum of **1b** shows two absorption maxima at 306 nm and at 376 nm as described in literature.[36] After reaction with dioxygen the spectrum changed and new absorption bands at 349 nm with a shoulder at 363 nm as well as at 393, 420 and 446 nm were observed. The infrared spectrum showed a Cr–O–Cr stretching vibration at 844 cm^{-1}. The spectroscopic data compare well with other μ-oxido chromium complexes described previously.[67-69]

Avoiding chloride as an additional ligand we performed the reaction of $Cr(OTf)_2 \cdot 4\ H_2O$ with tmpa in acetonitrile. From this reaction we obtained crystals suitable for crystallographic analysis that showed that a bis(μ-hydroxido) chromium(III) complex was obtained. The molecular structure of the cation of $[Cr(tmpa)OH]_2(OTf)_4$ (**1c**) is reported in Chapter 3. The

same reaction has been previously observed by Gafford *et al.* when [Cr(tmpa)](ClO$_4$)$_2$ reacted with dioxygen in ethanol.[67] This bis(μ-hydroxido) chromium(III) dimer has also been reported by Hodgson *et al.*[70] and Gafford *et al.*[71] with perchlorate or bromide as anions. All these bis(μ-hydroxido) complexes showed a similar UV/Vis spectrum with absorption maxima at 386 nm and 540 nm (the spectrum can be found in Chapter 3).
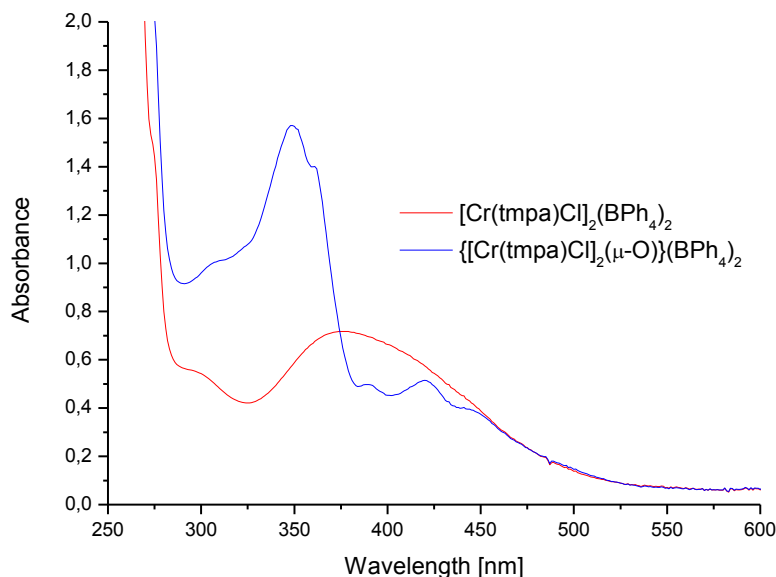
Figure 2-3: UV/Vis spectrum of **1b** (red line) and product complex (blue line) after passing dioxygen through the solution (CH$_3$CN, 25.0 °C, complex concentration = 0.8 mmol·L^{-1}).

Using the synthetic protocol of Robertson *et al.* for the tmpa complexes we prepared the according complexes with the ligands Me$_2$uns-penp, Me$_4$apme and Me$_6$tren in a similar way without any problems. Crystals suitable for structural analysis could be obtained at approx. –40 °C for the complexes described below. The crystallographic data are summarized in Tables 2-1, 2-3, 2-5 and 2-7.

The crystallographic data of [Cr(Me$_2$uns-penp)Cl$_2$] (**2a**) are reported in Chapter 3. Its molecular structure is very similar to **1a**. In both complexes the two chloride anions are coordinated to the chromium ion. The molecular structure of the cation of [Cr(Me$_2$uns-penp)Cl]$_2$(BPh$_4$)$_2$ (**2b**) is presented in Figure 2-4. Selected bond lengths and angles are summarized in Table 2-2. **2b** crystallized as a dimer. One unit of this complex has a distorted square pyramidal coordination (τ = 0.31).[72] Two of these units are connected through two chloride bridges. The bond length Cr–Cl(1)* is longer than the bond length between chromium and the coordinated chloride. Cr(1)–Cl(1)* = 3.278 Å *vs.* Cr(1)–Cl(1) = 2.3358(9) Å. This observation is in accordance to the observations for the tmpa complex as described previously by Robertson *et al.*[36]
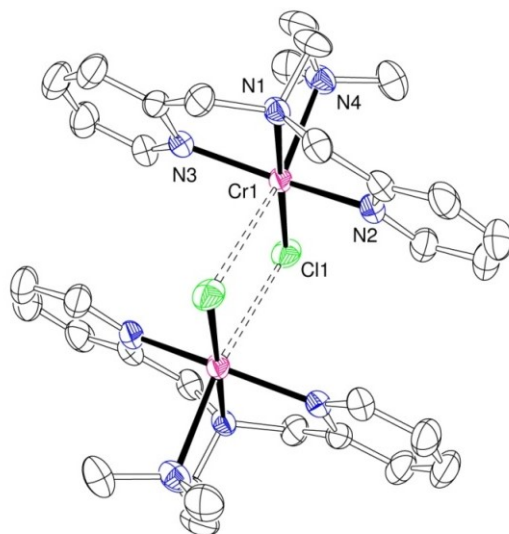
Figure 2-4: Molecular dimer structure of the cation of **2b** shown as an ORTEP plot with thermal ellipsoids set at 50 % probability.

Table 2-1: Crystallographic data and structure refinement of **2b**.

	2b
Formula	$C_{40}H_{42}BClCrN_4$
Formula weight	677.04 g·mol^{-1}
Temperature	193(2) K
Wavelength	0.71073 Å
Crystal system	monoclinic
Space group	P2$_1$/n
Unit cell dimensions	a = 14.9600(3) Å α = 90° b = 16.2770(3) Å β = 117.35(3)° c = 15.9060(3) Å γ = 90°
Cell volume	3440.2(12) Å^3
Z/Calculated density	4, 1.307 Mg/m^3
Absorption coefficient	0.445 mm^{-1}
F(000)	1424
θ range	2.83 to 28.12°
Limiting indices	−19<=h<=19, −20<=k<=20, −20<=l<=21
Reflections collected / unique	30871 / 8273 [R(int) = 0.0924]
Completeness to θ	98.4 %
Absorption correction	none
Refinement method	Full-matrix least-squares on F^2
Data / restraints / parameters	8273 / 0 / 426
Goodness-of-fit on F^2	0.839

Final R indices [I>2σ(I)]	$R_1 = 0.0471$, $wR_2 = 0.1027$
R indices (all data)	$R_1 = 0.1002$, $wR_2 = 0.1153$
Largest diff. peak and hole	0.515 and –0.385 e.Å^3

Table 2-2:   Selected bond lengths (Å) and bond angles (°) of **2b**.

	2b		**2b**
Cl(1)–Cr(1)	2.3358(9)	N(2)–Cr(1)–N(3)	158.71(9)
Cl(1)*–Cr(1)	3.278	N(2)–Cr(1)–N(1)	79.83(9)
Cr(1)–N(2)	2.076(2)	N(3)–Cr(1)–N(1)	81.41(9)
Cr(1)–N(3)	2.090(2)	N(2)–Cr(1)–N(4)	97.94(9)
Cr(1)–N(1)	2.110(2)	N(3)–Cr(1)–N(4)	88.86(9)
Cr(1)–N(4)	2.402(2)	N(1)–Cr(1)–N(4)	80.71(8)
		N(2)–Cr(1)–Cl(1)	98.00(7)
		N(3)–Cr(1)–Cl(1)	100.46(7)
		N(1)–Cr(1)–Cl(1)	177.42(7)
		N(4)–Cr(1)–Cl(1)	101.05(6)
		Cl(1)–Cr(1)–Cl(1)*	95.18

Crystals of **3a** suitable for crystal structure analysis could be obtained, but refinement was not possible. However, complex [Cr(Me$_4$apme)Cl]BPh$_4$ (**3b**) could be crystallized. Figure 2-5 shows the molecular structure of the cation of **3b** (selected bond lengths and angles are summarized in Table 2-4). In contrast to **1b** and **2b** it crystallized as a monomer. The arrangement is best described as an intermediate between a square pyramidal and trigonal bipyramidal coordination (τ = 0.57).[72]
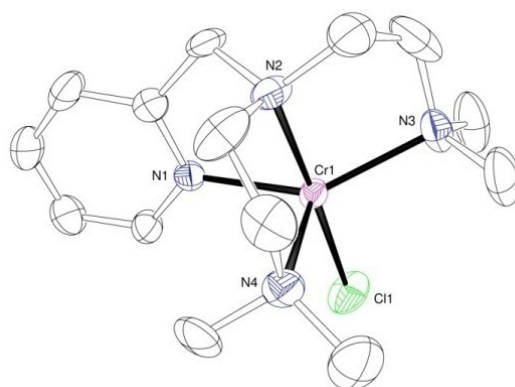
Figure 2-5:   Molecular structure of the cation of **3b** shown as an ORTEP plot with thermal ellipsoids set at 50 % probability.

Table 2-3: Crystallographic data and structure refinement of **3b**.

	3b
Formula	$C_{38}H_{46}BClCrN_4$
Formula weight	657.05 g·mol^{-1}
Temperature	193(2) K
Wavelength	0.71073 Å
Crystal system	orthorhombic
Space group	Pbca
Unit cell dimensions	a = 16.2700(3) Å α = 90° b = 16.6890(3) Å β = 90° c = 25.4950(5) Å γ = 90°
Cell volume	6923(2) Å^3
Z/Calculated density	8, 1.261 Mg/m^3
Absorption coefficient	0.440 mm^{-1}
F(000)	2784
θ range	1.92 to 24.22°
Limiting indices	−18<=h<=18, −19<=k<=19, −29<=l<=29
Reflections collected / unique	40311 / 5555 [R(int) = 0.1426]
Completeness to θ	99.7 %
Absorption correction	none
Refinement method	Full-matrix least-squares on F^2
Data / restraints / parameters	5555 / 0 / 410
Goodness-of-fit on F^2	0.827
Final R indices [I>2σ(I)]	$R_1 = 0.0510$, $wR_2 = 0.1143$
R indices (all data)	$R_1 = 0.1140$, $wR_2 = 0.1299$
Largest diff. peak and hole	0.596 and −0.269 e.Å^3

Table 2-4: Selected bond lengths (Å) and bond angles (°) of **3b**.

	3b		**3b**
Cl(1)–Cr(1)	2.3180(13)	N(2)–Cr(1)–N(3)	83.83(17)
Cr(1)–N(2)	2.107(4)	N(2)–Cr(1)–N(1)	79.70(14)
Cr(1)–N(3)	2.142(4)	N(3)–Cr(1)–N(1)	143.15(15)
Cr(1)–N(1)	2.110(4)	N(2)–Cr(1)–N(4)	80.28(15)
Cr(1)–N(4)	2.337(4)	N(3)–Cr(1)–N(4)	111.30(15)
		N(1)–Cr(1)–N(4)	98.13(15)
		N(2)–Cr(1)–Cl(1)	177.52(12)
		N(3)–Cr(1)–Cl(1)	98.52(12)
		N(1)–Cr(1)–Cl(1)	97.90(11)
		N(4)–Cr(1)–Cl(1)	99.54(11)

Furthermore, a chromium(III) complex with the ligand Me$_4$apme, [Cr(Me$_4$apme)Cl$_3$] (**3d**), could be crystallized as a by-product of the synthesis of complex **3a**. Upon crystallization we obtained a mixture of **3a** and **3d** that allowed picking of crystals of both compounds suitable for crystal structure analysis. Obviously, some part of the chromium(II) complex has been oxidized during the synthesis leading to this mixture. The molecular structure of [Cr(Me$_4$apme)Cl$_3$] (**3d**) is shown in Figure 2-6 (selected bond lengths and angles can be found in Table 2-6). This complex is sixfold coordinated with three chloride ligands and three N-donor atoms of the ligand Me$_4$apme. One aliphatic arm of the ligand is not coordinated, because it has been replaced by a chloride ion. This behavior is well-known from related copper chemistry.[73]
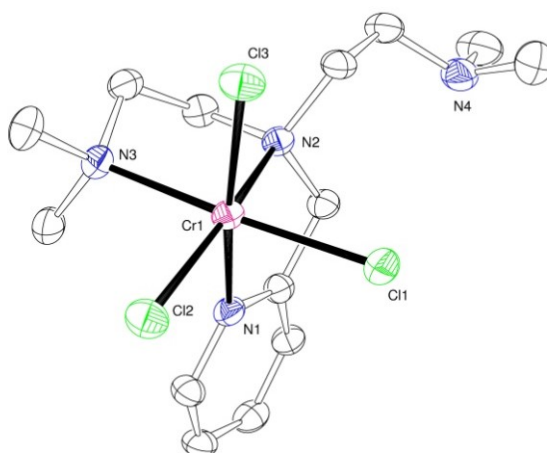
Figure 2-6: Molecular structure of **3d** shown as an ORTEP plot with thermal ellipsoids set at 50 % probability.

Table 2-5: Crystallographic data and structure refinement of **3d**.

	3d
Formula	C$_{14}$H$_{26}$Cl$_3$CrN$_4$
Formula weight	408.74 g·mol^{-1}
Temperature	190(2) K
Wavelength	0.71073 Å
Crystal system	triclinic
Space group	P–1
Unit cell dimensions	a = 7.1750(14) Å α = 97.88(3)° b = 8.7870(18) Å β = 93.92(3)° c = 16.2250(3) Å γ = 112.27(3)°
Cell volume	929.6(3) Å^3
Z/Calculated density	2, 1.460 Mg/m^3
Absorption coefficient	1.048 mm^{-1}
F(000)	426
θ range	2.54 to 27.46°

Limiting indices	$-9 <= h <= 9$, $-11 <= k <= 11$, $-21 <= l <= 20$
Reflections collected / unique	15992 / 4250 [R(int) = 0.0973]
Completeness to θ	99.7 %
Absorption correction	none
Refinement method	Full-matrix least-squares on F^2
Data / restraints / parameters	4250 / 0 / 303
Goodness-of-fit on F^2	1.029
Final R indices [I>2σ(I)]	$R_1 = 0.0523$, $wR_2 = 0.1297$
R indices (all data)	$R_1 = 0.0777$, $wR_2 = 0.1425$
Largest diff. peak and hole	1.015 and -0.809 e.Å^3

Table 2-6:   Selected bond lengths (Å) and bond angles (°) of **3d**.

	3d		**3d**
Cl(1)–Cr(1)	2.3406(11)	N(2)–Cr(1)–N(3)	83.88(10)
Cl(2)–Cr(1)	2.3150(13)	N(2)–Cr(1)–N(1)	78.56(10)
Cl(3)–Cr(1)	2.3161(11)	N(3)–Cr(1)–N(1)	92.27(11)
Cr(1)–N(2)	2.153(2)	N(2)–Cr(1)–Cl(1)	91.05(8)
Cr(1)–N(3)	2.168(3)	N(3)–Cr(1)–Cl(1)	174.92(7)
Cr(1)–N(1)	2.096(3)	N(1)–Cr(1)–Cl(1)	87.10(8)

Furthermore, complexes with Me$_6$tren as ligand were structurally characterized. Figure 2-7 shows the molecular structure of the cation of [Cr(Me$_6$tren)Cl]Cl (**4a**). In contrast to the complexes **1a** and **2a** complex **4a** is coordinated only by one chloride ligand. The complex is fivefold coordinated and has a trigonal bipyramidal coordination (τ = 1).[72] Therefore complex **4a** is quite similar to [Cr(Me$_6$tren)Cl]BPh$_4$ (**4b**). The molecular structure and crystallographic data of **4b** are reported in Chapter 3. **4b** again crystallizes as a monomeric unit that has a perfect trigonal bipyramidal coordination (τ = 1).[72]
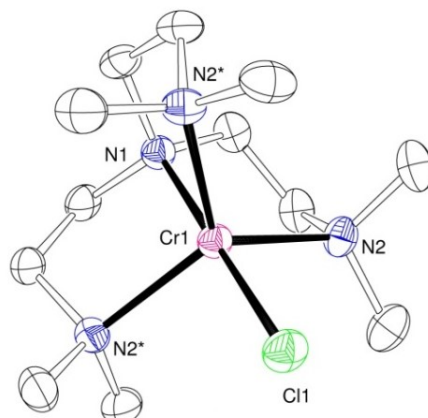
Figure 2-7:   Molecular structure of the cation of **4a** shown as an ORTEP plot with thermal ellipsoids set at 50 % probability.

Table 2-7: Crystallographic data and structure refinement of **4a**.

	4a
Formula	$C_{12}H_{30}Cl_2CrN_4$
Formula weight	353.30 g·mol^{-1}
Temperature	193(2) K
Wavelength	0.71073 Å
Crystal system	cubic
Space group	$P2_13$
Unit cell dimensions	a = 11.9655(14) Å α = 90° b = 11.9655(14) Å β = 90° c = 11.9655(14) Å γ = 90°
Cell volume	1713.1(3) Å^3
Z/Calculated density	4, 1.370 Mg/m^3
Absorption coefficient	0.974 mm^{-1}
F(000)	752
θ range	3.81 to 28.07°
Limiting indices	–14<=h<=15, –15<=k<=15, –14<=l<=15
Reflections collected / unique	15301 / 1404 [R(int) = 0.1200]
Completeness to θ	99.6 %
Absorption correction	none
Refinement method	Full-matrix least-squares on F^2
Data / restraints / parameters	1404 / 0 / 76
Goodness-of-fit on F^2	0.977
Final R indices [I>2σ(I)]	R_1 = 0.0427, wR_2 = 0.0896
R indices (all data)	R_1 = 0.0647, wR_2 = 0.0974
Largest diff. peak and hole	0.407 and –0.411 e.Å^3

Table 2-8: Selected bond lengths (Å) and bond angles (°) of **4a**.

	4a		4a
Cl(1)–Cr(1)	2.3346(18)	N(2)–Cr(1)–N(3)	118.46(3)
Cr(1)–N(2)	2.219(3)	N(2)–Cr(1)–N(1)	82.82(8)
Cr(1)–N(3)	2.219(3)	N(3)–Cr(1)–N(1)	82.82(8)
Cr(1)–N(1)	2.114(5)	N(2)–Cr(1)–N(4)	118.46(3)
Cr(1)–N(4)	2.219(3)	N(3)–Cr(1)–N(4)	118.46(3)
		N(1)–Cr(1)–N(4)	82.82(8)
		N(2)–Cr(1)–Cl(1)	97.18(8)
		N(3)–Cr(1)–Cl(1)	97.18(7)
		N(1)–Cr(1)–Cl(1)	180.00(7)
		N(4)–Cr(1)–Cl(1)	97.18(8)

2.3.1 Oxidation of Toluene

All synthesized chromium complexes were tested for their potential as catalysts for the oxidation of toluene in comparison with the analogous reaction of the according copper complexes reported previously.[20] For this investigation the complexes were dissolved in a minimum of a mixture of acetone and toluene and then dioxygen was passed through the solution. The resulting product solutions were analyzed by GC-MS spectrometry. **1a**, **2a**, **3a** and **4a** showed no oxidation potential towards toluene. GC-MS measurements showed no oxidation products of toluene. In contrast, complexes of the type [Cr(L)Cl]BPh$_4$ demonstrated oxidation potential towards toluene. GC-MS measurements showed that similar to the copper complexes benzaldehyde was formed with a maximum yield for complex **3b** of 25 %. Thus, the chromium complexes unfortunately were not better than analogous copper compounds: maximum yield of benzaldehyde with copper complexes was approx. 40 % with L = tmpa.[20,57] The yields of all chromium complexes are summarized in Figure 2-8. Due to the quite low yields no further detailed studies were performed on these oxidation reactions.
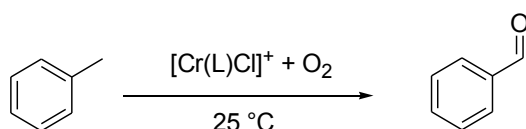
Complex	Yield (in %)
1b (L = tmpa)	8
2b (L = Me$_2$uns-penp)	5
3b (L = Me$_4$ampe)	25
4b (L = Me$_6$tren)	0

Figure 2-8:   Oxidation of toluene and yield of benzaldehyde in %.

The low yields of benzaldehyde are a consequence of several side reactions that cause formation of e. g. phenylbenzene or 4-phenyl-3-buten-2-one (reaction of benzaldehyde with acetone) in combination with simple oxidation reactions of the chromium(II) complex to a chromium(III) compound.

Whereas it is principally not correct to assume that solid-state structures are retained in solution, one could at least speculate if this is the case for the chromium complexes discussed above. This would give a possible explanation for the different yields of benzaldehyde obtained by oxidation with the four complexes discussed in this study. The nearly perfect trigonal bipyramidal coordination of **4b** seems to suppress reactivity towards a substrate whereas **3b** with an arrangement between square pyramidal and trigonal

bipyramidal supports the oxidation reaction of toluene to benzaldehyde. With complexes **1b** and **2b** lower yields were most likely observed due to equilibria of dimers and monomers. Two different mechanistic pathways were suggested by Lucas *et al.* for the oxidation of toluene by copper complexes.[57] However, these proposed mechanisms so far are not based on solid kinetic studies and might be different for the chromium complexes described in here anyway.

2.3.2 Low Temperature Stopped-Flow Spectroscopy

In regard to the finding that some toluene oxidation was observed with **3b**, its reaction with dioxygen was furthermore investigated by low temperature stopped-flow measurements. When **3b** (the spectrum is presented as black line in Figure 2-9 b) reacted with dioxygen, a new complex rapidly formed (red line in Figure 2-9 b).
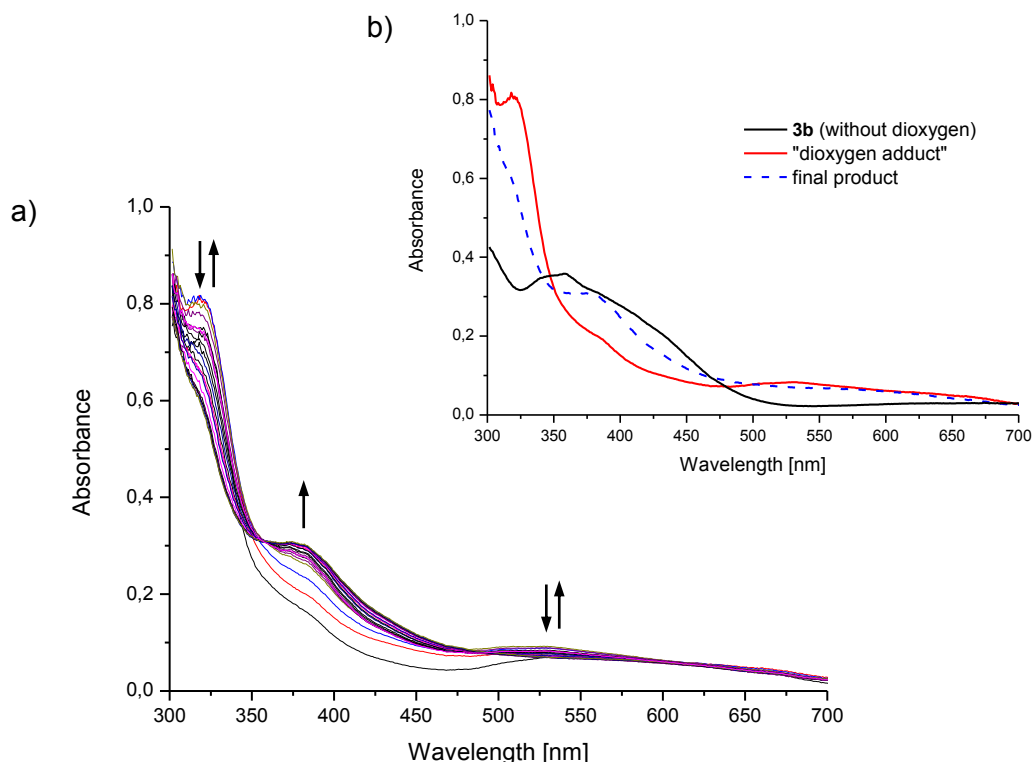
Figure 2-9:   a) Time resolved spectra for the reaction of a 0.5 mmol·L^{-1} solution of **3b** in acetonitrile with dioxygen [0.01 mol·L^{-1}] at –40.0 °C (overall reaction time = 450 s, Δ = 1.5 ms). b) UV/Vis spectrum of **3b** (0.5 mmol·L^{-1} in acetonitrile) and selected single spectra from the stopped-flow experiment.

The spectral features of this new compound (320, 381, 528 and 631 nm) are similar to the reported data for the end-on superoxido chromium(III) complex by Nam and co-workers.[29] Unfortunately it was not possible to further characterize this intermediate because in a slower consecutive reaction a different complex formed (dashed blue line in Figure 2-9 b, absorbance maxima at 319 (shoulder), 378 and 574 nm). So far, the final product of this

reaction is unknown. Efforts to isolate and characterize this product complex failed. Furthermore, a detailed kinetic analysis was not possible due to a more complex reaction behavior (parallel reactions – no isosbestic points were observed). In regard to these problems together with low yields on the oxidation of toluene this reaction further was not investigated

2.4 Conclusions

It was demonstrated that chromium(II) complexes with tripodal ligands in principle can be used to oxidize organic substrates with dioxygen as an oxidant. Furthermore, it was shown that this reactivity strongly depends on the tripodal ligand used. Unfortunately, our hope that using chromium complexes as an alternative to copper or iron complexes would simplify our understanding of these reaction mechanisms turned out to be too naive. Similar to related copper chemistry, the reaction behavior of chromium complexes with dioxygen is quite complicated to analyze. Furthermore, we were not able to structurally characterize some of the postulated reactive intermediate chromium "dioxygen adduct" complexes so far. However, the reactivity of the chromium(II) complexes in principle is promising. Optimizations of these reactions using different "better" ligands might lead to an alternative way for oxidation reactions in organic chemistry.

2.5 Experimental Section

2.5.1 Materials

Reagents and solvents used were commercially available. Chromium(II) triflate tetrahydrate was prepared according to literature.[74] Furthermore, all tripodal ligands were synthesized according to published procedures.[35]

2.5.2 Equipment

UV/Vis absorption spectra were recorded using an Agilent 8453-spectrometer. The measurements were performed using quartz cuvettes. GC-MS data were obtained using a Quadrupol-MS HP MSD 5971 (EI) with a J&W quartz glass GC column (30 m x 0.25 mm, 0.25 µmDB-5 MS). Stopped-flow experiments at ambient pressures were performed using a commercially available Hi Tech Limited SF-61SX2 (Salisbury, UK) instrument. IR measurements were performed using a JASCO FT/IR-4100 spectrometer. Elemental analyes were obtained using a vario EL III element analyzer from Elementar.

2.5.3 Synthesis of the Complexes with the Ligands L = tmpa, Me₂uns-penp, Me₄apme and Me₆tren

The synthesis of these complexes is based on the preparation of the complex [Cr(tmpa)Cl₂] (**1a**) and [Cr(tmpa)Cl]₂(BPh₄)₂ (**1b**) described in literature.[36] Complex [Cr(tmpa)OH]₂(OTf)₄ (**1c**) was also synthesized according to literature.[67]

2.5.3.1 [Cr(Me₂uns-penp)Cl₂] (2a)

Anhydrous CrCl₂ (0.05 g, 0.37 mmol) and Me₂uns-penp (2-dimethyl-aminoethyl)bis(2-pyridylmethyl)-amine) (0.10 g, 0.37 mmol) were stirred in tetrahydrofuran under inert atmosphere. The solution was stirred and a brown precipitate occurred. The solid was collected, dissolved in a minimum of acetonitrile and filtered. Brown crystals could be obtained by diethyl ether diffusion at –40 °C. Yield: 0.08 g (55 %). Anal.: $C_{16}H_{22}N_4Cl_2Cr$ (393.27); C 48.46 (calc. 48.86); H 5.65 (5.64); N 14.73 (14.25) %. UV/Vis (CH₃CN): λ_{max} (lg ε): 257 nm (3.7), 346 nm (3.1), IR (KBr): 3020, 2985, 2927, 1661, 1604, 1472, 1437, 1288, 1156, 1028, 818, 765, 650.

2.5.3.2 [Cr(Me₂uns-penp)Cl]₂(BPh₄)₂ (2b)

Anhydrous CrCl₂ (0.05 g, 0.37 mmol) and NaBPh₄ (0.13 g, 0.37 mmol) were stirred with Me₂uns-penp (0.10 g, 0.37 mmol) in tetrahydrofuran under inert atmosphere. The resulting precipitate was collected, dried and dissolved in acetonitrile at 70 °C. The solution was filtered hot and brown crystals could be obtained by diethyl ether diffusion at –40 °C. Yield: 0.06 g (22 %). Anal.: $C_{80}H_{84}N_8B_2Cl_2Cr_2$ (1354.10); C 69.90 (calc. 70.96); H 6.31 (6.25); N 8.97 (8.28) %. UV/Vis (CH₃CN): λ_{max} (lg ε): 350 nm (3.1), 426 nm (2.8). IR (KBr): 3052, 2994, 2983, 2833, 2370, 2309, 1945, 1881, 1816, 1677, 1607, 1579, 1478, 1439, 1424, 1288, 1266, 1160, 1097, 1054, 1030, 985, 845, 732, 706, 612.

2.5.3.3 [Cr(Me₄apme)Cl]Cl (3a)/[Cr(Me₄apme)Cl₃] (3d)

Anhydrous CrCl₂ (0.05 g, 0.40 mmol) and Me₄apme (bis(2-dimethyl-aminoethyl)(2-pyridylmethyl)amine) (0.10 g, 0.40 mmol) were stirred in tetrahydrofuran under inert atmosphere. The solution was stirred and a green precipitate occurred. The solid was collected, dissolved in a minimum of acetonitrile and filtered. During crystallization two species were obtained. Green crystals of **3d** were suitable for structural analysis (Figure 2-6). Brown crystals of **3a** were measurable, but refinement was not possible. Anal.: $C_{14}H_{26}N_4Cl_3Cr$ (408.74): C 41.00 (calc. 41.14); H 6.24 (6.41); N 13.50 (13.71) %. UV/Vis (CH₃CN): λ_{max} (lg ε): 366 nm (2.8), IR (KBr): (3062, 3024, 2966), 2919, 1606, (1566), 1474, (1438), 1293, 1156, 1099, 1027, 934, 809, 773.

2.5.3.4 [Cr(Me$_4$apme)Cl]BPh$_4$ (3b)

Anhydrous CrCl$_2$ (0.05 g, 0.40 mmol) and NaBPh$_4$ (0.14 g, 0.40 mmol) were stirred with Me$_4$apme (0.10 g, 0.40 mmol) in tetrahydrofuran under inert atmosphere. The resulting precipitate was collected, dried and dissolved in a minimum of acetonitrile at 70 °C. The solution was filtered hot and green crystals could be obtained by diethyl ether diffusion at –40 °C. Yield: 0.12 g (45 %). Anal.: C$_{38}$H$_{46}$N$_4$BClCr (657.05); C 69.00 (calc. 69.46); H 7.24 (7.06); N 8.59 (8.53) %. UV/Vis (CH$_3$CN): λ_{max} (lg ε): 365 nm (2.8). IR (KBr): 3052, 2998, 2982, 2965, 2366, 2309, 1941, 1892, 1817, 1606, 1577, 1475, 1437, 1427, 1300, 1265, 1155, 1090, 1052, 1022, 985, 930, 806, 770, 752, 734, 704, 609.

2.5.3.5 [Cr(Me$_6$tren)Cl]Cl (4a)

Anhydrous CrCl$_2$ (0.05 g, 0.43 mmol) and Me$_6$tren (tris(2-dimethylaminoethyl)amine) (0.10 g, 0.43 mmol) were stirred in tetrahydrofuran under inert atmosphere. The resulting precipitate was collected, dried and dissolved in a minimum of acetonitrile. Light blue crystals were obtained by diethyl ether diffusion at –40 °C. Yield: 0.11 g (72 %). Anal.: C$_{12}$H$_{30}$N$_4$Cl$_2$Cr (353.30); C 40.21 (calc. 40.80); H 8.56 (8.56); N 15.39 (15.86) %. UV/Vis (CH$_3$CN): λ_{max} (lg ε): 900 nm (2.3), IR (KBr): 2970, 2895, 2427, 1637, 1560, 1469, 1289, 1174, 1100, 1018, 966, 933, 802, 772, 594, 492.

2.5.3.6 [Cr(Me$_6$tren)Cl]BPh$_4$ (4b)

Anhydrous CrCl$_2$ (0.05 g, 0.43 mmol) and NaBPh$_4$ (0.15 g, 0.43 mmol) were stirred with Me$_6$tren (0.10 g, 0.43 mmol) in tetrahydrofuran under inert atmosphere. The resulting precipitate was collected, dried and dissolved in acetonitrile at 70 °C. The solution was filtered hot and green crystals could be obtained by diethyl ether diffusion at –40 °C. Yield: 0.09 g (33 %). Anal.: C$_{36}$H$_{50}$N$_4$BClCr (637.07); C 66.22 (calc. 67.87); H 7.68 (7.91); N 8.68 (8.79) %. UV/Vis (CH$_3$CN): λ_{max} (lg ε): 900 nm (2.3), IR (KBr): 3054, 2999, 2981, 2892, 2839, 1958, 1891, 1822, 1579, 1474, 1466, 1428, 1348, 1286, 1266, 1244, 1173, 1133, 1098, 1038, 1017, 932, 897, 845, 802, 768, 734, 705, 611.

2.5.4 Oxidation of Toluene

Complexes (10 mg) were dissolved in acetone (0.7 mL) und the same quantity of toluene was added. Accordingly dioxygen was passed through the solutions (ca. 1 min). To determine the oxidation products and the yields after a reaction time of 7 days GC-MS measurements were conducted. Analysis of the toluene oxidation products were confirmed by comparison with the database (Spectral Database for Organic Compounds SDBS), specifically benzaldehyde. The yields of the product signals were calculated on the basis of comparisons to a calibration curve according to the internal standard xylene. Also control

reactions with chromium(II) chloride and potassium dichromate were carried out and showed no reaction. And the blank only with acetone and toluene yielded no benzaldehyde.

2.5.5 X-ray Diffraction

The X-ray crystallographic data of the complexes **2b**, **3b** and **4a** were collected on a STOE IPDS-diffractometer equipped with a low temperature system (Karlsruher Glastechnisches Werk). Mo-K$_\alpha$ radiation (λ = 0.71073 Å) and a graphite monochromator. No absorption corrections were applied. The structures were solved by direct methods in SHELXS97 and refined by using full-matrix least squares in SHELXL97.[75-76] All hydrogen atoms were positioned geometrically and all non-hydrogen atoms were refined anisotropically.

The X-ray crystallographic data of **3d** were collected with a BRUKER NONIUS KappaCCD system using a BRUKER NONIUS FR591 rotating anode as radiation source and an OXFORD CRYOSYSTEMS low temperature system. Mo-K$_\alpha$ radiation with wavelength 0.71073 Å and a graphite monochromator was used. The PLATON MULABS semi-empirical absorption correction using multiple scanned reflection was applied. The structures were solved by direct methods in SHELXS97 and refined with SHELXL97 using full-matrix least squares. [75-76] All non-hydrogen atoms were refined anisotropically. Only the 50 % occupied hydrogen atoms were positioned geometrically.

Crystallographic data for the structures reported in this paper have been deposited with the Cambridge Crystallographic Data Centre as supplementary publication no. CCDC-924632 for **1c**, CCDC-924633 for **2b**, CCDC-924634 for **3b** and CCDC-924635 for **4a** and CCDC-924636 for **3d**. Copies of the data can be obtained, free of charge from The Cambridge Crystallographic Data Centre via www.ccdc.cam.ac.uk/data_request/cif. The crystallographic data for **2a** and **4b** are not deposited (see Chapter 3). Chapter 3 also includes the crystallographic data and selected bond lengths and angles of compounds of **1c**, **2a** and **4b**.

3 Supporting Information and Unpublished Results for Chapter 2

3.1 Supporting Information

3.1.1 Crystal Structure and Structural Data of 1c

[Cr(tmpa)OH]$_2$(OTf)$_4$ (1c). Chromium(II) triflate tetrahydrate (0.06 g, 0.14 mmol) was dissolved in acetonitrile. Afterwards, the ligand tmpa (0.05 g, 0.17 mmol) was added to the blue solution. The solution was stirred for two days in inert atmosphere. When the solution was added to diethyl ether, a purple solid precipitated. Crystals suitable for crystal structure analysis could be obtained (Figure 3-1). UV/Vis (CH$_3$CN): λ_{max} (lg ε): 386 nm (2.5), 540 nm (2.4), IR (KBr): 3294, 2966, 2255, 2028, 1613, 1446, 1266, 1157, 1026, 772, 636, 573, 557, 530, 516, 495.

A similar reaction was also observed by Gafford *et al.* when [Cr(tmpa)](ClO$_4$)$_2$ reacted with dioxygen in ethanol.[67] The chromium(III) bis(μ-hydroxido) dimer was furthermore reported by Hodgson *et al.*[70] and Gafford *et al.*[71] with perchlorate or bromide as anions. All these bis(μ-hydroxido) complexes showed similar UV/Vis spectra with absorption maxima at 386 nm and 540 nm (Figure 3-2).
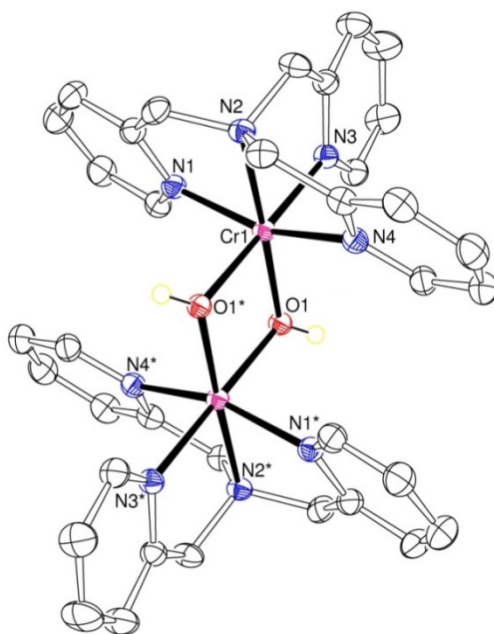
Figure 3-1: Molecular structure of the cation of **1c** shown as an ORTEP plot with thermal ellipsoids set at 50 % probability.

Table 3-1: Crystallographic data and structure refinement of **1c**.

	1c
Formula	$C_{40}H_{38}Cr_2F_{12}N_8O_{14}S_4 \cdot 3\ CH_3CN$
Formula weight	1438.19 g·mol^{-1}
Temperature	170(2) K
Wavelength	0.71073 Å
Crystal system	monoclinic
Space group	C2/c
Unit cell dimensions	a = 31.2830(6) Å α = 90° b = 9.7260(19) Å β = 123.56(3)° c = 23.3810(5) Å γ = 90°
Cell volume	5928(2) Å^3
Z/Calculated density	4, 1.611 Mg/m^3
Absorption coefficient	0.616 mm^{-1}
F(000)	2928
θ range	1.56 to 30.03°
Limiting indices	−44<=h<=44, −13<=k<=13, −32<=l<=32
Reflections collected / unique	51208 / 8658 [R(int) = 0.04341]
Completeness to θ	99.8 %
Absorption correction	semi-empiric
Refinement method	Full-matrix least-squares on F^2
Data / restraints / parameters	8658 / 0 / 492
Goodness-of-fit on F^2	1.043
Final R indices [I>2σ(I)]	R$_1$ = 0.0378, wR$_2$ = 0.0986
R indices (all data)	R$_1$ = 0.0531, wR$_2$ = 0.1068
Largest diff. peak and hole	0.537 and −0.619 e.Å^3

Table 3-2: Selected bond lengths (Å) and bond angles (°) of **1c**.

	1c		**1c**
Cr(1)–O(1)	1.9440(11)	N(2)–Cr(1)–N(1)	81.33(5)
Cr(1)–O(1)*	1.9680(11)	N(3)–Cr(1)–N(1)	84.53(5)
Cr(1)–N(2)	2.0593(12)	N(2)–Cr(1)–N(4)	79.77(5)
Cr(1)–N(3)	2.0342(13)	N(3)–Cr(1)–N(4)	90.44(5)
Cr(1)–N(1)	2.0536(17)	N(1)–Cr(1)–N(4)	160.86(5)
Cr(1)–N(4)	2.0493(16)	N(3)–Cr(1)–O(1)	99.79(5)
		N(4)–Cr(1)–O(1)	99.66(5)
		N(1)–Cr(1)–O(1)	90.44(5)
		N(2)–Cr(1)–O(1)	176.27(5)
		O(1)–Cr(1)–O(1)*	79.52(5)

30

The literature procedures are different from our synthetic protocol since the complexes described therein were prepared in aqueous solutions. The reported crystal structures contain four or eight water molecules in the unit cell, in contrast to **1c** where no coordinated water molecules are present. All complexes crystallized in roughly octahedral coordination. As expected, all complexes display similar bond lengths and angles.
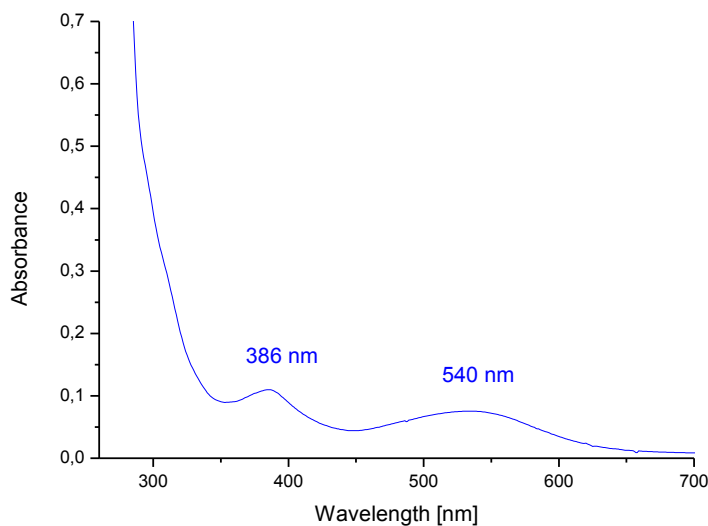
Figure 3-2: UV/Vis spectrum of **1c** in acetonitrile at 25.0 °C (complex concentration = 0.3 mmol·L^{-1}).

3.1.2 Crystal Structure and Structural Data of 2a
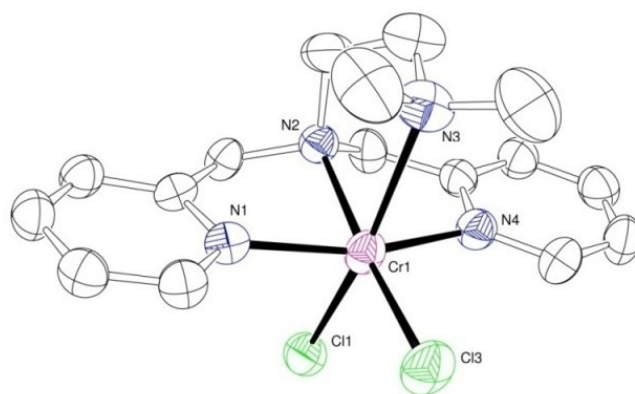
Figure 3-3: Molecular structure of the cation of **2a** shown as an ORTEP plot with thermal ellipsoids set at 50 % probability.

31

Table 3-3:   Crystallographic data and structure refinement of **2a**.

	2a
Formula	$C_{18}H_{25}CrCl_2N_5 \cdot 0.25\ H_2O$
Formula weight	438.83 g·mol^{-1}
Temperature	170(2) K
Wavelength	0.71073 Å
Crystal system	tetragonal
Space group	P4(2)/n
Unit cell dimensions	a = 22.992(3) Å α = 90° b = 22.992(3) Å β = 90° c = 8.2180(16) Å γ = 90°
Cell volume	4344.3(12) Å^3
Z/Calculated density	8, 1.342 Mg/m^3
Absorption coefficient	0.785 mm^{-1}
F(000)	1828
θ range	2.51 to 27.86°
Limiting indices	–23<=h<=30, –28<=k<=29, –9<=l<=10
Reflections collected / unique	28561 / 5173 [R(int) = 0.0818]
Completeness to θ	100.0 %
Absorption correction	none
Refinement method	Full-matrix least-squares on F^2
Data / restraints / parameters	5173 / 0 / 267
Goodness-of-fit on F^2	1.058
Final R indices [I>2σ(I)]	R_1 = 0.0528, wR_2 = 0.1296
R indices (all data)	R_1 = 0.1043, wR_2 = 0.1469
Largest diff. peak and hole	0.717 and –0.322 e.Å^3

Table 3-4:   Selected bond lengths (Å) and bond angles (°) of **2a**.

	2a		**2a**
Cl(1)–Cr(1)	2.04(4)	N(2)–Cr(1)–N(3)	76.86
Cl(3)–Cr(1)	2.377(3)	N(2)–Cr(1)–N(1)	80.00(9)
Cr(1)–N(2)	2.130(3)	N(3)–Cr(1)–N(1)	94.55
Cr(1)–N(3)	2.567	N(2)–Cr(1)–N(4)	80.44(10)
Cr(1)–N(1)	2.097(3)	N(3)–Cr(1)–N(4)	84.34
Cr(1)–N(4)	2.098(3)	N(1)–Cr(1)–N(4)	160.13(10)
		N(2)–Cr(1)–Cl(1)	96.6(10)
		N(3)–Cr(1)–Cl(1)	171.18
		N(1)–Cr(1)–Cl(1)	89.5(5)
		N(4)–Cr(1)–Cl(1)	89.4(5)
		Cl(1)–Cr(1)–Cl(3)	91.6(10)
		N(1)–Cr(1)–Cl(3)	99.43(9)

N(4)–Cr(1)–Cl(3)	100.43(9)
N(2)–Cr(1)–Cl(3)	171.70(12)
N(3)–Cr(1)–Cl(3)	95.08

3.1.3 Crystal Structure and Structural Data of 4b
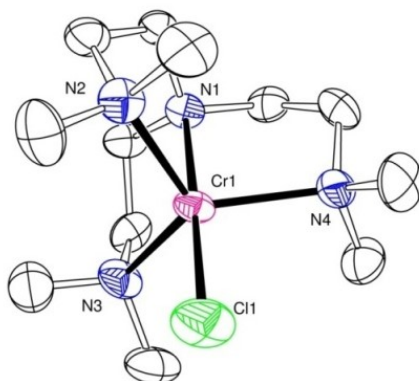
Figure 3-4: Molecular structure of the cation of **4b** shown as an ORTEP plot with thermal ellipsoids set at 50 % probability.

Table 3-5: Crystallographic data and structure refinement of **4b**.

	4b	
Formula	$C_{36}H_{50}CrN_4BCl$	
Formula weight	636.62 g·mol^{-1}	
Temperature	193(2) K	
Wavelength	0.71073 Å	
Crystal system	monoclinic	
Space group	Pc	
Unit cell dimensions	a = 12.493(3) Å	α = 90°
	b = 12.502(3) Å	β = 90.99(3)°
	c = 23.561(5) Å	γ = 90°
Cell volume	3679.5(13) Å^3	
Z/Calculated density	7, 1.224 Mg/m^3	
Absorption coefficient	0.417 mm^{-1}	
F(000)	1448	
θ range	2.30 to 25.97°	
Limiting indices	−15<=h<=15, −15<=k<=15, −29<=l<=28	
Reflections collected / unique	25749 / 13520 [R(int) = 0.1481]	
Completeness to θ	97.9 %	

33

Absorption correction	none
Refinement method	Full-matrix least-squares on F^2
Data / restraints / parameters	13520 / 2 / 843
Goodness-of-fit on F^2	1.021
Final R indices [I>2σ(I)]	R_1 = 0.1075, wR_2 = 0.2780
R indices (all data)	R_1 = 0.1277, wR_2 = 0.2943
Largest diff. peak and hole	1.250 and –1.125 e.Å^3

Table 3-6: Selected bond lengths (Å) and bond angles (°) of **4b**.

	4b		**4b**
Cr(1)–Cl(1)	2.319(3)	N(2)–Cr(1)–N(3)	118.8(3)
Cr(1)–N(2)	2.231(8)	N(2)–Cr(1)–N(1)	82.2(3)
Cr(1)–N(3)	2.238(7)	N(3)–Cr(1)–N(1)	82.3(3)
Cr(1)–N(1)	2.130(6)	N(2)–Cr(1)–N(4)	117.6(3)
Cr(1)–N(4)	2.210(8)	N(3)–Cr(1)–N(4)	118.3(3)
		N(1)–Cr(1)–N(4)	82.6(3)
		N(2)–Cr(1)–Cl(1)	96.9(2)
		N(3)–Cr(1)–Cl(1)	97.7(2)
		N(1)–Cr(1)–Cl(1)	178.9(2)
		N(4)–Cr(1)–Cl(1)	98.4(2)

3.2 Unpublished Results

3.2.1 Synthesis of the Chromium(II) Complexes with the Ligand tmpa

3.2.1.1 [Cr(tmpa)Cl$_2$] (1a)

Anhydrous CrCl$_2$ (0.04 g, 0.34 mmol) and tmpa (tris(2-pyridylmethyl)amine) (0.10 g, 0.34 mmol) were stirred in tetrahydrofuran in inert atmosphere. The resulting precipitate was collected, dried and dissolved in a minimum amount of acetonitrile. Purple crystals were obtained by diffusion of diethyl ether at –40 °C. Yield: 0.04 g (29 %). UV/Vis (CH$_3$CN): λ_{max} (lg ε): 376 nm (2.9), IR (KBr): 3020, 2914, 1604, 1472, 1437, 1283, 1152, 1090, 1051, 1024, 765, 650.

3.2.1.2 [Cr(tmpa)Cl]$_2$(BPh$_4$)$_2$ (1b)

Anhydrous CrCl$_2$ (0.04 g, 0.34 mmol) and NaBPh$_4$ (0.12 g, 0.34 mmol) were stirred with tmpa (0.10 g, 0.34 mmol) in tetrahydrofuran in inert atmosphere. The resulting precipitate was collected, dried and dissolved in acetonitrile at 70 °C. The solution was filtered hot and red-brown crystals could be obtained by diffusion of diethyl ether at –40 °C. Yield: 0.15 g (63 %). UV/Vis (CH$_3$CN): λ_{max} (lg ε): 379 nm (2.9), 421 nm (2.9), IR (KBr): 3053, 2998, 2982, 1942,

1882, 1818, 1609, 1577, 1480, 1440, 1426, 1286, 1266, 1159, 1092, 1054, 1030, 843, 733, 703, 612.

3.2.2 Synthesis of Chromium Complexes with Triflate as Anion

The complexes were synthesized according to the previously described protocol for the preparation of [Cr(tmpa)OH]$_2$(OTf)$_4$ (**1c**). Unfortunately, no crystals for crystal structure analysis could be obtained. The synthetic protocols with the spectral data are reported below.

3.2.2.1 [Cr(Me$_2$uns-penp)OH]$_2$(OTf)$_4$ (2c)

Chromium(II) triflate tetrahydrate (0.08 g, 0.18 mmol) and Me$_2$uns-penp (0.06 g, 0.22 mmol) were stirred in acetonitrile in inert atmosphere. The solution was stirred for a couple of days. When the solution was added to diethyl ether a red precipitate was obtained. UV/Vis (CH$_3$CN): λ_{max} (lg ε): 264 nm (4.0), 404 nm (2.6), 528 nm (2.2), IR (KBr): 3362, 3078, 1665, 1611, 1558, 1485, 1452, 1260, 1161, 1028, 769, 636, 573, 514.

3.2.2.2 [Cr(Me$_4$apme)OH]$_2$(OTf)$_4$ (3c)

Chromium(II) triflate tetrahydrate (0.14 g, 0.33 mmol) and Me$_4$apme (0.10 g, 0.40 mmol) were stirred in acetonitrile in inert atmosphere. The solution was stirred for a couple of days. When the solution was added to diethyl ether a grey precipitate was obtained. UV/Vis (CH$_3$CN): λ_{max} (lg ε): 259 nm (3.8), 414 nm (2.4), 560 nm (2.2), IR (KBr): 3459, 3074, 1592, 1476, 1266, 1158, 1028, 760, 634, 571, 514.

3.2.2.3 [Cr(Me$_6$tren)OH]$_2$(OTf)$_4$ (4c)

Chromium(II) triflate tetrahydrate (0.15 g, 0.36 mmol) was dissolved in acetonitrile. The ligand Me$_6$tren (0.10 g, 0.43 mmol) was added to the blue solution. The solution was stirred for a couple of days in inert atmosphere and turned light blue. When the solution was added to diethyl ether a light blue precipitate was obtained. UV/Vis (CH$_3$CN): λ_{max} (lg ε): 263 nm (2.4), IR (KBr): 3113, 2831, 1482, 1268, 1155, 1032, 960, 923, 757, 638, 573, 518.

3.2.3 Oxidation of Toluene by Using the Chromium(II) Complexes and Dioxygen

According to the previously described oxidation experiments with copper peroxido complexes[20], the synthesized chromium(II) complexes with tetraphenylborate as anion were used for the oxidation of toluene. Additionally, chromium(II) complexes with chloride as anion were applied, but no oxidation products could be identified. The same accounted for blank tests with chromium(II) chloride and potassium dichromate, which as well yielded no oxidation products.

3.2.3.1 Reaction of [Cr(tmpa)Cl]$_2$(BPh$_4$)$_2$ and Dioxygen with Toluene

In a small vessel, [Cr(tmpa)Cl]$_2$(BPh$_4$)$_2$ (10.0 mg, 0.01 mmol) was dissolved in acetone (0.7 mL) and toluene (0.7 mL) was added in inert atmosphere. Afterwards, dioxygen was passed through the solution for ca. 1 min. The complex was not completely dissolved. The mixture was stored for 7 days at room temperature on the bench. Afterwards, the mixture was analyzed by GC-MS measurement, the spectrum is presented in Figure 3-5. Yield: approx. 8 % benzaldehyde and by-products.
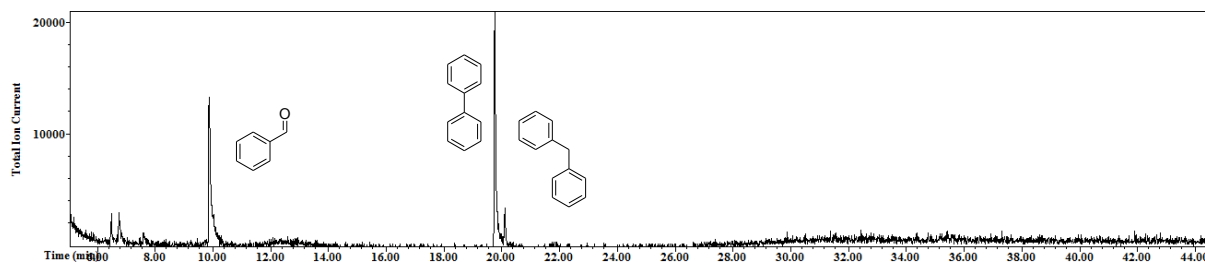
Figure 3-5: GC-MS spectrum of the reaction mixture of [Cr(tmpa)Cl]$_2$(BPh$_4$)$_2$ with dioxygen in toluene/acetone (1:1) after a reaction time of 7 days.

The first small peaks result from the different substituted xylene derivates (internal standard). Benzaldehyde was detected at a retention time of 9.87 min. At retention times of 19.76 min biphenyl and at 20.11 min diphenylmethane where observed, respectively.

3.2.3.2 Reaction of [Cr(Me$_2$uns-penp)Cl]$_2$(BPh$_4$)$_2$ and Dioxygen with Toluene

[Cr(Me$_2$uns-penp)Cl]$_2$(BPh$_4$)$_2$ (10.0 mg, 0.01 mmol) was treated as previously described (3.2.3.1). The complex was not completely dissolved as well. The mixture was stored for 7 days at room temperature on the bench. The resulting GC-MS is shown in Figure 3-6. Yield: approx. 5 % benzaldehyde and by-products.
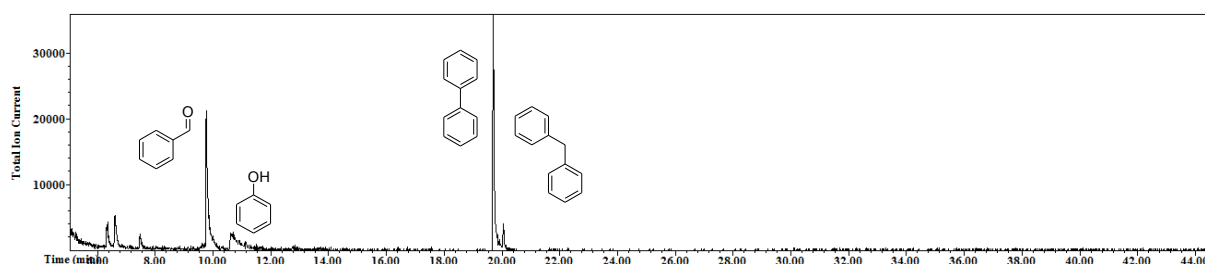
Figure 3-6: GC-MS spectrum of the reaction mixture of [Cr(Me$_2$uns-penp)Cl]$_2$(BPh$_4$)$_2$ with dioxygen in toluene/acetone (1:1) after a reaction time of 7 days.

The first small peaks result from the different substituted xylene derivates (internal standard). Benzaldehyde was detected at a retention time of 9.80 min. Phenole could be found at a retention time of 10.64 min. At retention times of 19.71 min diphenyl and at 20.06 min diphenylmethane were observed, respectively.

36

3.2.3.3 Reaction of [Cr(Me₄apme)Cl]BPh₄ and Dioxygen with Toluene

[Cr(Me₄apme)Cl]BPh₄ (10.0 mg, 0.02 mmol) was treated as previously described (3.2.3.1). The complex was completely dissolved. After storage for 7 days at room temperature the mixture was analyzed by GC-MS measurement, the spectrum is shown in Figure 3-7. Yield: approx. 25 % benzaldehyde and by-products.
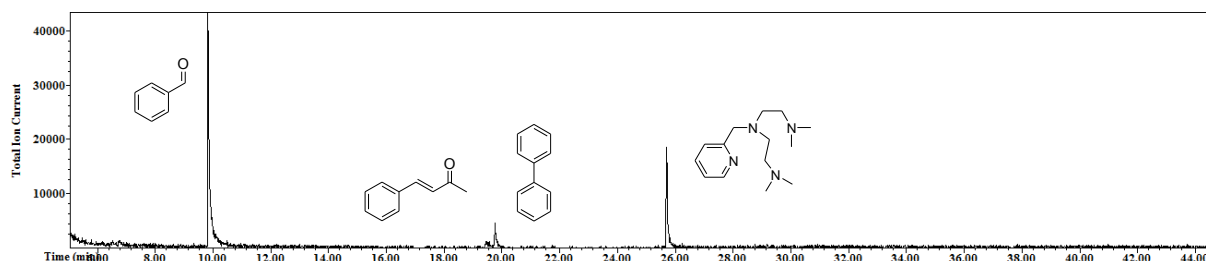
Figure 3-7: GC-MS spectrum of the reaction mixture of [Cr(Me₄apme)Cl]BPh₄ with dioxygen in toluene/acetone (1:1) after a reaction time of 7 days.

The first small peaks result from the different substituted xylene derivates (internal standard). Benzaldehyde was detected at a retention time of 9.83 min. 4-phenyl-3-buten-2-one could be found at a retention of 19.49 min. At retention times of 19.77 min diphenyl and at 25.71 min the ligand Me₄apme were observed, respectively.
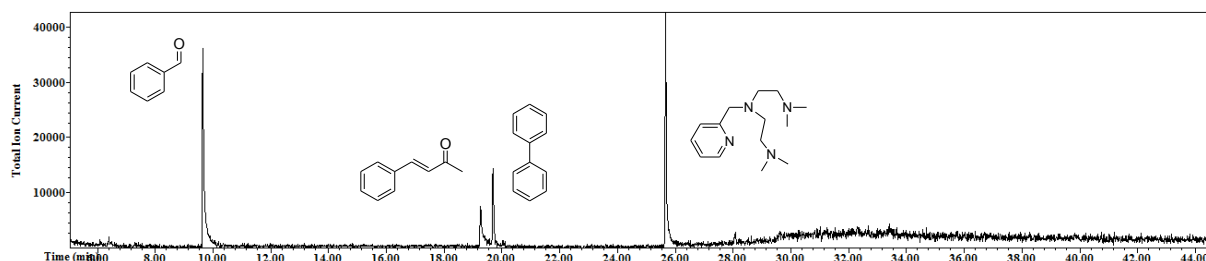
Figure 3-8: GC-MS spectrum of the reaction mixture of [Cr(Me₄apme)Cl]BPh₄ with dioxygen in toluene/acetone (1:1) after a reaction time of a couple of days.

By comparing the GC-MS spectra in Figure 3-7 and Figure 3-8 it can be noticed that after a reaction time of two more weeks the peak area of benzaldehyde at the retention time of 9.83 min has decreased whereas the peak area of 4-phenyl-3-buten-2-one at 19.49 min has increased. This could be explained by the reaction of benzaldehyde with the solvent acetone. The reaction equation is shown in Figure 3-9.
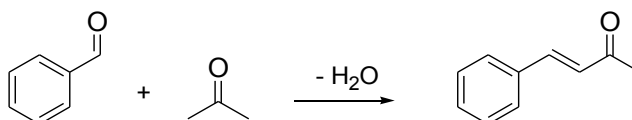
Figure 3-9: Reaction scheme of the condensation reaction of benzaldehyde with acetone to 4-phenyl-3-buten-2-one.

3.2.3.4 Reaction of [Cr(Me₆tren)Cl]BPh₄ and Dioxygen with Toluene

[Cr(Me$_6$tren)Cl]BPh$_4$ (10.0 mg, 0.02 mmol) was treated as previously described (3.2.3.1). The complex was completely dissolved, after a couple of days a precipitate had formed. The mixture was stored for 7 days at room temperature on the bench. Afterwards, the mixture was analyzed by GC-MS measurement and the resulting spectrum is shown in Figure 3-10. Herein, no benzaldehyde could be detected.
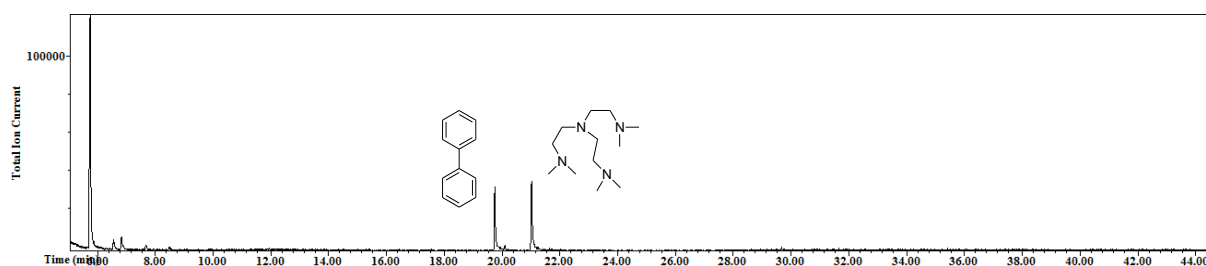
Figure 3-10: GC-MS spectrum of the reaction mixture of [Cr(Me$_6$tren)Cl]BPh$_4$ with dioxygen in toluene/acetone (1:1) after a reaction time of 7 days.

The first small peaks result from the different substituted xylene derivates (internal standard). At a retention time of ca. 10 min no benzaldehyde could be detected. At retention times of 19.75 min diphenyl of 21.02 min, the ligand Me$_6$tren were observed, respectively.

By-products such as diphenyl are believed to be formed by a radical reaction of the anion tetraphenylborate.

4 Reactivity of Chromium Complexes with N-benzyl-N,N',N'-tris(2-methylpyridyl)-ethylenediamine (bztpen) as a Ligand

This work is ready for submission to *Zeitschrift für Anorganische und Allgemeine Chemie*

Sabrina Schäfer, Sabine Löw and Christian Würtele

4.1 Abstract

Chromium(II) complexes containing the tetradentate ligand bztpen (N-benzyl-N,N',N'-tris(2-methylpyridyl)-ethylenediamine) were prepared and investigated with regard to their reactivity towards dioxygen. Especially the reactivity towards hydrogen peroxide together with triethlyamine was tested. It was possible to structurally characterize the complexes [Cr(bztpen)Cl]Cl and [Cr(bztpen)(CH$_3$OH)](OTf)$_2$. The complexes showed reactions with dioxygen and hydrogen peroxide, but it was not possible to fully characterize intermediates of these reactions. The reactions were followed spectroscopically. However, it was possible to prepare and structurally characterize the complex [Cr(bztpen)(NO)Cl]Cl from the related reaction with NO instead of O$_2$.

4.2 Indroduction

Metalloenzymes play an important role for aerobic life. Mainly enzymes with iron or copper ions in the active site are involved in the activation of dioxygen and subsequent oxidation reactions. There is great interest to model these reactions using low molecular transition metal complexes in regard to find new catalysts for selective oxidations of substrates such as hydrocarbons, e. g. methane. In the past, especially iron complexes were synthesized and investigated in that regard.[11-13,77-78] However, despite the goal to use air/dioxygen as direct oxidant together with a catalyst, mainly hydrogen peroxide or organic peroxides have been used instead.[3,79-81] In that regard iron complexes with the ligand Rtpen, especially with R = bz (bztpen = N-benzyl-N,N',N'-tris(2-methylpyridyl)-ethylenediamine, Figure 4-1) turned out to be quite useful for such studies.[13,37-40,82]
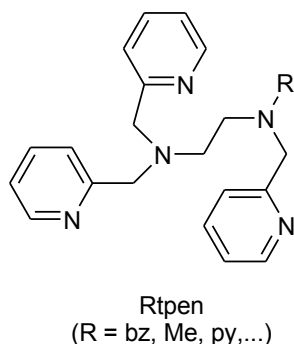
Rtpen
(R = bz, Me, py,...)

Figure 4-1:   The ligand Rtpen (bztpen with R = bz).

It was observed that iron complexes with the ligand bztpen formed quite stable hydroperoxido as well as peroxido complexes according to the mechanism shown in Figure 4-2.[37,40,83-85] The purple iron hydroperoxido complex [Fe(bztpen)OOH]$^{2+}$ can be deprotonated with bases such as triethylamine to form the blue, most likely side-on coordinated, peroxido complex [Fe(bztpen)O$_2$]$^+$.
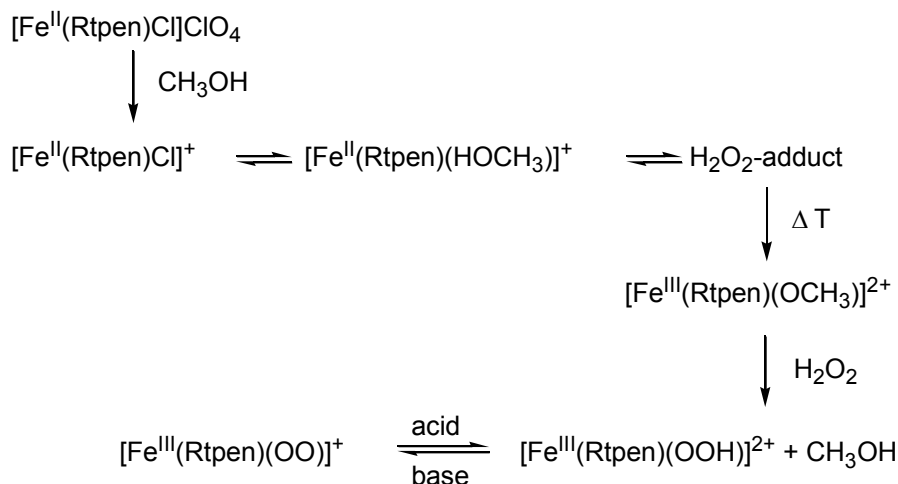
Figure 4-2:   Postulated mechanism for the formation of iron hydroperoxido and peroxido complexes.[37]

Hydroperoxido and peroxido complexes can act as precursors for the formation of iron oxido complexes. An iron oxido complex with the ligand bztpen could be characterized spectroscopically.[79]

Despite the fact that the hydroperoxido as well as the peroxido complex of the iron bztpen system are quite stable, all efforts to isolate and structurally characterize one of these complexes failed so far. Furthermore, it was not possible to isolate a superoxido or peroxido complex from the reaction of dioxygen with iron(II) bztpen complexes. In contrast, it was possible to obtain a molecular structure of the according iron(III) nitrosyl complex [Fe(bztpen)NO](OTf)$_2$, that should be structurally similar with the analogous iron superoxido complex.[37]

Due to the high stability of chromium peroxido complexes[86] it was promised that it should be possible to isolate and structurally characterize chromium "dioxygen adduct complexes" with

the ligand bztpen as "model compounds" for the analogous iron intermediate complexes. Thus, the synthesis of chromium(II) bztpen complexes together with their reactivity towards dioxygen, hydrogen peroxide and nitrogen oxide is reported herein.

4.3 Results and Discussion

While chromium(III) Rtpen (with R = py, thus leading to a hexadentate ligand with four pyridyl N-donor atoms) complexes are known in literature,[87] chromium(II) complexes of Rtpen have not been reported so far.

A chromium(II) complex with the ligand bztpen (Figure 4-1) was prepared by adding the ligand solution in methanol to a chromium(II) chloride solution in inert atmosphere. The molecular structure of the obtained complex [Cr(bztpen)Cl]Cl (**1**) is shown in Figure 4-3. Crystallographic data are summarized in Table 4-1 and selected bond lengths and angles in Table 4-2. Complex **1** crystallizes in monoclinic crystal system and has distorted octahedral coordination. The chromium(II) cation is coordinated by the three pyridyl donor groups and two amine nitrogen atoms of the ligand bztpen. One coordination position is occupied by a chloride ligand, which is disordered. The Cr(1)–Cl(3) bond has a length of 2.368(2) Å, similar to other Cr–Cl bond lengths (see Chapter 2).
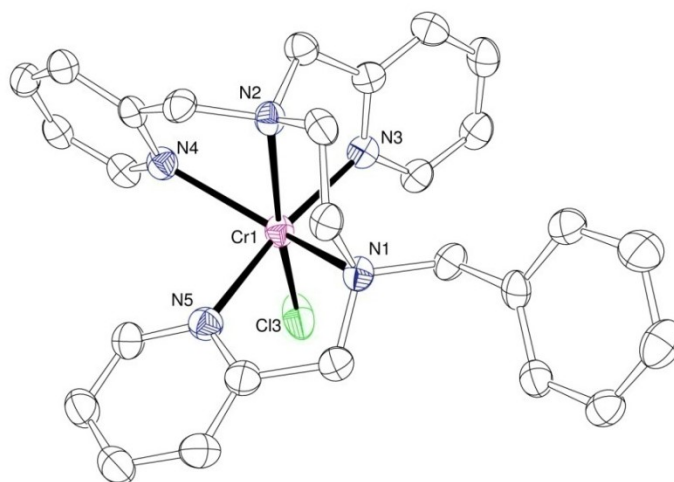
Figure 4-3: Molecular structure of the cation of **1** shown as an ORTEP plot with thermal ellipsoids set at 50 % probability.

Table 4-1: Crystallographic data and structure refinement of **1**.

	1
Formula	$C_{27}H_{29}Cl_2Cr\,N_5$
Formula weight	546.45 g·mol^{-1}
Temperature	293(2) K

Wavelength	0.71073 Å	
Crystal system	monoclinic	
Space group	Cc	
Unit cell dimensions	a = 15.847(3) Å	α = 90°
	b = 9.5260(19) Å	β = 102.45(3)°
	c = 17.100(3) Å	γ = 90°
Cell volume	2520.7(9) Å^3	
Z/Calculated density	4/1.440 Mg/m^3	
Absorption coefficient	0.692 mm^{-1}	
F(000)	1136	
θ range	2.44 to 30.04°	
Limiting indices	–22<=h<=20, –10<=k<=13, –24<=l<=23	
Reflections collected / unique	10544/6139 [R(int)=0.0520]	
Completeness to θ	99.6 %	
Absorption correction	none	
Refinement method	Full-matrix least-squares on F^2	
Data / restraints / parameters	6139 / 2 / 432	
Goodness-of-fit on F^2	0.993	
Final R indices [I>2σ(I)]	R$_1$=0.0477, wR$_2$=0.0876	
R indices (all data)	R$_1$=0.0783, wR$_2$=0.1012	
Largest diff. peak and hole	0.470 and –0.392 e.Å^3	

Table 4-2: Selected bond lengths (Å) and bond angles (°) of **1**.

	1		**1**
Cr(1)–N(1)	2.407(3)	N(1)–Cr(1)–N(3)	96.1(2)
Cr(1)–N(2)	2.318(3)	N(1)–Cr(1)–N(5)	74.4(2)
Cr(1)–N(3)	2.111(3)	N(1)–Cr(1)–N(2)	75.4(2)
Cr(1)–N(4)	2.357(3)	N(1)–Cr(1)–N(4)	137.8(2)
Cr(1)–N(5)	2.154(3)	N(2)–Cr(1)–N(3)	76.0(2)
Cr(1)–Cl(3)	2.368(2)	N(2)–Cr(1)–N(4)	71.9(2)
		N(2)–Cr(1)–N(5)	103.2(2)
		N(3)–Cr(1)–N(4)	101.0(2)
		N(3)–Cr(1)–N(5)	170.2(2)
		N(4)–Cr(1)–N(5)	87.7(2)
		N(2)–Cr(1)–Cl(3)	168.22(8)
		N(3)–Cr(1)–Cl(3)	93.21(9)
		N(1)–Cr(1)–Cl(3)	111.00(7)
		N(4)–Cr(1)–Cl(3)	106.12(8)
		N(5)–Cr(1) - Cl(3)	88.17(8)

Chloride anions are known to be strongly coordinating ligands and are quite difficult to be substituted with weaker ligands. Therefore, the reaction of chromium(II) triflate with bztpen,

which yielded the complex [Cr(bztpen)(CH₃OH)](OTf)₂ (**2**) was investigated. The molecular structure of the cation of **2** is shown in Figure 4-4. Crystallographic data are summarized in Table 4-3 and selected bond length and angles in Table 4-4.
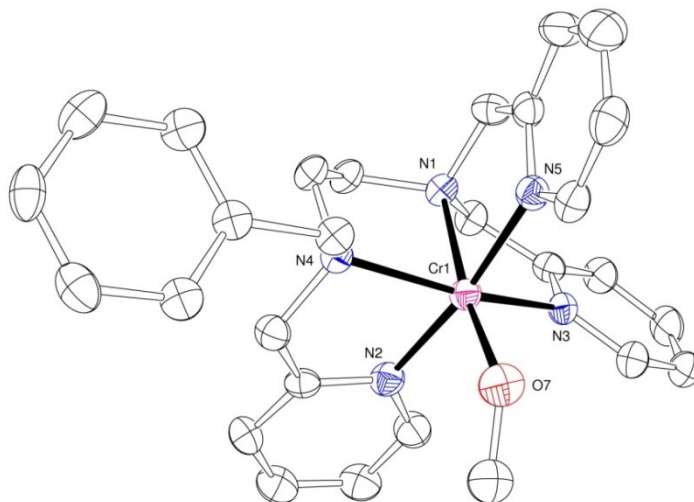
Figure 4-4: Molecular structure of the cation of **2** shown as an ORTEP plot with thermal ellipsoids set at 50 % probability.

Table 4-3: Crystallographic data and structure refinement of **2**.

	2
Formula	$C_{30}H_{33}CrF_6N_5O_7S_2$
Formula weight	805.73 g·mol^{-1}
Temperature	190(2) K
Wavelength	0.71073 Å
Crystal system	orthorhombic
Space group	Pbca
Unit cell dimensions	a = 19.178(4) Å α = 90° b = 17.133(3) Å β = 90° c = 20.267(4) Å γ = 90°
Cell volume	6659(2) Å^3
Z/Calculated density	8/1.607 Mg/m^3
Absorption coefficient	0.558 mm^{-1}
F(000)	3312
θ range	2.57 to 27.48°
Limiting indices	–22<=h<=24, –22<=k<=20, –25<=l<=26
Reflections collected / unique	44456/7615 [R(int)=0.1108]
Completeness to θ	99.6 %
Absorption correction	empirical
Refinement method	Full-matrix least-squares on F^2

43

Data / restraints / parameters	7615 / 0 / 588
Goodness-of-fit on F^2	1.008
Final R indices [I>2σ(I)]	R_1=0.0550, wR_2=0.0993
R indices (all data)	R_1=0.1083, wR_2=0.1168
Largest diff. peak and hole	0.308 and –0.430 e.$Å^3$

Table 4-4: Selected bond lengths (Å) and bond angles (°) of **2**.

	2		**2**
Cr(1)–N(1)	2.122(2)	N(1)–Cr(1)–N(3)	78.4(2)
Cr(1)–N(2)	2.065(3)	N(1)–Cr(1)–N(5)	81.6(2)
Cr(1)–N(3)	2.068(3)	N(1)–Cr(1)–N(2)	94.4(2)
Cr(1)–N(4)	2.136(2)	N(1)–Cr(1)–N(4)	84.5(2)
Cr(1)–N(5)	2.050(3)	N(2)–Cr(1)–N(3)	91.7(2)
Cr(1)–O(7)	1.853(3)	N(2)–Cr(1)–N(4)	81.9(2)
		N(2)–Cr(1)–N(5)	171.9(2)
		N(3)–Cr(1)–N(4)	161.3(2)
		N(3)–Cr(1)–N(5)	94.3(2)
		N(4)–Cr(1)–N(5)	90.6(2)
		N(2)–Cr(1)–O(7)	92.8(2)
		N(3)–Cr(1)–O(7)	99.1(2)
		N(1)–Cr(1)–O(7)	172.3(2)
		N(4)–Cr(1)–O(7)	98.6(2)
		N(5)–Cr(1)–O(7)	91.3(2)

In complex **2** a methanol molecule from the solvent is coordinated instead of the chloride anion in **1**. The bond length between the chromium(II) ion and the oxygen atom of the coordinated methanol molecule amounts 1.853(3) Å, which is significantly shorter than the bond length between the chromium(II) cation and the chloride ligand in **1**.

As expected, the two complexes behave different in solution. This was documented by their UV/Vis spectra. Complex **1** shows four absorption maxima at 261 nm, 295 nm, 341 nm and 488 nm whereas complex **2** shows absorption maxima at 420 nm and 620 nm and shoulders at 344 nm and 502 nm.

4.3.1 Reactivity towards Dioxygen

When complex **1** reacted with dioxygen at low temperatures in a benchtop experiment, a color change of the solution from deep red color to a deep blue was observed. Low temperature stopped-flow measurements were carried out to gain more detailed insight into the reaction mechanism. Figure 4-5 shows time-resolved spectra for the reaction of **1** with dioxygen in methanol at –92 °C.
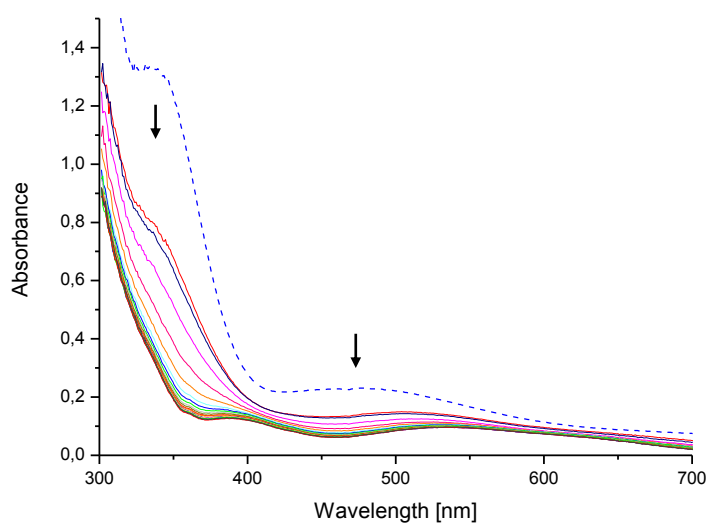
Figure 4-5: Time-resolved spectra for the reaction of a 0.2 mmol·L⁻¹ solution of **1** in methanol with dioxygen (8.5 mmol·L⁻¹, –92 °C, overall reaction time = 0.075 s, Δ = 1.5 ms). **1** prior to its reaction with dioxygen (blue dashed line).

The reaction of complex **1** with dioxygen is too fast for a detailed kinetic analysis. The two absorption maxima at 344 nm and 488 nm disappeared immediately during mixing. Afterwards, in a fast consecutive reaction, absorption maxima at 360 nm, 390 nm, 536 nm and 630 nm formed. The resulting solution is stable at room temperature, however no crystals could be obtained for structural characterization of the product. The UV/Vis data are similar to data reported by Nam and co-workers for a chromium(III) end-on superoxido complex using the macrocyclic ligand TMC (1,4,8,11-tetramethyl-1,4,8,11-tetraazacyclotetradecane).[29] It is also similar to previously reported results with the ligand Me₄apme by our group.[88] The assumption that a chromium end-on superoxido complex with the ligand bztpen is formed is furthermore supported by the infrared spectrum of this complex in the solid state at room temperature. Herein, two new absorption bands at 1160 cm⁻¹ and 554 cm⁻¹ were observed after the reaction with dioxygen. The band at 1160 cm⁻¹ is a good indicator of the presence of an end-on superoxido ligand.[45] Nam and co-workers described this band in the resonance Raman spectrum of their superoxido complex as O–O stretching vibration (in acetonitrile at –20 °C).[29] The band at 554 cm⁻¹ can be assigned to a ν(Cr–O) stretching vibration.[89]

In contrast to our expectations, the reaction of complex **2** with dioxygen at low temperatures (Figure 4-6) turned out to be complex. After very fast reaction, an intermediate with absorption maxima at 443 nm and 623 nm was formed (red solid line) followed by a fast consecutive reaction during which this intermediate decomposed showing two isosbestic points at 544 nm and 672 nm. The final product (black dashed line) arises with absorption maxima at 479 nm and 601 nm. Unfortunately, so far it is not fully understood, which reaction

occurs here. The resulting absorption maxima could be indicative for the formation of a simple chromium(III) complex without any dioxygen ligand.[45]
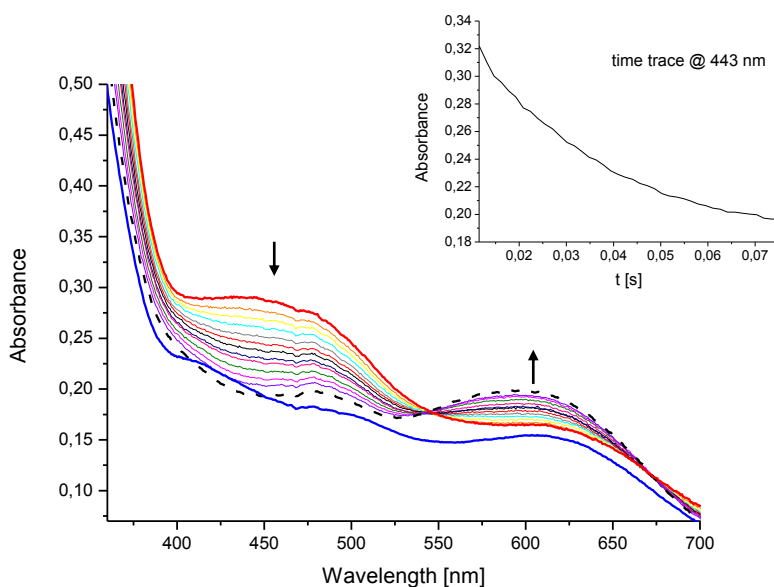
Figure 4-6: Time-resolved spectra for the reaction of a 4 mmol·L^{-1} solution of **2** in methanol with dioxygen (8.5 mmol·L^{-1}, −92 °C, overall reaction time = 0.075 s, Δ = 1.5 ms). Complex **2** prior to its reaction with dioxygen (blue line). Insert: Time trace of the reaction at 443 nm. Some data points at the beginning were disregarded due to the mixing time of the solution.

4.3.2 Reactivity towards Hydrogen Peroxide

In analogy to the reaction of the iron bztpen complex with hydrogen peroxide, a similar reaction is expected for the chromium complexes. The reaction with hydrogen peroxide should produce a hydroperoxido intermediate. All reactions were performed with excess hydrogen peroxide. Both compounds showed nearly the same UV/Vis spectrum with hydrogen peroxide (black line in Figure 4-7, UV/Vis spectrum of compound **2** with hydrogen peroxide and triethylamine can be found in Chapter 5). The formation of a hydroperoxido intermediate could not be confirmed spectroscopically; and the intermediate could so far not be identified. A spectroscopic change can be traced by addition of the base triethylamine to the solution. The time-resolved spectra of the reactions for compound **1** are shown in Figure 4-7 (Reaction for compound **2** Chapter 5). Despite the fact that compound **1** and **2** showed different reaction behavior towards dioxygen, the UV/Vis spectra showed similar absorption maxima at approx. 372 nm and a shoulder at 476 nm. The comparison of the UV/Vis spectra with the literature furthermore allowed no suggestions about the nature of the final product.

In contrast to the reaction of the iron complexes with hydrogen peroxide and trietylamine the reaction with the chromium complexes is much slower. The progress of the reaction had been followed for a couple of days.
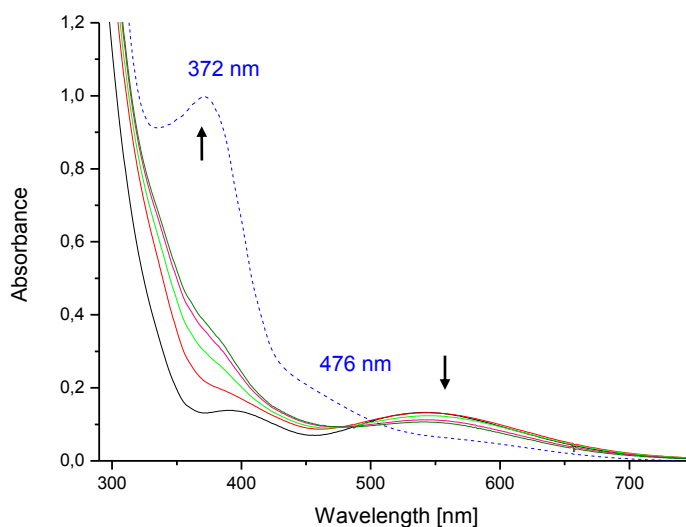
Figure 4-7: Compound **1** with hydrogen peroxide (black line) after a couple of days. The dashed line shows the solution after reaction with triethylamine for three days (complex concentration = 0.8 mmol·L^{-1}).

Unfortunately, again it was not possible to isolate a product suitable for structural characterization.

4.3.3 Reactivity towards Nitric Oxide

In contrast to the unsuccessful attempts to characterize the products of the reaction with dioxygen or hydrogen peroxide, the product of the reaction with nitric oxide could be isolated. A solution of complex **1** in methanol was flushed for ca. 1 min with nitric oxide at approx. –40 °C. The solution turned dark green. After recrystallization from acetone crystals of the complex [Cr(bztpen)(NO)Cl]Cl (**3**) suitable for structural analysis could be obtained. The molecular structure of the cation of **3** is presented in Figure 4-8. Crystallographic data are summarized in Table 4-5 and selected bond lengths and angles in Table 4-6.
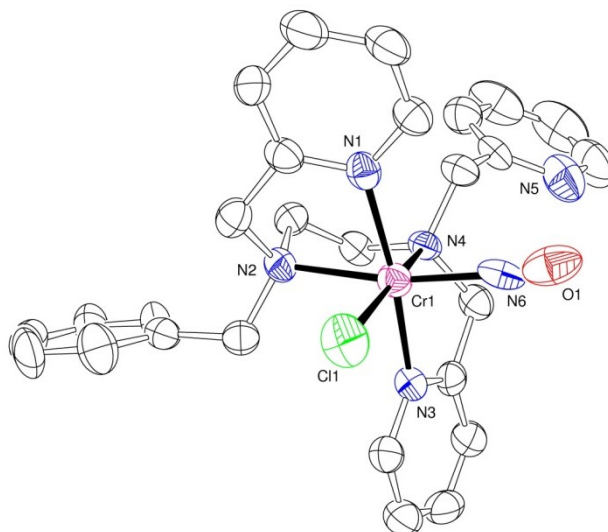
Figure 4-8: Molecular structure of the cation of **3** shown as an ORTEP plot with thermal ellipsoids set at 50 % probability.

Table 4-5: Crystallographic data and structure refinement of **3**.

	3
Formula	$C_{108}H_{116}Cl_9Cr_4N_{24}O_4$
Formula weight	2341.30 g·mol^{-1}
Temperature	356(2) K
Wavelength	0.71073 Å
Crystal system	monoclinic
Space group	P2$_1$/n
Unit cell dimensions	a = 11.429(2) Å α = 90° b = 11.653(2) Å β = 97.32(3)° c = 20.298(4) Å γ = 90°
Cell volume	2681.3(9) Å^3
Z/Calculated density	1/1.450 Mg/m^3
Absorption coefficient	0.684 mm^{-1}
F(000)	1213
θ range	1.95 to 22.99°
Limiting indices	$-12<=h<=12$, $-12<=k<=12$, $-21<=l<=22$
Reflections collected / unique	13861 / 3717 [R(int)=0.1857]
Completeness to θ	99.7 %
Absorption correction	none
Refinement method	Full-matrix least-squares on F^2
Data / restraints / parameters	3717 / 1 / 471
Goodness-of-fit on F^2	1.015
Final R indices [I>2σ(I)]	R$_1$=0.0665, wR$_2$=0.1498

48

R indices (all data)	R$_1$=0.1092, wR$_2$=0.1711
Largest diff. peak and hole	0.427 and −0.471 e.Å^3

Table 4-6: Selected bond lengths (Å) and bond angles (°) of **3**.

	3		**3**
Cr(1)–N(1)	2.065(5)	N(1)–Cr(1)–N(3)	172.4(2)
Cr(1)–N(2)	2.172(4)	N(1)–Cr(1)–N(2)	78.1(2)
Cr(1)–N(3)	2.065(5)	N(1)–Cr(1)–N(4)	99.1(2)
Cr(1)–N(4)	2.142(4)	N(2)–Cr(1)–N(3)	94.3(2)
Cr(1)–Cl(1)	2.337(2)	N(2)–Cr(1)–N(4)	82.5(2)
Cr(1)–N(6)	1.872(6)	N(3)–Cr(1)–N(4)	78.9(2)
N(6)–O(7)	0.871(6)	N(1)–Cr(1)–N(6)	95.7(2)
		N(2)–Cr(1)–N(6)	168.3(2)
		N(3)–Cr(1)–N(6)	91.6(2)
		N(4)–Cr(1)–N(6)	88.8(2)
		N(1)–Cr(1)–Cl(1)	87.8(2)
		N(2)–Cr(1)–Cl(1)	91.9(2)
		N(3)–Cr(1)–Cl(1)	93.1(2)
		N(4)–Cr(1)–Cl(1)	169.9(2)
		N(6)–Cr(1)–Cl(1)	97.7(2)
		Cr(1)–N(6)–O(1)	170.7(9)

The chromium ion is coordinated by two pyridyl groups and two amine nitrogen atoms of the ligand bztpen. One of the pyridyl arms of the ligand is not coordinated, because it was replaced by the nitrosyl ligand. The strong bonding chloride ligand is still coordinated. The Cr(1)–Cl(1) bond length of 2.337(2) Å in complex **3** is similar to the Cr(1)–Cl(3) bond length of 2.3682(11) Å in complex **1**. The bond length of the coordinated nitrosyl ligand with 1.872(6) Å is similar to the bond lengths of other metal nitrosyl complexes.[41] The coordination of the nitrosyl ligand is nearly linear with the angle Cr(1)–N(6)–O(1) = 170.7(9)°. The bond length between the coordinated nitrogen atom and the oxygen atom is untypically very small with 0.871(6) Å. The usual length is 1.18 Å.[90-91] The coordination of a nitrosyl ligand is supported by the infrared spectrum. Figure 4-9 shows the infrared spectrum of compound **1** in comparison with compound **3**.
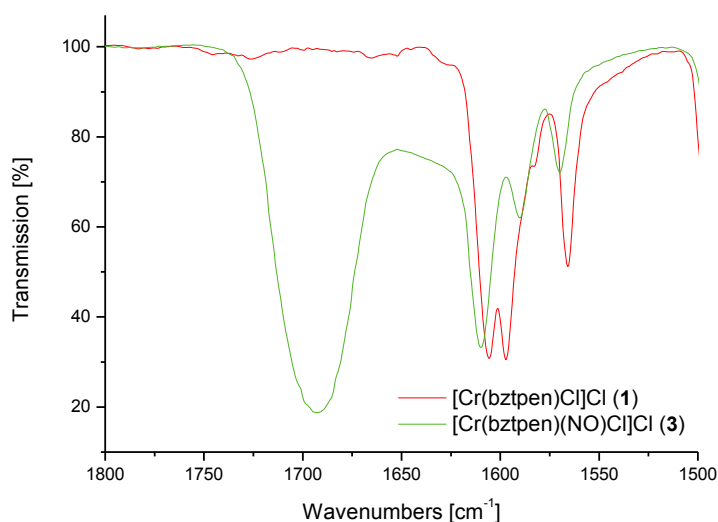
Figure 4-9: Comparison of the IR spectra of compound **1** (red line) and **3** (green line). (KBr-pellet)

The strong band at 1692 cm^{-1} indicated the coordination of a nitrosyl ligand. Nam and co-workers described the same strong NO band in the infrared spectrum of a chromium(II) nitrosyl complex with the macrocyclic ligand 12-TMC.[32] Furthermore, Ardon *et al.* described a N–O stretching frequency in the range of 1600–1750 cm^{-1}.[91] Analogous regions have also been observed for other metal nitrosyl complexes. For example, the iron(III) nitrosyl complex with the ligand bztpen [Fe(bztpen)NO](OTf)$_2$ showed a bond at 1671.4 cm^{-1}.[37]

The UV/Vis spectrum of compound **3** shows three absorption maxima at 460 nm, 623 nm and 677 nm (see Chapter 5). Low temperature stopped-flow measurements at –75 °C in methanol showed that the formation of the nitrosyl complex is too fast to follow the reaction spectroscopically.

To the best of our knowledge, this is the first molecular structure of a chromium nitrosyl complex with a simple organic ligand. Nam and co-workers investigated the reaction of the chromium(II) complex using 12-TMC with nitric oxide, but they were not able to solve the crystal structure of the complex. However, they succeeded to structurally characterize the according end-on superoxido complex with the related ligand 14-TMC. Most recently, Nam and co-workers furthermore investigated in detail the reaction of chromium peroxido[32] and chromium superoxido[92] complexes with nitric oxide.

The molecular structure of the [Cr(14-TMC)(O$_2$)Cl]Cl complex is similar to the structure of the related NO complex [Cr(12-TMC)(NO)Cl]Cl proposed by Nam and co-workers.[32] In regard to these and previous findings, it is assumed that the molecular structure of [Cr(bztpen)(O$_2$)Cl]Cl should be quite similar to [Cr(bztpen)(NO)Cl]Cl.

4.4 Conclusions

Whereas the idea to obtain chromium hydroperoxido or peroxido complexes with the ligand bztpen as "model compounds" for the analogous iron complexes did not yield the desired results, the starting materials [Cr(bztpen)Cl]Cl and [Cr(bztpen)(CH$_3$OH)](OTf)$_2$ could be characterized for the first time. Furthermore, the formation of an end-on superoxido complex, [Cr(bztpen)(O$_2$)Cl]Cl during the reaction of [Cr(bztpen)Cl]Cl with dioxygen could be strongly supported. Most exciting however was the fact that for the first time a chromium–NO complex with a simple organic ligand could be structurally characterized.

4.5 Experimental Section

4.5.1 Materials

Reagents and solvents used were commercially available. Chromium(II) triflate tetrahydrate was prepared according to the literature.[74] Bztpen was synthesized according to published procedures.[82] Nitric oxide was prepared by reaction of a sulfuric acid/iron(II) sulfate suspension with sodium nitrite under argon. The gas was further purified by passing it through a 2 M sodium hydroxide solution and solid sodium hydroxide.[37] Preparation and handling of air-sensitive compounds were carried out in a glove box filled with argon (MBraun, Germany; water and dioxygen less than 1 ppm) or using Schlenk techniques.

4.5.2 Equipment

UV/Vis absorption spectra were recorded with an Agilent 8453-spectrometer. The measurements were performed using quartz cuvettes. Stopped-flow experiments at ambient pressures were performed using a commercially available Hi Tech Limited SF-61SX2 (Salisbury, UK) instrument. Detailed description of low temperature stopped-flow experiments were published previously.[64] IR spectroscopic measurements were performed using a JASCO FT/IR-4100 spectrometer. Elemental analyses were obtained using a vario EL III element analyzer from Elementar.

4.5.3 [Cr(bztpen)Cl]Cl (1)

Anhydrous CrCl$_2$ (0.12 g, 1 mmol) and bztpen (N-benzyl-N,N',N'-tris(2-methylpyridyl)-ethylenediamine) (0.42 g, 1 mmol) were dissolved in methanol. The ligand solution was added dropwise to the chromium(II) solution. The resulting solution was stirred for 2 h in inert atmosphere. After filtration the complex was precipitated in diethyl ether. Red crystals could be obtained by diffusion of diethyl ether at –40 °C. Yield: 0.43 g (78 %). Anal.: C$_{27}$H$_{29}$N$_5$Cl$_2$Cr (546.45); C 58.06 (calcd. 59.34); H 5.43 (5.35); N 12.48 (12.82) %. UV/Vis (CH$_3$OH): λ_{max} (lg ε): 261 nm (3.7), 295 nm (3.3), 341 nm (3.1), 488 nm (2.4), IR (KBr): 3056, 3039, 2991,

2954, 2930, 2904, 2857, 1606, 1597, 1565, 1478, 1441, 1431, 1376, 1363, 1337, 1312, 1294, 1245, 1186, 1154, 1145, 1084, 1075, 1058, 1034, 1019, 1005, 959, 944, 937, 924, 891, 847, 815, 796, 767, 750, 725, 714, 666, 651, 620, 607, 589, 486, 449, 423.

4.5.4 [Cr(bztpen)(CH$_3$OH)](OTf)$_2$ (2)

Cr(OTf)$_2 \cdot$ 4H$_2$O (0.11 g, 0.25 mmol) and bztpen (0.11 g, 0.25 mmol) were dissolved in methanol. The ligand solution was added dropwise to the chromium(II) solution. The solution was stirred for 1.5 h in inert atmosphere. The complex solution was precipitated in diethyl ether. Green crystals could be obtained by diffusion of diethyl ether at –40 °C. Yield: 0.12 g (58 %). Anal.: C$_{30}$H$_{33}$N$_5$F$_6$O$_7$S$_2$Cr (805.73); C 44.93 (calcd. 44.72); H 4.29 (4.13); N 8.72 (8.69); S 8.42 (7.96) %. UV/Vis (CH$_3$OH): λ_{max} (lg ε): 344 nm (2.7), 420 nm (2.1), 502 nm (2.0) shoulder, 620 nm (1.9), IR (KBr): 3513, 3074, 2956, 2924, 2863, 2793, 2373, 2289, 1610, 1571, 1472, 1444, 1268, 1223, 1154, 1058, 1028, 936, 873, 845, 636, 571, 516, 425.

4.5.5 [Cr(bztpen)(NO)Cl]Cl (3)

Nitric oxide was purged for ca. 1 min through a solution of compound **1** in methanol under argon at –40 °C. The color of the solution changed from dark red to deep green. When the solution was added to diethyl ether a green precipitate was obtained. Crystals suitable for crystal structure analysis could be obtained by recrystallization in acetone. UV/Vis (CH$_3$OH): λ_{max} (lg ε): 460 nm (1.9), 623 nm (1.3), 677 nm (1.3), IR (KBr): 3410, 3058, 3032, 2953, 2787, 1692, 1609, 1589, 1568, 1482, 1437, 1299, 1157, 1110, 1053, 1028, 997, 955, 931, 867, 807, 754, 723, 706, 666, 609, 586, 501.

4.5.6 X-ray Diffraction

The X-ray crystallographic data of complexes **1**, **2**, and **3** were collected with a BRUKER NONIUS KappaCCD system using a BRUKER NONIUS FR591 rotating anode as radiation source and an OXFORD CRYOSYSTEMS low temperature system. Mo-K$_\alpha$ radiation with wavelength 0.71073 Å and a graphite monochromator was used. The PLATON MULABS semi-empirical absorption correction using multiple scanned reflection was applied. The structures were solved by direct methods in SHELXS97 and refined with SHELXL97 using full-matrix least squares.[75-76] All non-hydrogen atoms were refined anisotropically. Only the 50 % occupied hydrogen atoms were positioned geometrically.

5 Supporting Information for Chapter 4

5.1 Infrared Spectrum of the Reaction of [Cr(bztpen)Cl]Cl with Dioxygen

The resulting solution from the reaction of [Cr(bztpen)Cl]Cl with dioxygen, which is stable at room temperature, was precipitated in diethyl ether. The precipitate was dried and the solid was used to record an infrared spectrum using a KBr-pellet. The spectrum was compared with the spectrum of the starting complex.

As mentioned in Chapter 4, the assumption that a chromium end-on superoxido complex is formed by the reaction of [Cr(bztpen)Cl]Cl with dioxygen is supported by the infrared spectrum. Figure 5-1 and Figure 5-2 show sections of the IR spectrum with the relevant bands. The red line in Figure 5-1 shows the complex prior to the reaction with dioxygen. After the reaction, a new absorption band at 1160 cm^{-1} is observed. This band can be assigned as a ν(O–O) stretching vibration.[45] Nam and co-workers also described this band in the resonance Raman spectrum of their superoxido complex and compared this observation with other chromium(III) superoxido complexes in literature.[29]
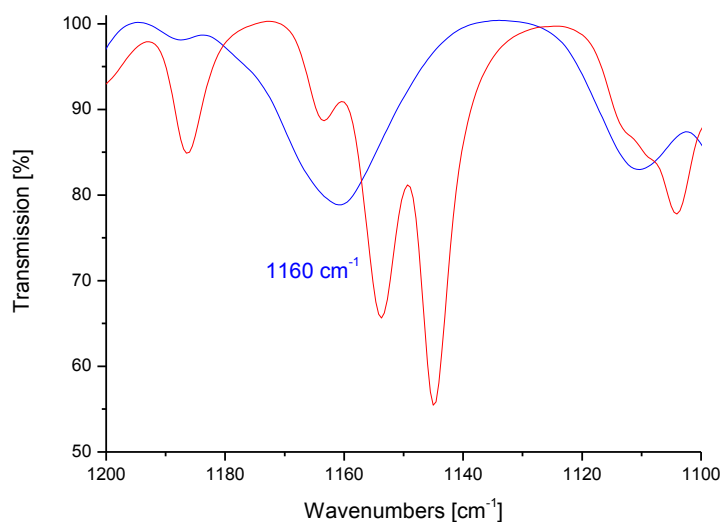
Figure 5-1: Infrared spectrum of compound **1** (red line) and compound **1** after reacting with dioxygen (blue line) in the range of 1200–1100 cm^{-1}. (KBr-pellet)

Figure 5-2 shows the resulting band at 554 cm^{-1} after the reaction with dioxygen (blue line). This band can be assigned to a ν(Cr–O) stretching vibration.[89]

554 cm^{-1}
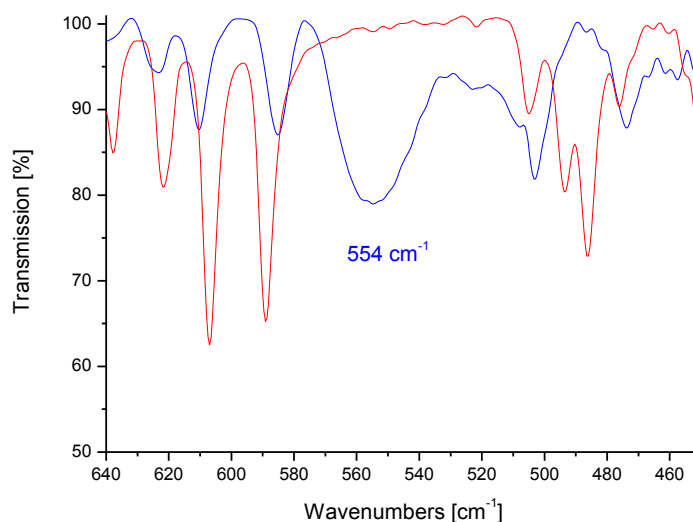
Figure 5-2: Infrared spectrum of compound **1** (red line) and compound **1** after reacting with dioxygen (blue line) in the range of 640–450 cm^{-1}. (KBr-pellet)

5.2 UV/Vis Spectra of the Reaction of [Cr(bztpen)(CH$_3$OH)](OTf)$_2$ with Hydrogen Peroxide and Triethylamine

The reaction of [Cr(bztpen)(CH$_3$OH)](OTf)$_2$ with hydrogen peroxide showed a similar UV/Vis spectrum than that of [Cr(bztpen)Cl]Cl. The spectrum with [Cr(bztpen)Cl]Cl is presented in Chapter 4 Figure 4-7. Figure 5-3 shows the spectroscopical changes when triethylamine as a base was added to the solution of [Cr(bztpen)(CH$_3$OH)](OTf)$_2$ in methanol together with hydrogen peroxide. The arising absorption maximum at 374 nm and a shoulder at 473 nm showed similar absorption maxima than the spectrum of the reaction of [Cr(bztpen)Cl]Cl, which is described in Chapter 4.
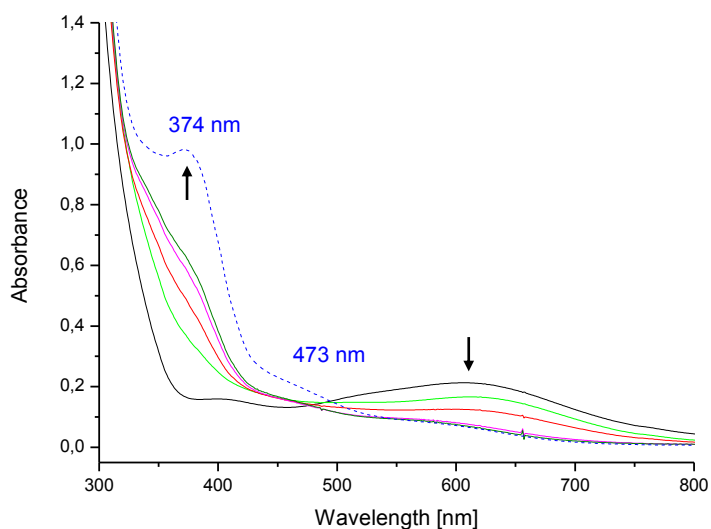
Figure 5-3: Compund **2** with hydrogen peroxide (black line) after a couple of days. The dashed line shows the solution after reaction with triethylamine for three days (complex concentration = 0.8 mmol·L^{-1}).

5.3 UV/Vis Spectrum of [Cr(bztpen)(NO)Cl]Cl

As described in Chapter 4, a chromium–NO complex [Cr(bztpen)(NO)Cl]Cl could be structurally characterized for the first time with a simple organic ligand. The complex was dissolved in methanol and the obtained UV/Vis spectrum showed three absorption maxima at 460 nm, 623 nm and 677 nm. The spectrum is shown in Figure 5-4.
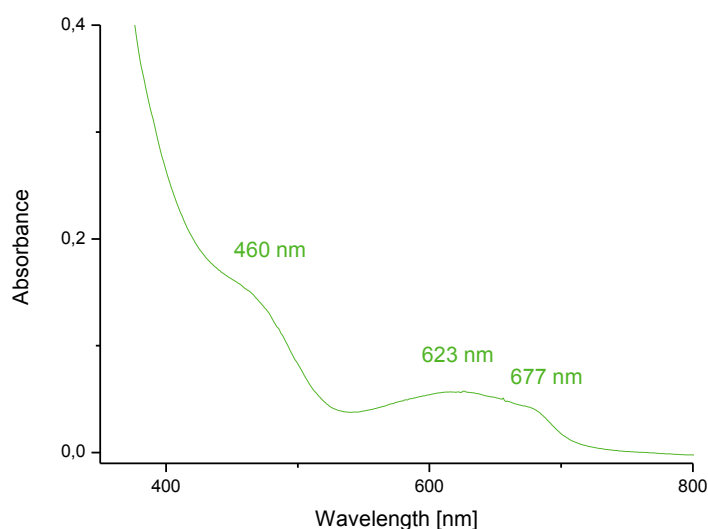
Figure 5-4: UV/Vis spectrum of **3** in methanol (complex concentration approx. 6 mmol·L^{-1}).

6 Oxidation of Bis(benzene)chromium in Organic Solvents with Dioxygen

This work is ready for submission to *Zeitschrift für Anorganische und Allgemeine Chemie*

Sabrina Schäfer, Christian Kleeberg and Christian Würtele

6.1 Abstract

In this work the reactivity of bis(benzene)chromium(0) towards dioxygen was investigated. By passing dioxygen through the complex in organic solution a yellow precipitate was obtained. This oxidation product could be structurally characterized as the mixed-valence chromium salt $[Cr(C_6H_6)_2]_2[Cr_2O_7]$. A reaction equation for the formation of the salt was proposed. It decomposed at room temperature after a couple of days.

6.2 Introduction

Bis(benzene)chromium(0) (**1**) (Figure 6-1) is a well-known compound. It was first synthesized in 1955 by Fischer and Hafner[44,93] and was the first sandwich complex with "two neutral benzene molecules π-bonded to a neutral, zero valent metal atom".[46] Different methods to synthesize this compound have been established in the past.[46,94-95] Furthermore, Elschenbroich *et al.* reported a η^6-coordination with unsubstituted pyridine for the first time.[53]
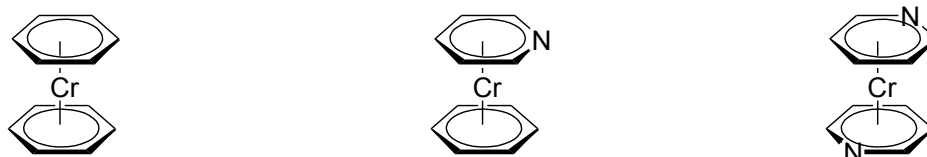
bis(η^6-benzene)chromium   (η^6-benzene)(η^6-pyridine)chromium   bis(η^6-pyridine)chromium

Figure 6-1:   Structural formula of a selection of bis(arene)chromium complexes.[53]

The reactivity of **1** was extensively investigated. The redox processes were studied in detail by electrochemical measurements.[96-97] It was found that the preparation of chromium(I) salts from the sandwich complex could be carried out by air oxidation in water followed by addition of an aqueous solution of different salts e. g. NH_4PF_6.[98] During these studies it was observed that $[Cr(C_6H_6)_2]^+$ salts are stable in neutral or basic aqueous solutions.[46] In 1971, Gribov *et al.*

reported the formation of a hydroxide $[Cr(C_6H_6)_2][OH]$ in the presence of moisture.[99-101] These compounds are interesting in the field of crystal engineering.[102]

The reaction of **1** with dioxygen under aprotic and anhydrous conditions has not been studied in detail. Elschenbroich investigated the reactivity of **1** towards sulfur dioxide in an non aqueous solution,[103] which led to the formation of $[Cr(C_6H_6)_2]^+$ salts with $[S_2O_6 \cdot 2SO_2]^{2-}$ as anion. In organic solutions compound **1** showed unusual oxidation behavior with dioxygen forming a yellow precipitate. This product could not be characterized so far, but it was proposed that the reaction might be similar to the oxidation of cobaltocene. The oxidation product of cobaltocene is proposed as $[Co(C_5H_5)_2]_2O_2$ with an oxygen bridge between two cyclopentadienyl groups.[54-55] Unpublished calculations by Holthausen, however, indicated the formation of a chromium peroxido complex.[56]

Furthermore, in anhydrous solutions the oxidation products $[Cr(C_6H_6)_2][CrO_4]$ and $[Cr(C_6H_6)_2]_2[CrO_4] \cdot [Cr(C_6H_6)_2]_2[Cr_2O_7]$ were proposed mainly from IR spectroscopic measurements.[99,104-105] However, so far none of these complexes was structurally characterized. It was therefore decided to investigate the reactivity of **1** towards dioxygen in organic solvents in more detail.

6.3 Results and Discussion

Different protocols for the synthesis of the starting material bis(benzene)chromium (**1**) are described in literature.[44,93-95] Herein, the method with aluminum chloride in a bomb tube was applied. In the first step of the reaction the bis(benzene)chromium(I) cation is formed (equation 1). In the next step the intermediate is reduced with dithionite to the final product **1** (equation 2). The resulting dark brown solid of **1** was dried under vacuum and finally sublimed under argon at 160 °C to yield the product in pure form.

(1) $3\ CrCl_3\ +\ 2\ Al\ +\ AlCl_3\ +\ 6\ C_6H_6\ \xrightarrow[\text{bomb tube}]{\text{24 h, 140 °C}}\ 3\ [Cr]^+\ AlCl_4^-$

(2) $2\ [Cr]^+\ +\ S_2O_4^{2-}\ +\ 4\ OH^-\ \longrightarrow\ 2\ [Cr]^0\ +\ 2\ SO_3^{2-}\ +\ 2\ H_2O$
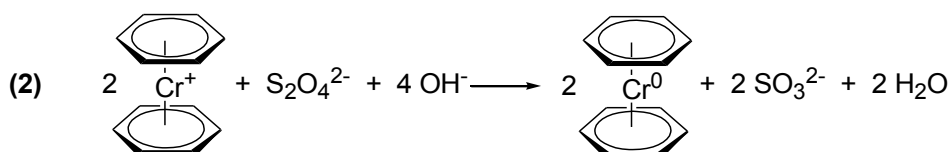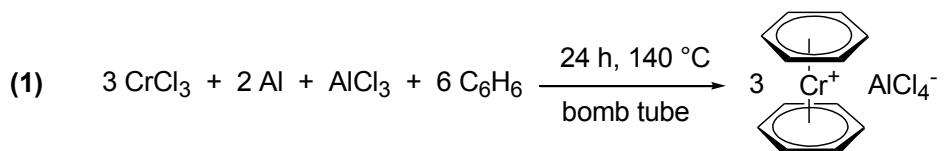
When **1** was dissolved in tetrahydrofuran and stored at –80 °C, crystals suitable for structure analysis could be obtained. The molecular structure of **1** was confirmed and the synthesis product was thus identified. The UV/Vis spectrum of compound **1** in methanol shows an absorption maximum at 310 nm (Figure 6-2). When passing dioxygen through the solution clear spectral changes could be observed. The resulting spectrum showed two new absorption maxima at 272 nm (lg ε = 4.0) and 334 nm (lg ε = 4.0). It is similar to a spectrum of a bis(benzene)chromium(I) cation in aqueous solution previously described in literature.[106]
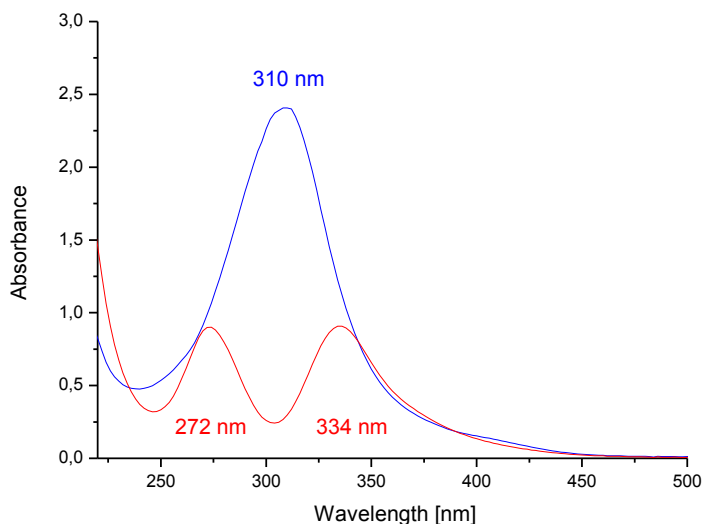
Figure 6-2:   UV/Vis spectra of **1** (blue line) in methanol before and after passing dioxygen through the solution (**2**) (red line) (complex concentration approx. 0.1 mmol·L^{-1}).

To characterize the yellow colored product, the oxidation reaction was performed in a more concentrated solution. A yellow precipitate immediately formed. For complete precipitation the reaction mixture was stored at –20 °C. The isolated precipitate is only stable at low temperatures. Dissolving the yellow product in a minimum amount of acetonitrile followed by diethyl ether diffusion at –20 °C yielded yellow crystals suitable for crystal structure analysis. The yellow oxidation product was identified as $[Cr(C_6H_6)_2]_2[Cr_2O_7]\cdot CH_3CN$ (**2**) and its molecular structure is shwon in Figure 6-3. Crystallographic data and structure refinement can be found in Table 6-1, selected bond lengths and angles Table 6-2.

The oxidation product is a mixed-valence chromium salt composed of two bis(benzene)chromium(I) cations $[Cr(C_6H_6)_2]^+$ and one dichromate anion $[Cr_2O_7]^{2-}$. Furthermore, a solvent molecule of acetonitrile is located in the unit cell. Compound **2** crystallizes in orthorhombic crystal system.
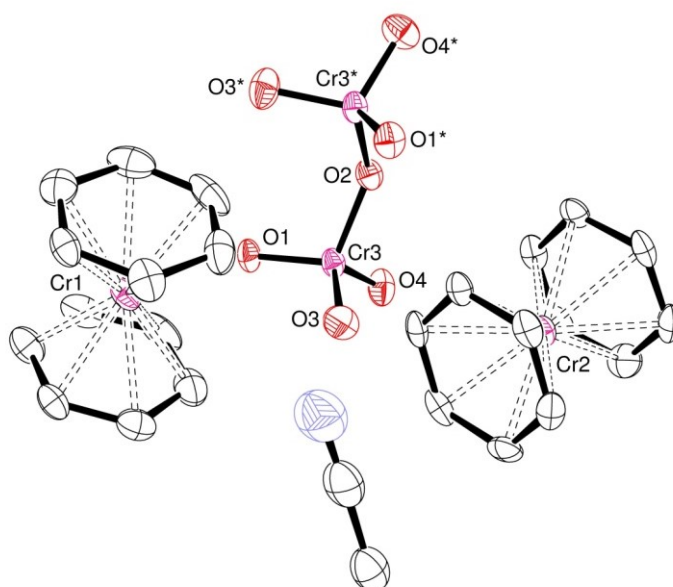
Figure 6-3: Molecular structure of **2** shown as an ORTEP plot with thermal ellipsoids set at 50 % probability. Hydrogen atoms and charges are omitted for clarity.

The formation of a similar mixed-valence chromium salt was previously observed by Braga *et al.*,[107] however, after following a different reaction method. They obtained crystals of the chromium salt [Cr(C$_6$H$_6$)$_2$][CrO$_3$(OCH$_3$)] as a minor by-product during their attempts to crystallize the bis(benzene)chromium(I) hydroxide from methanol.[107]

Table 6-1: Crystallographic data and structure refinement of **2**.

	2
Formula	C$_{26}$H$_{27}$Cr$_4$NO$_7$
Moiety formula	(C$_{12}$H$_{12}$Cr)$_2$, Cr$_2$O$_7$, CH$_3$CN
Formula weight	673.49 g·mol^{-1}
Temperature	100(2) K
Wavelength	0.71073 Å
Crystal system	orthorhombic
Space group	cmca
Unit cell dimensions	a = 17.0723(9) Å α = 90° b = 20.892(2) Å β = 90° c = 14.6597(9) Å γ = 90°
Cell volume	5228.9(5) Å^3
Z/Calculated density	8, 1.711 Mg/m^3
Absorption coefficient	1.665 mm^{-1}
F(000)	2736
θ range	2.39 to 25.00°
Limiting indices	−20<=h<=20, −24<=k<=24,

	–17<=l<=17
Reflections collected / unique	44635 / 2391 [R(int) = 0.1374]
Completeness to θ	99.9 %
Absorption correction	semi-empirical from equivalents
Refinement method	Full-matrix least-squares on F^2
Data / restraints / parameters	2391 / 0 / 186
Goodness-of-fit on F^2	1.042
Final R indices [I>2σ(I)]	R_1 = 0.0423, wR_2 = 0.0885
R indices (all data)	R_1 = 0.0783, wR_2 = 0.1018
Largest diff. peak and hole	0.494 and –0.378 e.$Å^3$

Table 6-2: Selected bond lengths (Å) and bond angles (°) of **2**.

2		**2**	
Cr(1)–C(1)	2.153(5)	C(1)–Cr(1)–C(2)	38.69(17)
Cr(1)–C(2)	2.146(4)	C(1)–Cr(1)–C(3)	69.55(16)
Cr(1)–C(3)	2.122(4)	C(1)–Cr(1)–C(4)	82.10(18)
Cr(1)–C(4)	2.132(4)	C(1)–Cr(1)–C(5)	69.05(19)
Cr(1)–C(5)	2.152(4)	C(1)–Cr(1)–C(6)	38.46(19)
Cr(1)–C(6)	2.143(4)	C(2)–Cr(1)–C(3)	38.34(15)
Cr(2)–C(7)	2.128(5)	C(2)–Cr(1)–C(4)	69.28(18)
Cr(2)–C(8)	2.144(4)	C(2)–Cr(1)–C(5)	82.15(17)
Cr(2)–C(9)	2.149(4)	C(2)–Cr(1)–C(6)	69.54(18)
Cr(2)–C(10)	2.158(6)	C(3)–Cr(1)–C(4)	38.25(15)
Cr(2)–C(11)	2.135(6)	C(3)–Cr(1)–C(5)	69.41(16)
Cr(2)–C(12)	2.131(4)	C(3)–Cr(1)–C(6)	81.90(16)
Cr(2)–C(13)	2.141(4)	C(4)–Cr(1)–C(5)	38.53(16)
Cr(2)–C(14)	2.148(6)	C(4)–Cr(1)–C(6)	68.87(17)
Cr(3)–O(1)	1.618(3)	C(5)–Cr(1)–C(6)	37.64(18)
Cr(3)–O(2)	1.789(2)	C(7)–Cr(2)–C(8)	38.43(12)
Cr(3)–O(3)	1.607(3)	C(7)–Cr(2)–C(9)	69.25(17)
Cr(3)–O(4)	1.618(3)	C(7)–Cr(2)–C(10)	82.00(2)
		C(8)–Cr(2)–C(9)	38.24(16)
		C(8)–Cr(2)–C(10)	69.38(17)
		C(9)–Cr(2)–C(10)	38.46(13)
		C(11)–Cr(2)–C(12)	38.47(12)
		C(11)–Cr(2)–C(13)	69.22(17)
		C(11)–Cr(2)–C(14)	82.20(2)
		C(12)–Cr(2)–C(13)	38.05(15)
		C(12)–Cr(2)–C(14)	69.41(18)
		C(13)–Cr(2)–C(14)	38.66(14)

O(1)–Cr(3)–O(2)	110.35(11)
O(1)–Cr(3)–O(3)	109.63(15)
O(1)–Cr(3)–O(4)	110.50(14)
O(2)–Cr(3)–O(3)	110.26(13)
O(2)–Cr(3)–O(4)	105.58(15)
O(3)–Cr(3)–O(4)	110.46(16)

A proposed reaction equation for the formation of **2** is presented in equation 3.

$$(3) \quad 8\ Cr^0 + 7\ O_2 \longrightarrow 2\ Cr_2O_7^{2-} + 4\ Cr^+ + 8$$
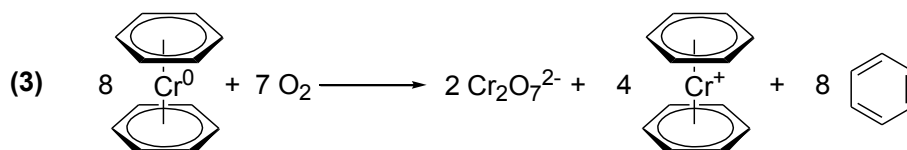
The release of benzene was detected by GC-MS measurements. Benzene was found at a retention time of 2.19 min. Dichromate was detected by addition of an acidic hydrogen peroxide solution to form the blue chromium(V) peroxide as described in literature and details are reported in the Experimental Section.[108]

As described above, the dried yellow oxidation product **2** is not stable at room temperature and turned green after a couple of days. The green color indicated a chromium(III) compound. The poor solubility of the resulting product suggests that chromium(III) oxide had formed. The reaction is proposed as follows.

$$(4) \quad 4\ Cr^+ + 2\ Cr_2O_7^{2-} \longrightarrow 4\ Cr_2O_3 + O_2 + 8$$
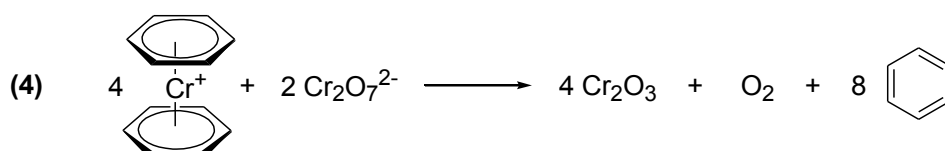
6.4 Conclusions

In contrast to the previously proposed structures the yellow product of the oxidation of bis(benzene)chromium could be structurally characterized as the mixed-valence chromium salt $[Cr(C_6H_6)_2]_2[Cr_2O_7]$. This offers a better understanding of the reaction behavior of chromium complexes. Reaction equations for the formation of the oxidation product and the consecutive decomposition at room temperature could be proposed.

6.5 Experimental Section

6.5.1 Materials

Reagents and solvents used were commercially available. Bis(benzene)chromium was synthesized according to a slightly modified literature method.[44,93] $[Cr(C_6H_6)_2]PF_6$ was prepared according the literature.[98] Preparation and handling of air-sensitive compounds were carried out in a glove box filled with argon (MBraun, Germany; water and dioxygen less than 1 ppm) or using Schlenk techniques.

6.5.2 Equipment

UV/Vis absorption spectra were recorded using an Agilent 8453-spectrometer. The measurements were performed using quartz cuvettes. GC-MS data were obtained using a Quadrupol-MS HP MSD 5971 (EI) with a J&W quartz glass GC column (30 m x 0.25 mm, 0.25 μm DB-5 MS).

6.5.3 Bis(benzene)chromium $Cr(C_6H_6)_2$ (1)

Anhydrous chromium(III) chloride (5.94 g, 0.04 mol), aluminum(III) chloride (12.00 g, 0.09 mol) and aluminum powder (0.78 g, 0.03 mol) were filled in a bomb tube (V = 75.4 cm^3). Afterwards, anhydrous benzene (19.5 mL) was added. The bomb tube was cooled in liquid nitrogen, evacuated and afterwards flame sealed. The bomb tube was stored for 24 h at 140 °C in a drying oven. During that time the bomb tube was frequently removed from the oven, shaked and returned to the oven. After the reaction time was completed, the bomb tube was again cooled in liquid nitrogen and opened. The resulting dark red colored product was transferred under a constant flow of argon into a 1 L three-necked flask. Afterwards, degassed distilled water (150 mL) was slowly added whilst cooling in an ice bath. After an exothermic reaction the color of the solution turned to green and the actual precipitate had dissolved. Degassed methanol (30 mL), potassium hydroxide (45 g, 0.80 mol) and sodium dithionite (45 g, 0.26 mol) were added whilst cooling in an ice bath. Thus, the bis(benzene)chromium cation was reduced to the final product bis(benzene)chromium. To separate the final product from the solution, degassed benzene (200 mL) was added and stirred for 2 h. The benzene phase turned brownish and the aqueous phase light green. The benzene phase was transferred into another flask (2 L). Furthermore, the solution was washed three times with degassed benzene (150 mL) until the benzene phase was only slightly colored. The benzene phase was dried over night with potassium hydroxide. After the benzene phase was transferred to a flask (1 L), the benzene was removed under vacuum (condensation). The resulting dark brown solid was dried under vacuum and finally sublimed

under argon at 160 °C. Yield: 3.24 g (63 %). ^{1}H NMR (400 MHz, C_6D_6, δ/ppm): 4.33 (s, 6 H). UV/Vis (CH_3OH): λ_{max}(lg ε): 310 nm (4.4).

6.5.4 $[Cr(C_6H_6)_2]_2(Cr_2O_7)\cdot CH_3CN$ (2)

1 was dissolved in THF in inert atmosphere. Afterwards, dioxygen was passed through the solution and a yellow precipitate formed immediately. For complete precipitation the reaction mixture was stored at –20 °C. The product is only stable at low temperatures. Dissolving the yellow product in a minimum amount of acetonitrile and subsequent diffusion of diethyl ether at –20 °C resulted in preparation of yellow crystals suitable for X-ray crystal structure determination.

6.5.5 GC-MS Measurements

1 was dissolved in dimethyl sulfoxide in inter atmosphere. Afterwards, dioxygen was passed through the solution. A part of the solution was diluted in dichlormethane and a GC-MS spectrum was recorded. Benzene was confirmed by comparison with a database (Spectral Database for Organic Compounds SDBS).

6.5.6 Detection of Chromium(VI)

Compound **2** was dissolved in distilled water whilst cooling in an ice bath. The resulting yellow solution was layered with diethyl ether and afterwards a 30 % solution of hydrogen peroxide was added. With addition of 1–2 drops of concentrated nitric acid the diethyl ether phase turned blue. The evidence is positive, because the blue chromium(V) peroxide is formed, which is stabilized in the diethyl ether phase.

Control reactions with **1** and $[Cr(C_6H_6)_2]PF_6$ were carried out and showed no positive results.

6.5.7 X-ray Diffraction

The crystal was mounted in inert perfluoroether oil on top of a human hair and rapidly transferred to the cold nitrogen gas stream of the diffractometer. The data were collected using an Oxford Diffraction Xcalibur E instrument using monochromated MoK_α radiation. The data were integrated and an empirical absorption correction was performed employing the CrysAlisPro software.[109] The structure was solved employing the program SHELXS-97 (direct methods) and refined anisotropically for all non-hydrogen atoms by full-matrix least squares on all F^2 using SHELXL-97.[110] All hydrogen atoms were refined using a riding model, with a common Uiso restrained to be 1.2 (1.5 for methyl groups) times the equivalent isotropic displacement parameter of the parent atom.

7   Supporting Information for Chapter 6

7.1   Illustration of the Bis(benzene)chromium Synthesis

In the following pictures some parts of the synthesis of bis(benzene)chromium are illustrated. Figure 7-1 a) shows the purpose-built bomb tube. After loading with the educts, the bomb tube was flame sealed. To store the bomb tube over 24 h in a drying oven it was placed in a vessel as shown in Figure 7-1 b).

Figure 7-1:   a) The bomb tube for the synthesis. b) Vessel with which the bomb tube was placed in the oven.

After the reaction the product was transferred into a 1 L flask and further treated. Figure 7-2 shows the flask with the final product in aqueous solution before separation with benzene. The added benzene turned brown and separation was repeated until the aqueous phase was light green. It was transferred into a flask with potassium hydroxide. (Figure 7-2 b))

Figure 7-2:   a) Final product before separation. b) Separation of the final product with benzene. The benzene was transferred into a flask with potassium hydroxide.

After drying the benzene phase was separated from potassium hydroxide and transferred into another flask. Benzene was then removed under vacuum (condensation). This step is shown in Figure 7-3.

Figure 7-3: Condensation of benzene.

The resulting dark brown solid of bis(benzene)chromium was dried under vacuum and finally sublimated in inert atmosphere at 160 °C. Figure 7-4 a) shows the equipment. Figure 7-4 b) shows the cold trap with crystals of bis(benzene)chromium.

Figure 7-4: a) Sublimation of bis(benzene)chromium. b) Cold trap with crystals of bis(benzene)chromium.

8 Summary/Zusammenfassung

8.1 Summary

Oxidation reactions in nature are an interesting topic since these reactions occur under ambient conditions, which is the reason why modeling these systems for industrial use has become a lucrative and well investigated field of science. Metalloenzymes with iron or copper ions located in the active site are essential compounds in nature. Therefore, in recent years, a number of iron or copper complexes have been studied as functional model complexes for these enzymes. It turned out that investigation of these complexes can be complicated, because of the instability of the "dioxygen adduct complexes". In contrast to that, handling of "dioxygen adduct complexes" of chromium proved to be less difficult and stable chromium peroxido and oxido complexes have been reported in literature. Therefore, chromium complexes with ligands of which iron and copper complexes are already known, were investigated in this thesis.

Firstly, chromium(II) complexes with the following tripodal amine ligands based on the related tren system (Figure 8-1) were synthesized.

tmpa   Me$_2$uns-penp   Me$_4$apme   Me$_6$tren
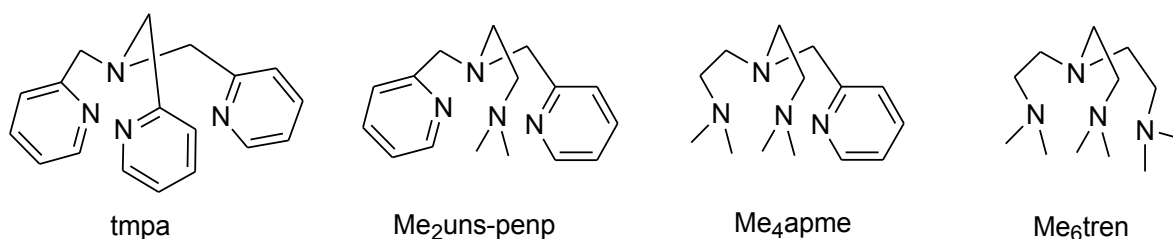
Figure 8-1: Tripodal Ligands.

The complexes [Cr(tmpa)Cl$_2$] and [Cr(tmpa)Cl]$_2$(BPh$_4$)$_2$ could be prepared according to the literature. Furthermore, spectroscopic data for the reaction of [Cr(tmpa)Cl]$_2$(BPh$_4$)$_2$ with dioxygen to form a chromium(III) μ-oxido complex were reported. A chromium(III) bis(μ-hydroxido) complex [Cr(tmpa)OH]$_2$(OTf)$_4$ was structurally characterized. This complex is already known in literature with different counter anions.

Similar to the reported chromium(II) complexes, [Cr(Me$_2$uns-penp)Cl]$_2$(BPh$_4$)$_2$, [Cr(Me$_6$tren)Cl]Cl and [Cr(Me$_4$apme)Cl]BPh$_4$ were synthesized and structurally characterized. Furthermore, a chromium(III) complex [Cr(Me$_4$apme)Cl$_3$] was structurally characterized.

The oxidation behavior of these complexes towards organic substrates like toluene was investigated. By using the complex [Cr(Me$_4$apme)Cl]BPh$_4$ a maximum yield (25 %) of benzaldehyde could be observed. Low temperature stopped-flow measurements led to the

suggestion that the reaction of [Cr(Me$_4$apme)Cl]BPh$_4$ with dioxygen formed an end-on superoxido intermediate.

Another object of this thesis was the investigation of "dioxygen adduct complexes" of chromium(II) complexes with the ligand bztpen (Figure 8-2).

Figure 8-2: The ligand bztpen.

The starting materials [Cr(bztpen)Cl]Cl and [Cr(bztpen)(CH$_3$OH)](OTf)$_2$ could be structurally characterized. Based on these compounds, the reactivity towards dioxygen was investigated using low temperature stopped-flow techniques. For the reaction with [Cr(bztpen)(CH$_3$OH)](OTf)$_2$ the decompositi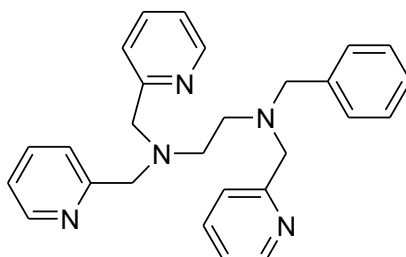on of an unknown species could be tracked spectroscopically. However, the absorption maxima could not be clearly assigned to a "dioxygen adduct complex". During the reaction of [Cr(bztpen)Cl]Cl with dioxygen strong support for the formation of an end-on superoxido complex [Cr(bztpen)(O$_2$)Cl]Cl could be obtained.

Due to the fact that NO$^-$ and dioxygen are isoelectronic, a comparison of NO–metal complexes with "dioxygen adduct complexes" is very interesting. During these investigations a chromium–NO complex was structurally characterized and thus useful structural information about the presence of the dioxygen intermediates was obtained. [Cr(bztpen)(NO)Cl]Cl is the first structural characterized chromium–NO complex with a simple organic ligand.

Moreover, the reactivity of bis(benzene)chromium toward dioxygen using organic solvents was investigated in this work. The formation of a yellow oxidation product was repeatedly observed, the structural characterization, however, repeatedly failed due to the fact that the yellow precipitate was only stable at low temperatures and decomposed to a green species after a couple of days at room temperature. Different suggestions about the structure of the yellow precipitate were made. Elschenbroich suggested that the oxidation product might be similar to the reaction of cobaltocene and dioxygen. Herein it is proposed that the oxygen is bridged between two cyclopentadienyl groups. Holthausen suggested a chromium peroxido complex based of DFT calculations. The resulting yellow precipitate could be structurally characterized as a mixed-valence chromium salt [Cr(C$_6$H$_6$)$_2$]$_2$[Cr$_2$O$_7$]·CH$_3$CN. (Figure 8-3)

Furthermore, a reaction equation for the formation of the oxidation product was suggested. GC-MS measurements and a chromium(VI) detection proved the proposed equation.
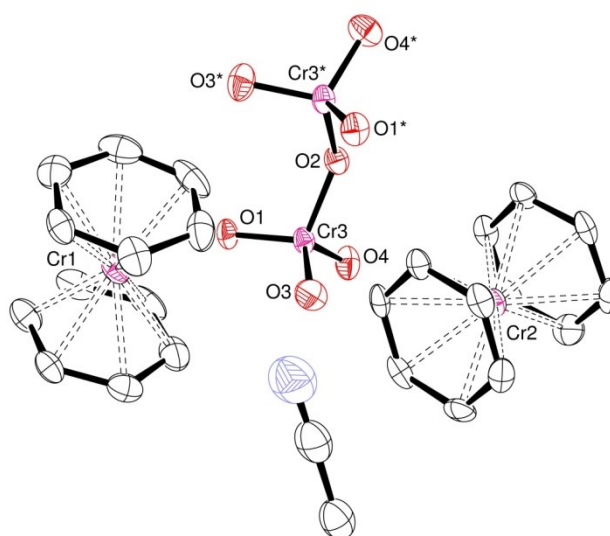

Figure 8-3: Molecular structure of the mixed-valence chromium salt $[Cr(C_6H_6)_2]_2[Cr_2O_7] \cdot CH_3CN$.

8.2 Zusammenfassung

Oxidationsreaktionen in der Natur sind von besonderer Bedeutung, da sie auf effiziente und selektive Weise unter milden Bedingungen ablaufen. Daher besteht großes Interesse, solche Oxidationsreaktionen mit Hilfe von Modellkomplexen nachzuahmen und so industriell nutzbar zu machen. Es ist bekannt, dass für diese Reaktionen in der Natur Metallenzyme benötigt werden, die Eisen- oder Kupferionen im aktiven Zentrum enthalten. In den vergangenen Jahren wurden deshalb bereits zahlreiche Modellkomplexe mit Eisen- und Kupferionen untersucht. Dabei stellte sich heraus, dass die Untersuchung dieser Komplexe aufgrund der Instabilität der „Sauerstoff Addukt Komplexe" oft sehr schwierig ist. Dagegen hat Chrom die Eigenschaft stabile „Sauerstoff Addukt Komplexe" zu bilden, was die eingehende Untersuchung dieser Verbindungen ermöglicht. So wurden bereits Peroxido und Oxido Komplexe des Chroms isoliert und charakterisiert. Aus diesem Grund wurden in der vorliegenden Arbeit verschiedene Chromkomplexe mit Liganden untersucht, von denen die entsprechenden Eisen- und Kupferkomplexe bereits bekannt sind.

Zunächst wurden folgende tripodale Aminliganden mit tren-Gerüst (Abb. 9-1) zur Synthese von Chrom(II) Komplexen eingesetzt.

| tmpa | Me$_2$uns-penp | Me$_4$apme | Me$_6$tren |
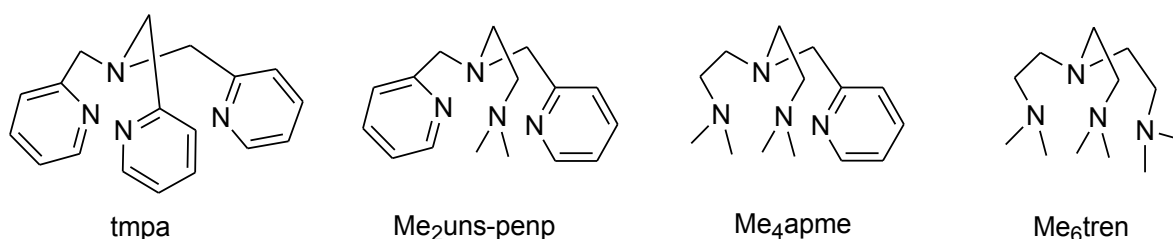
Abb. 9-1: Tripodale Liganden.

Die Komplexe [Cr(tmpa)Cl$_2$] und [Cr(tmpa)Cl]$_2$(BPh$_4$)$_2$ konnten, wie in der Literatur beschrieben, dargestellt werden. Außerdem konnten die spektroskopischen Daten der Reaktion von [Cr(tmpa)Cl]$_2$(BPh$_4$)$_2$ mit Sauerstoff zu einem Chrom(III) µ-oxido Komplex aufgenommen werden. Mit dem Liganden tmpa konnte zudem ein Chrom(III) bis(µ-hydroxido) Komplex [Cr(tmpa)OH]$_2$(OTf)$_4$ kristallographisch charakterisiert werden. Dieser ist bisher nur mit anderen Gegenionen in der Literatur bekannt.

Analog zu den oben genannten Chrom(II)komplexen konnten die Komplexe [Cr(Me$_2$uns-penp)Cl]$_2$(BPh$_4$)$_2$, [Cr(Me$_6$tren)Cl]Cl und [Cr(Me$_4$apme)Cl]BPh$_4$ dargestellt und kristallographisch charakterisiert werden. Außerdem konnte ein Chrom(III)komplex [Cr(Me$_4$apme)Cl$_3$] dargestellt und ebenfalls kristallographisch charakterisiert werden.

Die dargestellten Chrom(II)komplexe wurden dahingehend untersucht, ob sie in der Lage sind organische Substrate wie Toluol zu oxidieren. Die Oxidation von Toluol zu Benzaldehyd konnte beobachtet werden, wobei der Einsatz des Komplexes [Cr(Me$_4$apme)Cl]BPh$_4$ mit

25 % die größte Ausbeute lieferte. Mit Hilfe von Tieftemperatur „Stopped-Flow" Untersuchungen konnte belegt werden, dass die Reaktion dieses Komplexes mit Sauerstoff über ein instabiles end-on Superoxido Intermediat verläuft.

Ein weiteres Ziel dieser Arbeit war die Untersuchung aktiver Sauerstoffintermediate der Chrom(II)komplexe mit dem Liganden bztpen (Abb. 9-2).

Abb. 9-2:   Der Ligand bztpen.

Für die Untersuchungen konnten die Chrom(II)komplexe [Cr(bztpen)Cl]Cl und [Cr(bztpen)(CH$_3$OH)](OTf)$_2$ erfolgreich dargestellt und kristallographisch charakterisiert werden. Ausgehend von diesen Verbindungen wurde d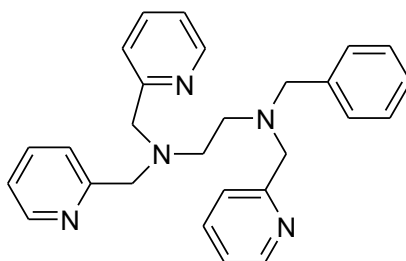ie Reaktion mit Sauerstoff mit Hilfe von Tieftemperatur „Stopped-Flow" Messungen verfolgt. Bei der Reaktion von [Cr(bztpen)(CH$_3$OH)](OTf)$_2$ ließ sich der Abbau einer Spezies spektroskopisch verfolgen. Die Banden konnten nicht eindeutig einem „Sauerstoff Addukt Komplex" zugeordnet werden, aber bei der Reaktion von [Cr(bztpen)Cl]Cl mit Sauerstoff konnten Hinweise auf die Bildung eines end-on Superoxido Komplexes [Cr(bztpen)(O$_2$)Cl]Cl erhalten werden.

Da NO$^-$ isoelektronisch zu Sauerstoff ist, ist ein Vergleich von NO–Metallkomplexen mit „Sauerstoff Addukt Komplexen" interessant. Im Rahmen dieser Untersuchungen konnte ein Chrom–Stickstoffmonoxid Komplex kristallographisch charakterisiert werden. Dadurch konnten strukturelle Hinweise über das Vorliegen der „Sauerstoff Addukt Komplexe" gewonnen werden. Dabei stellt [Cr(bztpen)(NO)Cl] den ersten kristallographisch charakterisierten Chrom–NO Komplex mit einem einfachen organischen Liganden dar.

Im Rahmen dieser Arbeit wurde weiterhin die Reaktion von Bis(benzol)chrom mit Sauerstoff in organischen Lösungsmitteln untersucht. Die Entstehung eines gelben Oxidationsproduktes konnte schon mehrfach beobachtet werden, allerdings gelang eine Charakterisierung bisher noch nicht. Das gelbe Produkt ist nur bei tiefen Temperaturen stabil und wandelt sich bei Raumtemperatur nach einigen Tagen zu einer grünen Spezies um.

Elschenbroich vermutete, dass es sich um eine ähnliche Struktur handelte, die für das Oxidationsprodukt von Cobaltocen vorgeschlagen ist. Hier befindet sich eine Sauerstoff-Brücke zwischen den Cyclopentadienylgruppen. Holthausen postulierte das Vorliegen eines Chrom Peroxido Komplexes. Der entstehende gelbe Niederschlag konnte erfolgreich als

gemischt valentes Chromsalz [Cr(C$_6$H$_6$)$_2$]$_2$[Cr$_2$O$_7$]·CH$_3$CN kristallographisch charakterisiert werden. (Abb. 9-3) Außerdem konnte eine Reaktionsgleichung angegeben werden, die die Bildung des Oxidationsproduktes beschreibt. GC-MS Messungen und ein Chrom(VI)-Nachweis bestätigen diese Gleichung.
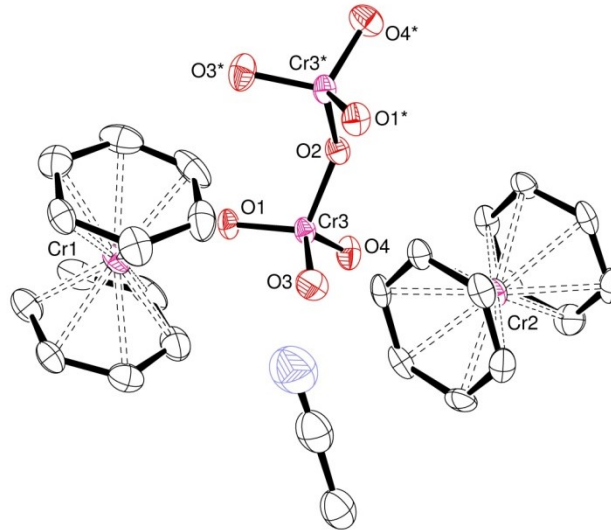
Abb. 9-3:   Molekülstruktur des gemischt valenten Chromsalzes [Cr(C$_6$H$_6$)$_2$]$_2$[Cr$_2$O$_7$]·CH$_3$CN.

Der Lebenslauf wurde aus der elektronischen Version der Arbeit entfernt.

The curriculum vitae was removed from the electronic version of the paper.

Publications and Presentations

Journal Article

- **Investigation of Chromium Complexes with a Series of Tripodal Ligands**
  S. Schäfer, J. Becker, A. Beitat, C. Würtele *Z. Anorg. Allg. Chem.*, **2013**, *639*, 2269.

Presentations

- Poster presentation: *Bestimmung des löslichen Anteils der A-Fraktion – Eine Hilfe zur Beurteilung der Gefährdungssituation am Arbeitsplatz*
  53. Wissenschaftlichen Jahrestagung der Deutschen Gesellschaft für Arbeitsmedizin und Umweltmedizin e.V., Bregenz

- Poster presentation: *Thermoanalytische Untersuchungen einer standardisierten Probe zur Bestimmung des löslichen Anteils der alveolengängigen Staub-Fraktion*
  20. Ulm-Freiberger Kalorimetrietage, Freiberg

- Poster presentation: *Thermoanalytische und elektronenmikroskopische Charakterisierung einer standardisierten Staubprobe zur Bestimmung des löslichen Anteils der alveolengängigen Fraktion im Rahmen des durch die DFG festgelegten neuen Allgemeinen Staubgrenzwertes*
  GEFTA-SKT-Joint Meeting on Thermal Analysis and Calorimetry, Saarbrücken

- Poster presentation: *Untersuchungen des Oxidationspotentials von Chromkomplexen mit tripodalen Liganden gegenüber organischen Substraten*
  GDCh-Wissenschaftsforum, Bremen

- Oral presentation: *Reaktivitätsuntersuchungen von Chromkomplexen mit Sauerstoff*
  7. Koordinationschemie-Treffen, Stuttgart

- Poster presentation: *Reactivity of Chromium Complexes towards Dioxygen*
  3rd European Chemistry Congress, Nürnberg

9 References

(1)   Special Issue on Dioxygen Activation by Metalloenzymes and Models (Ed.: Nam, W.) *Acc. Chem. Res.* **2007**, *40*, 465.

(2)   Schindler, S. *Eur. J. Inorg. Chem.* **2000**, 2311.

(3)   Costas, M.; Mehn, M. P.; Jensen, M. P.; Que, L. *Chem. Rev.* **2004**, *104*, 939.

(4)   Lewis, E. A.; Tolman, W. B. *Chem. Rev.* **2004**, *104*, 1047.

(5)   Mirica, L. M.; Ottenwaelder, X.; Stack, T. D. P. *Chem. Rev.* **2004**, *104*, 1013.

(6)   Reedijk, J.; Bouwman, E. *Bioinorganic Catalysis*; 2. ed.; Marcel Dekker: New York, 1999.

(7)   Simandi, L. I. *Advances in Catalytic Activation of Dioxygen by Metal Complexes*; Kluwer Academic Publisher: Dordrecht, Boston, London, 2003; Vol. 26.

(8)   Kitajima, N.; Moro-oka, Y. *Chem. Rev.* **1994**, *94*, 737.

(9)   Tolman, W. B. *Acc. Chem. Res.* **1997**, *30*, 227.

(10)   Than, R.; Feldmann, A. A.; Krebs, B. *Coord. Chem. Rev.* **1999**, *182*, 211.

(11)   Tshuva, E. Y.; Lippard, S. J. *Chem. Rev.* **2004**, *104*, 987.

(12)   Kryatov, S. V.; Rybak-Akimova, E. V.; Schindler, S. *Chem. Rev.* **2005**, *105*, 2175.

(13)   Que, L. *Acc. Chem. Res.* **2007**, *40*, 493.

(14)   McDonald, A. R.; Que, L. *Coord. Chem. Rev.* **2013**, *257*, 414.

(15)   de Visser, S. P.; Rohde, J.-U.; Lee, Y.-M.; Cho, J.; Nam, W. *Coord. Chem. Rev.* **2013**, *257*, 381.

(16)   Kitajima, N.; Fujisawa, K.; Morooka, Y.; Toriumi, K. *J. Am. Chem. Soc.* **1989**, *111*, 8975.

(17)   Jacobson, R. R.; Tyeklar, Z.; Farooq, A.; Karlin, K. D.; Liu, S.; Zubieta, J. *J. Am. Chem. Soc.* **1988**, *110*, 3690.

(18)   Tyeklar, Z.; Jacobson, R. R.; Wei, N.; Murthy, N. N.; Zubieta, J.; Karlin, K. D. *J. Am. Chem. Soc.* **1993**, *115*, 2677.

(19)   Komiyama, K.; Furutachi, H.; Nagatomo, S.; Hashimoto, A.; Hayashi, H.; Fujinami, S.; Suzuki, M.; Kitagawa, T. *Bull. Chem. Soc. Jpn.* **2004**, *77*, 59.

(20)   Würtele, C.; Sander, O.; Lutz, V.; Waitz, T.; Tuczek, F.; Schindler, S. *J. Am. Chem. Soc.* **2009**, *131*, 7544.

(21)   Hoppe, T.; Schaub, S.; Becker, J.; Würtele, C.; Schindler, S. *Angew. Chem. Int. Ed.* **2013**, *52*, 870.

(22)   Kent, B. E. *Coord. Chem. Rev.* **2010**, *254*, 1607.

(23)   Cho, J.; Sarangi, R.; Nam, W. *Acc. Chem. Res.* **2012**, *45*, 1321.

(24)   Cho, J.; Jeon, S.; Wilson, S. A.; Liu, L. V.; Kang, E. A.; Braymer, J. J.; Lim, M. H.; Hedman, B.; Hodgson, K. O.; Valentine, J. S.; Solomon, E. I.; Nam, W. *Nature* **2011**, *478*, 502.

(25)   Rohde, J.-U.; In, J.-H.; Lim, M. H.; Brennessel, W. W.; Bukowski, M. R.; Stubna, A.; Münck, E.; Nam, W.; Que, L. *Science* **2003**, *299*, 1037.

(26)   Vollhardt, K. P. C.; Schore, N. E. *Organische Chemie*; 4. ed.; Wiley-VCH: Weinheim, 2005.

(27)   Qin, K.; Incarvito, C. D.; Rheingold, A. L.; Theopold, K. H. *Angew. Chem. Int. Ed.* **2002**, *41*, 2333.

(28)   Ramsey, C. M.; Cage, B.; Nguyen, P.; Abboud, K. A.; Dalal, N. S. *Chem. Mater.* **2003**, *15*, 92.

(29)   Cho, J.; Woo, J.; Nam, W. *J. Am. Chem. Soc.* **2010**, *132*, 5958.

(30)   Cho, J.; Woo, J.; Han, J. E.; Kubo, M.; Ogura, T.; Nam, W. *Chem. Sci.* **2011**, *2*, 2057.

(31)   Cho, J.; Woo, J.; Nam, W. *J. Am. Chem. Soc.* **2012**, *134*, 11112.

(32)   Yokoyama, A.; Han, J. E.; Cho, J.; Kubo, M.; Ogura, T.; Siegler, M. A.; Karlin, K. D.; Nam, W. *J. Am. Chem. Soc.* **2012**, *134*, 15269.

(33)   Blackman, A. G. *Polyhedron* **2005**, *24*, 1.

(34)   Anderegg, G.; Wenk, F. *Helv. Chim. Acta* **1967**, *50*, 2330.

(35)   Britovsek, G. J. P.; England, J.; White, A. J. P. *Inorg. Chem.* **2005**, *44*, 8125.

(36)   Robertson, N. J.; Carney, M. J.; Halfen, J. A. *Inorg. Chem.* **2003**, *42*, 6876.

(37)   Nebe, T.; Beitat, A.; Wuertele, C.; Duecker-Benfer, C.; van, E. R.; McKenzie, C. J.; Schindler, S. *Dalton Trans.* **2010**, *39*, 7768.

(38)   Rohde, J.-U.; Torelli, S.; Shan, X.; Lim, M. H.; Klinker, E. J.; Kaizer, J.; Chen, K.; Nam, W.; Que, L. *J. Am. Chem. Soc.* **2004**, *126*, 16750.

(39)   Klinker, E. J.; Kaizer, J.; Brennessel, W. W.; Woodrum, N. L.; Cramer, C. J.; Que, L. *Angew. Chem. Int. Ed.* **2005**, *44*, 3690.

(40)   Hazell, A.; McKenzie, C. J.; Nielsen, L. P.; Schindler, S.; Weitzer, M. *J. Chem. Soc., Dalton Trans.* **2002**, 310.

(41)   Eisenberg, R.; Meyer, C. D. *Acc. Chem. Res.* **1975**, *8*, 26.

(42)   Hayton, T. W.; Legzdins, P.; Sharp, W. B. *Chem. Rev.* **2002**, *102*, 935.

(43)   Theopold, K. H.; Kucharczyk, R. R. *Encyclopedia of Inorganic and Bioinorganic Chemistry*; John Wiley & Sons, Ltd: 2011.

(44)   Fischer, E. O.; Hafner, W. *Z. Naturforschg.* **1955**, *10b*, 665.

(45)   Janiak, C.; Klapötke, T. M.; Meyer, H.-J. *Moderne Anorganische Chemie*; 2. ed.; Walter de Gruyter: Berlin, New York, 2003.

(46)   Seyferth, D. *Organometallics* **2002**, *21*, 2800.

(47) Weiss, E.; Fischer, E. O. *Z. Anorg. Allg. Chem.* **1956**, *286*, 142.

(48) Jellinek, F. *Nature* **1960**, *187*, 871.

(49) Cotton, F. A.; Dollase, W. A.; Wood, J. S. *J. Am. Chem. Soc.* **1963**, *85*, 1543.

(50) Ibers, J. A. *J. Chem. Phys.* **1964**, *40*, 3129.

(51) Keulen, E.; Jellinek, F. *J. Organometal. Chem.* **1966**, *5*, 490.

(52) Fischer, E. O.; Fritz, H.-P. *Angew. Chem.* **1961**, *11*, 353.

(53) Elschenbroich, C.; Koch, J.; Kroker, J.; Wünsch, M.; Massa, W.; Baum, G.; Stork, G. *Chem. Ber.* **1988**, *121*, 1983.

(54) Elschenbroich, C. *Private Publication*.

(55) Kojima, H.; Takahashi, S.; Hagihara, N. *Chem. Commun.* **1973**, 230.

(56) Holthausen, M. C. *Private Publication*.

(57) Lucas, H. R.; Li, L.; Sarjeant, A. A. N.; Vance, M. A.; Solomon, E. I.; Karlin, K. D. *J. Am. Chem. Soc.* **2009**, *131*, 3230.

(58) Bäckvall, J.-E. *Modern Oxidation Methods*; Wiley-VCH: Weinheim, 2004.

(59) Karlin, K. D.; Wei, N.; Jung, B.; Kaderli, S.; Niklaus, P.; Zuberbuehler, A. D. *J. Am. Chem. Soc.* **1993**, *115*, 9506.

(60) Ward, A. L.; Elbaz, L.; Kerr, J. B.; Arnold, J. *Inorg. Chem.* **2012**, *51*, 4694.

(61) Karlin, K. D.; Hayes, J. C.; Juen, S.; Hutchinson, J. P.; Zubieta, J. *Inorg. Chem.* **1982**, *21*, 4106.

(62) Allen, C. S.; Chuang, C.-L.; Cornebise, M.; Canary, J. W. *Inorg. Chim. Acta* **1995**, *239*, 29.

(63) Schatz, M.; Becker, M.; Thaler, F.; Hampel, F.; Schindler, S.; Jacobson, R. R.; Tyeklar, Z.; Murthy, N. N.; Ghosh, P.; Chen, Q.; Zubieta, J.; Karlin, K. D. *Inorg. Chem.* **2001**, *40*, 2312.

(64) Weitzer, M.; Schatz, M.; Hampel, F.; Heinemann, F. W.; Schindler, S. *J. Chem. Soc., Dalton Trans.* **2002**, 686.

(65) Weitzer, M.; Schindler, S.; Brehm, G.; Schneider, S.; Hörmann, E.; Jung, B.; Kaderli, S.; Zuberbühler, A. D. *Inorg. Chem.* **2003**, *42*, 1800.

(66) Zhang, C. X.; Kaderli, S.; Costas, M.; Kim, E.-i.; Neuhold, Y.-M.; Karlin, K. D.; Zuberbühler, A. D. *Inorg. Chem.* **2003**, *42*, 1807.

(67) Gafford, B. G.; Holwerda, R. A.; Schugar, H. J.; Potenza, J. A. *Inorg. Chem.* **1988**, *27*, 1126.

(68) Li, S.; Wang, S.-B.; Zhang, F.-L.; Tang, K. *Acta Cryst. Section E* **2008**, *64*, m2.

(69) DiVaira, M.; Mani, F. *Inorg. Chem.* **1984**, *23*, 409.

(70) Hodgson, D. J.; Zietlow, M. H.; Pedersen, E.; Toftlund, H. *Inorg. Chim. Acta* **1988**, *149*, 111.

(71) Gafford, B. G.; Holwerda, R. A. *Inorg. Chem.* **1989**, *28*, 60.

(72)   Addison, A. W.; Rao, T. N.; Reedijk, J.; van Rijn, J.; Verschoor, G. C. *J. Chem. Soc., Dalton Trans.* **1984**, 1349.

(73)   Eckenhoff, W. T.; Biernesser, A. B.; Pintauer, T. *Inorg. Chem.* **2012**, *51*, 11917.

(74)   Jubb, J.; Larkworthy, L. F.; Oliver, L. F.; Povey, D. C.; Smith, G. W. *J. Chem. Soc., Dalton Trans.* **1991**, 2045.

(75)   Sheldrick, G. M.; SHELXS-90, Program for Crystal Structure Solution, University of Göttingen, Germany, 1990.

(76)   Sheldrick, G. M.; SHELXL-97, Program for Crystal Structure Refinement, University of Göttingen, Germany, 1997.

(77)   Sono, M.; Roach, M. P.; Coulter, E. D.; Dawson, J. H. *Chem. Rev.* **1996**, *96*, 2841.

(78)   Que, L.; Ho, R. Y. N. *Chem. Rev.* **1996**, *96*, 2607.

(79)   Park, M. J.; Lee, J.; Suh, Y.; Kim, J.; Nam, W. *J. Am. Chem. Soc.* **2006**, *128*, 2630.

(80)   Nielsen, A.; Larsen, F. B.; Bond, A. D.; McKenzie, C. J. *Angew. Chem. Int. Ed.* **2006**, *45*, 1602.

(81)   Westerheide, L.; Müller, F. K.; Than, R.; Krebs, B.; Dietrich, J.; Schindler, S. *Inorg. Chem.* **2001**, *40*, 1951.

(82)   Bernal, I.; Jensen, I. M.; Jensen, K. B.; McKenzie, C. J.; Toftlund, H.; Tuchagues, J.-P. *J. Chem. Soc., Dalton Trans.* **1995**, 3667.

(83)   Horner, O.; Jeandey, C.; Oddou, J.-L.; Bonville, P.; McKenzie, C. J.; Latour, J.-M. *Eur. J. Inorg. Chem.* **2002**, 3278.

(84)   Duelund, L.; Hazell, R.; McKenzie, C. J.; Preuss, N. L.; Toftlund, H. *J. Chem. Soc., Dalton Trans.* **2001**, 152.

(85)   Jensen, K. B.; McKenzie, C. J.; Nielsen, L. P.; Zacho, P. J.; Svendsen, H. M. *Chem. Commun.* **1999**, 1313.

(86)   Cotton, F. A.; Wilkinson, G. *Advanced Inorganic Chemistry*; 5. ed. New York [u.a.], 1988.

(87)   Eriksen, J.; Goodson, P.; Hazell, A.; Hodgson, D. J.; Michelsen, K.; Monsted, O.; Rasmussen, J. C.; Toftlund, H. *Acta Chem. Scand.* **1999**, *53*, 1083.

(88)   Schäfer, S.; Becker, J.; Beitat, A.; Würtele, C. *Z. Anorg. Allg. Chem.* **2013**, *639*, 2269.

(89)   Gutmann, N.; Müller, B. *J. Solid State Chem.* **1996**, *122*, 214.

(90)   Shibahara, T.; Akashi, H.; Asano, M.; Wakamatsu, K.; Nishimoto, K.; Mori, M. *Inorg. Chem. Commun.* **2001**, *4*, 413.

(91)   Ardon, M.; Cohen, S. *Inorg. Chem.* **1993**, *32*, 3241.

(92)   Yokoyama, A.; Cho, K.-B.; Karlin, K. D.; Nam, W. *J. Am. Chem. Soc.* **2013**.

(93)   Fischer, E. O.; Hafner, W. *Z. Anorg. Allg. Chem.* **1956**, *286*, 146.

(94)   Fischer, E. O.; Seeholzer, J. *Z. Anorg. Allg. Chem.* **1961**, *312*, 244.

(95)   Fehlhammer, W. P.; Herrmann, W. A.; Öfele, K. *Handbuch der Präparativen Anorganischen Chemie*; 3. ed.; Brauer, G., Ed.; Ferdinand Enke Verlag: Stuttgart, 1981, 1840.

(96)   Elschenbroich, C.; Bilger, E.; Metz, B. *Organometallics* **1991**, *10*, 2823.

(97)   Tsierkezos, N. G. *J. Solution Chem.* **2008**, *37*, 1437.

(98)   Grepioni, F.; Cojazzi, G.; Draper, S. M.; Scully, N.; Braga, D. *Organometallics* **1998**, *17*, 296.

(99)   Gribov, B. G.; Mozzhukhin, D. D.; Suskina, I. A.; Salamatin, B. A. *Dokl. Akad. Nauk SSSR* **1971**, *196*, 586.

(100) Braga, D.; Costa, A. L.; Grepioni, F.; Scaccianoce, L.; Tagliavini, E. *Organometallics* **1996**, *15*, 1084.

(101) Braga, D.; Angeloni, A.; Maini, L.; Götz, A. W.; Grepioni, F. *New. J. Chem.* **1999**, 17.

(102) Braga, D. *Chem. Commun.* **2003**, 2751.

(103) Elschenbroich, C.; Gondrum, R.; Massa, W. *Angew. Chem.* **1985**, *97*, 976.

(104) Hagihara, N. *Ann. NY Acad. Sci.* **1965**, *125*, 98.

(105) Tsutsui, M. *Ann. NY Acad. Sci.* **1965**, *125*, 147.

(106) Feltham, R. D. *J. Inorg. Nucl. Chem.* **1961**, *16*, 197.

(107) Braga, D.; Grepioni, F.; Tagliavini, E.; Novoa, J. J.; Mota, F. *New. J. Chem.* **1998**, 755.

(108) Jander, G.; Blasius, E. *Lehrbuch der analytischen und präparativen anorganischen Chemie*; 14. neu bearb. ed.; Hirzel Verlag: Stuttgart, 1995.

(109) CrysAlisPro *Agilent Technologies* **2010**, *Version 1.171.34.44*.

(110) Sheldrick, G. M. *Acta Cryst.* **2008**, *A64*, 112.

Versicherung

Ich erkläre: Ich habe die vorgelegte Dissertation selbständig und ohne unerlaubte fremde Hilfe und nur mit den Hilfen angefertigt, die ich in der Dissertation angegeben habe. Alle Textstellen, die wörtlich oder sinngemäß aus veröffentlichten Schriften entnommen sind, und alle Angaben, die auf mündlichen Auskünften beruhen, sind als solche kenntlich gemacht. Bei den von mir durchgeführten und in der Dissertation erwähnten Untersuchungen habe ich die Grundsätze guter wissenschaftlicher Praxis, wie sie in der „Satzung der Justus-Liebig-Universität Gießen zur Sicherung guter wissenschaftlicher Praxis" niedergelegt sind, eingehalten.

_____

Sabrina Schäfer